Chemistry-Driven Dissection of Malaria Immunity and Resistance: Multiplex Antibody Analysis and Mechanistic Inhibition Studies

Elizabeth Momoh

A dissertation

submitted in partial fulfillment of the

requirements for the degree of

Doctor of Philosophy

University of Washington

2025

Reading Committee:

Pradipsinh K. Rathod, Co-chair

Ashleigh Theberge, Co-chair

Alshakim Nelson

Program Authorized to Offer Degree:

Chemistry

University of Washington

Abstract

Chemistry-Driven Dissection of Malaria Immunity and Resistance: Multiplex Antibody Analysis and Mechanistic Inhibition Studies

Elizabeth Momoh

Chairs of the Supervisory Committee:

Pradipsinh K. Rathod
Ashleigh Theberge

Department of Chemistry

This dissertation discusses the dissection of antimalarial immunity and resistance, with an emphasis on chemistry-driven tools for antibody analysis and parasite inhibition. Malaria remains a major global health burden, and despite the availability of frontline therapeutics, widespread resistance and incomplete immune protection underscore the urgent need for new strategies. To address these challenges, this work integrates chemical biology approaches to interrogate antibody responses, evaluate drug efficacy, and characterize host-parasite interactions during the erythrocytic life cycle.

First, bead-based multiplexing assays were developed and optimized as a platform for the simultaneous analysis of antibody responses against multiple malaria antigens. By applying advanced coupling chemistries and addressing limitations in antigen production and orientation, this platform enabled high-throughput, sensitive, and reproducible profiling of naturally acquired immunity. These innovations provide an improved chemical framework for antigen prioritization and vaccine candidate evaluation.

Second, mechanistic growth inhibition assays (GIAs) were employed to investigate parasite susceptibility to small molecules, monoclonal antibodies, and patient sera. Using well-characterized compounds such as Tartrolon E, DSM265, and artemisinin as pharmacological benchmarks, these assays established a robust comparative system for evaluating inhibitory potency. Parallel studies with monoclonal antibodies targeting key invasion ligands (MSP1, AMA1, EBA175) highlighted distinct inhibitory profiles and stage-

specific vulnerabilities, while patient sera from a malaria-endemic region revealed protective capacity that complements drug and antibody-mediated mechanisms.

Finally, resistance studies focused on dihydroorotate dehydrogenase (DHODH) inhibitors, a promising class of antimalarials. Cross-resistance analyses of DSM265-resistant *P. falciparum* mutant lines against a panel of novel DHODH inhibitors revealed susceptibility patterns. These findings provide critical insights into drug-target interactions and resistance evolution, informing future drug design strategies.

Together, this dissertation demonstrates how chemical tools and mechanistic assays can be harnessed to dissect the molecular basis of antimalarial immunity and drug resistance. The integration of multiplex immunoassays, pharmacological profiling, and resistance mapping establishes a versatile framework for advancing vaccine development, drug discovery, and malaria research.

Table of Contents

Acknowledgements

Writing this section brings tears to my eyes as I reflect on my PhD journey. It has truly been a rollercoaster of emotions from day one to this moment. The challenging, anxious, hopeful, good, and great days all played a critical role in shaping my path, and I am deeply grateful to everyone who walked alongside me.

I would like to thank Dr. Pradip Rathod for welcoming me into your lab and for your guidance in helping me grow as a scientist. Thank you for believing in my potential and for providing the resources that enabled me to complete this major milestone.

To my lab mentors, Dr. Devaraja Mudeppa and Dr. John White, I am profoundly grateful for your mentorship and teachings. You invested not only in my academic and professional development but also in my personal growth. Thank you for your patience, encouragement, and support.

To Dr. Ashleigh Theberge, I am deeply appreciative of your constant advocacy and guidance, especially as I finish up my program. Your support has been a major source of encouragement, helping me to navigate challenges and remain focused on my goals.

To Adewunmi and the wonderful friends I met along the way, thank you for being my companions on this graduate school journey. The memories we created together will always be cherished.

To my siblings, Daniel, Emmanuella, and Naomi, thank you for giving me the comfort of your presence whenever I needed to step away from the demands of research.

To my parents, thank you for instilling in me resilience and discipline, and for always checking in from thousands of miles away.

To my husband and best friend, you have been my anchor through every high and low. Thank you for being there and for the countless ways you lightened my load along the way.

Finally, to my Creator, thank You for walking with me every step of the way. All glory belongs to You.

Dedication

This dissertation is dedicated to Almighty God whose grace carried me through every step of this journey; to my parents, Barr. Abdulfathai and Mrs. Felicitas Momoh, whose wisdom and sacrifices inspired me to dream boldly and persevere; and to my husband, Ayomikun Oluwayemi, whose steadfast love and support made this accomplishment possible.

Chapter 1 | Introduction

1.1 Global Malaria Burden

Malaria remains one of the most significant infectious diseases worldwide, with progress in control stalling in recent years despite decades of concerted global efforts. In 2023, the World Health Organization (WHO) estimated 263 million malaria cases and 597,000 deaths, marking an increase from the 249 million cases and 608,000 deaths reported in 2022.[1-3] The vast majority of this burden occurs in sub-Saharan Africa, which in 2023 accounted for 94% of global cases and 95% of deaths.[2,4] Four countries alone: Nigeria (~30%), the Democratic Republic of the Congo (~12%), Niger (~6%), and Tanzania (~4%), were collectively responsible for more than half of global malaria deaths[3],[4]. Children under five years of age remain the most vulnerable group, contributing to about 76% of malaria deaths in 2022, equivalent to approximately 462,000 child deaths.[5] This equates to more than 1,200 young children dying every day from a preventable and treatable disease, reflecting both biological susceptibility and structural inequities in healthcare access.

Despite these sobering statistics, progress since the early 2000s highlights the effectiveness of large-scale interventions. Between 2000 and 2022, global malaria control measures, including insecticide-treated bed nets, indoor residual spraying, rapid diagnostic testing, and artemisinin-based combination therapies are estimated to have averted 2.1 billion cases and 11.7 million deaths.[6] Case incidence fell from around 81 per 1,000 population at risk in 2000 to 58 per 1,000 in 2022, while mortality dropped from 28.8 to 14.3 deaths per 100,000 population during the same period.[7] However, these gains have plateaued since 2015, with the COVID-19 pandemic further straining fragile malaria programs through disruptions in prevention campaigns, supply chains, and healthcare access.[7]

The malaria burden is highly heterogeneous and concentrated in a small number of endemic countries. The WHO has identified a group of 11 “High Burden to High Impact” (HBHI) countries, which together accounted for 67% of malaria cases and 73% of deaths in 2022[2]. Within these countries, health inequities, conflict, poverty, and weak health systems contribute to persistent transmission and high mortality.

For example, climate- and conflict-related displacement has exacerbated transmission in countries such as Sudan and the Democratic Republic of the Congo, where internally displaced populations have limited access to preventive tools or treatment.

Today, nearly half of the world's population lives in malaria-risk zones. The disease is caused by parasites of the genus *Plasmodium*, with *Plasmodium falciparum* and *Plasmodium vivax* responsible for most human infections. *P. falciparum*, predominant in Africa, is associated with the highest mortality due to its capacity for high parasite densities, sequestration in microvasculature, and immune evasion. *P. vivax,* widespread in Asia and the Americas, contributes significantly to morbidity through its ability to establish dormant liver stages (hypnozoites) that trigger relapses months after initial infection. The virulence of these parasites reflects their complex life cycle and immune-evasion strategies, which continue to pose challenges for vaccine development and sustained elimination.

In addition to biological challenges, emerging threats are undermining current control strategies. The spread of insecticide resistance in Anopheles mosquitoes and antimalarial drug resistance in *P. falciparum* are limiting the effectiveness of frontline interventions.[8] Climate change is also altering transmission patterns, with rising temperatures and rainfall variability expanding malaria risk zones into previously low-transmission areas. Together, these challenges threaten to reverse two decades of progress, reinforcing the urgent need for novel interventions, including next-generation vector control tools, new chemotherapeutics, and effective vaccines to achieve the global malaria elimination targets set by the WHO.

1.2 Malaria Parasite Life Cycle

The malaria parasite has a complex lifecycle that alternates between the human host and the female Anopheles mosquito vector. Transmission begins when an infected mosquito inoculates sporozoites into the skin during a blood meal. A small proportion of these sporozoites enter the bloodstream and rapidly migrate to the liver, where they invade hepatocytes and undergo asexual replication to form liver-stage schizonts containing thousands of merozoites.[1,9] Upon rupture of infected hepatocytes, merozoites are

released into the bloodstream, initiating the erythrocytic cycle. In *P. vivax* and *P. ovale*, a subset of parasites develop into dormant liver stages known as hypnozoites, which can remain quiescent for weeks to years before reactivating to cause clinical relapses.[10-12]

Within the erythrocytic cycle, merozoites invade red blood cells, where they progress through ring, trophozoite, and schizont stages before rupturing to release new merozoites. This cyclical invasion and destruction of erythrocytes results in the hallmark clinical manifestations of malaria, including fever, anemia, and in severe cases, organ dysfunction.[13] Some blood-stage parasites differentiate into sexual forms known as gametocytes, which are the transmissible stage of the parasite. When another mosquito takes a blood meal, gametocytes are ingested and mature into male and female gametes within the mosquito midgut, where fertilization produces zygotes that transform into motile ookinetes. Ookinetes penetrate the midgut epithelium and form oocysts, which develop into thousands of sporozoites. Mature sporozoites subsequently migrate to the mosquito salivary glands, enabling transmission to a new human host and completing the cycle.[14]

The complexity of the malaria parasite lifecycle underlies the difficulty of controlling and eliminating the disease. The parasite's ability to transition between distinct developmental stages, establish dormant reservoirs, and evade host immunity presents formidable barriers for both natural clearance and vaccine development.[15,16]

1.3 Current Treatments and Prevention: Antimalarial Successes and Challenges

Efforts to control malaria rely on a multipronged approach integrating chemotherapy, chemoprevention, and vector control interventions. Artemisinin-based combination therapies (ACTs) are the current standard of care for uncomplicated *Plasmodium falciparum* malaria and have been central to global reductions in mortality since their introduction in the early 2000s.[17, 18] ACTs pair a fast-acting artemisinin derivative with a partner drug to enhance efficacy and reduce the risk of resistance. Severe malaria is managed with intravenous artesunate, which has been shown to reduce mortality compared to quinine[19]. For *P. vivax* malaria, chloroquine remains effective in many regions, although resistance has emerged;

radical cures require the use of primaquine or tafenoquine to eliminate dormant liver-stage hypnozoites and prevent relapse.[19]

Chemopreventive strategies, such as intermittent preventive treatment in pregnancy (IPTp) with sulfadoxine-pyrimethamine, seasonal malaria chemoprevention (SMC) for children in highly seasonal transmission areas, and prophylaxis for travelers to endemic regions, are also critical tools.[20] Beyond pharmacological interventions, vector control measures remain the cornerstone of malaria prevention. Insecticide-treated nets (ITNs), indoor residual spraying (IRS), and larval source management have significantly reduced transmission, particularly in sub-Saharan Africa.[21]

In recent years, advances in malaria vaccine development have marked a major milestone. The RTS,S/AS01 vaccine, the first malaria vaccine recommended by the World Health Organization in 2021, demonstrated modest but significant protection against clinical malaria in young children.[22] More recently, the R21/Matrix-M vaccine has shown improved efficacy and scalability, offering hope for integration into broader control programs.[23]

Despite these successes, formidable challenges remain. The emergence and spread of drug resistance, particularly artemisinin partial resistance in Southeast Asia and increasingly in Africa, threatens the efficacy of ACTs.[24] Resistance to partner drugs such as piperaquine and lumefantrine further complicates treatment strategies. On the prevention front, widespread insecticide resistance among Anopheles mosquitoes is undermining the effectiveness of ITNs and IRS, while operational and financial constraints limit large-scale implementation in many endemic regions.[25] Vaccine rollout faces hurdles including limited efficacy, logistical demands of multi-dose schedules, and uncertain long-term protection.[22,23]

Taken together, global malaria control has achieved notable success over the past two decades, with significant declines in morbidity and mortality. However, the combination of parasite resistance, vector adaptation, and health system challenges underscores the need for sustained innovation, surveillance, and investment to accelerate progress toward malaria elimination.

1.4 Antigen Prioritization: Past, Current, and Novel Methods

Evasion of Host Immune Response and the Need for Antigen Prioritization

Antigenic variation refers to the ability of infectious organisms to systematically alter the immunogenic epitopes exposed to their host's immune system, thereby avoiding antibody recognition and enabling persistent infection and transmission.[26] In *Plasmodium falciparum*, antigenic variation manifests clinically as successive waves of parasitemia, with each wave representing antigenically distinct parasite populations that evade antibodies generated against previously expressed antigens.[27] This phenomenon complicates the development of protective immunity, as the parasite exploits a vast repertoire of antigens during different stages of its life cycle. Consequently, prioritizing parasite antigens that play critical roles in invasion and pathogenesis has become a central focus of malaria research.[28] However, identifying and characterizing immunologically relevant parasite antigens remains a challenge due to the parasite's structural complexity and antigenic diversity.

Approaches to Antigen Identification and Prioritization

Historically, antigen discovery relied heavily on serological assays, particularly the enzyme-linked immunosorbent assay (ELISA), which detects host antibody responses to individual recombinant antigens.[27] While informative, this approach is limited by its singleplex nature, requiring significant time and resources to evaluate numerous antigens individually. These early methods yielded valuable insights but were constrained in their capacity to capture the breadth of immune responses elicited by malaria infection.

Advances in Antigen Discovery: Current and Novel Methods

The advent of genomic technologies marked a turning point in antigen identification. Following the publication of the *P. falciparum* genome in 2003, researchers gained access to a complete catalogue of parasite genes, enabling systematic evaluation of putative antigens.[29] High-throughput platforms, such as protein microarrays, were developed to screen host antibody responses against hundreds to thousands of recombinant malaria proteins simultaneously, accelerating the identification of immune-reactive

candidates.[30-33] More recently, the Rathod lab developed a bead-based flow cytometric assays (e.g., Luminex) that allows multiplex detection of up to one hundred antibody responses in a single sample, offering both efficiency and scalability.[34]

Systems serology approaches that integrate functional antibody profiling with computational analysis have provided deeper insights into correlates of immunity.[35] Furthermore, reverse vaccinology and immunopeptidomics are increasingly employed to predict and validate antigens most likely to elicit protective responses.[36] Integration of these novel methods with longitudinal cohort studies and clinical trial data has refined the prioritization process, moving the field toward rational vaccine design and more targeted therapeutic development.[37]

1.5 Bead-Based Multiplexing for Antigen Prioritization

Principles of Bead-Based Multiplexing

Bead-based multiplexing has emerged as a powerful approach for antigen prioritization, enabling simultaneous interrogation of multiple antigens using a single patient sample, thereby reducing assay time, cost, and biological sample requirements.[38,39] The core components of the technology are flow cytometry, microspheres, and antibodies. Key advancements, including fluorophore-dyed microspheres, compact lasers, expanded antibody and fluorochrome repertoires, and advanced computational software in the late 1990s, enabled high-throughput multiplexing.[40]

A major development was Luminex Corporation's xMAP® technology, in which polystyrene microspheres are internally dyed with precise ratios of two fluorochromes. Each bead set is physically identical but spectrally distinct, allowing unique identification via emission spectra.[41] Beads conjugated with antigens are analyzed on instruments such as the Luminex 200® (later rebranded Bio-Plex 200®). Two lasers interrogate each bead: a 635 nm laser excites the internal classification dye, and a 532 nm laser excites the surface reporter fluorophore, typically R-phycoerythrin (PE). These signals enable simultaneous detection of bead identity and antigen-antibody binding events.[41,42]

Multiplexing offers several advantages over protein microarrays. Bead conjugation is simpler than array spotting, multiple antigens can interact with antibodies simultaneously mimicking in vivo binding, and up to 100 antigens can be assayed per well of a 96-well plate in under an hour, increasing throughput and reducing sample consumption.[43]

Multiplexing Applications in Malaria Antigen Studies

Bead-based multiplexing was first applied to malaria antigens in the mid-2000s.[44] Early studies demonstrated strong correlation with ELISA while requiring smaller serum volumes and offering greater dynamic range.[45,46] Initial studies commonly targeted three to five antigens implicated in naturally acquired immunity (NAI), using patient samples primarily from African cohorts, with fewer studies from South America and Southeast Asia and limited data from India.[34,46]

Standardized bead-coupling protocols, such as those in the Luminex "cookbook", employ carbodiimide chemistry using 1-ethyl-3-(3-dimethylaminopropyl) carbodiimide (EDC) and N-hydroxysulfosuccinimide (Sulfo-NHS) to covalently attach purified antigens to carbonylated beads.[47] Despite these advances, challenges remain. Many malaria antigens are membrane-bound or structurally complex, making purification difficult.[48] Additionally, carbodiimide coupling can result in non-uniform antigen presentation and occasional loss of conformational epitopes, leading to variability in antibody binding.[49]

Advances in Multiplex Chemistry

To address these limitations, affinity-based capture strategies are being explored, enabling direct isolation of tagged antigens from expression lysates without purification.[34] Traditional large tags like GST or MBP may interfere with epitope recognition, whereas smaller tags such as polyhistidine (His-tag) offer better compatibility but can yield lower purity.[50] Future improvements aim to achieve high selectivity, consistent antigen presentation, and preserved epitopes while maintaining high-throughput capabilities. Oriented linker chemistries are one approach that may improve assay reproducibility and epitope accessibility. Optimized bead-based multiplexing platforms will be critical for systems-level approaches to malaria antigen discovery and rational vaccine design.[51]

The primary goal of the work presented in the following chapter is to address current limitations in methods used to dissect antibody-mediated immune responses to malaria. Improving the technical aspects of immune assays will enhance the prioritization of antigen candidates and enable investigation of additional disease-relevant questions. A critical first step is ensuring the quality of antigens used in such studies; antigens must be expressed in full-length, functional form and isolated at high purity to maintain structural integrity and immunoreactivity. To achieve this, we harnessed the powerful expression capabilities of the eukaryotic wheat germ system based on a well-characterized protocol developed in the Rathod lab.[48] Furthermore, the methods used to immobilize antigens require optimization to present correctly folded epitopes without masking or loss of antibody-binding sites, necessitating reliable and controllable chemistries for attachment to solid surfaces. Developing strategies to gently release antigens from these surfaces could also provide insight into structural changes induced during immobilization. Finally, given the extensive repertoire of malaria antigens, it is highly advantageous to interrogate multiple antigens in parallel while minimizing the use of limited patient samples. The implementation of these technical improvements will not only save time and resources but also facilitate the development of a highly sensitive, high-throughput platform for the investigation of naturally acquired immunity targets, setting the stage for the experimental studies described in Chapter 2.

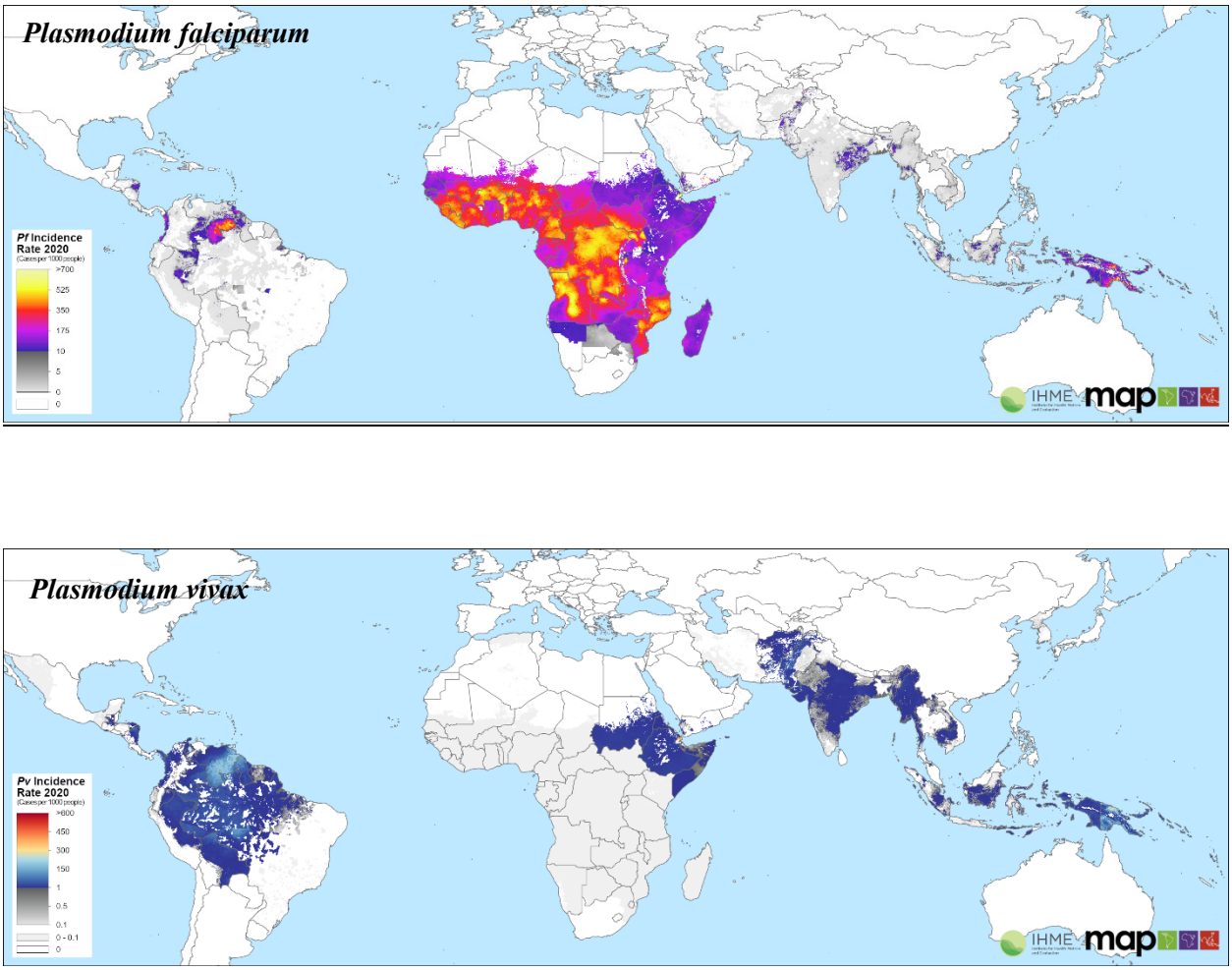

Figure 1.1: World map illustrating the spatial distribution of malaria burden, highlighting regional variation in *Plasmodium falciparum and vivax* prevalence and transmission intensity. Adapted from Lancet spatial and temporal modeling study. [52]

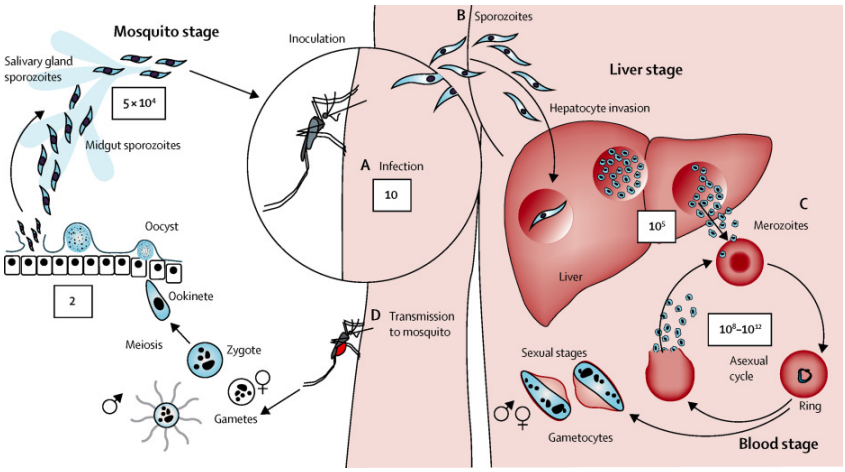

Figure 1.2: Life cycle of *Plasmodium falciparum*, illustrating the mosquito, liver, and blood stages. Following inoculation of sporozoites by an infected Anopheles mosquito, parasites invade hepatocytes and undergo replication, releasing thousands of merozoites into the bloodstream. In red blood cells, parasites multiply asexually in cycles of exponential growth, while a subset differentiates into sexual gametocytes that are taken up by mosquitoes, completing the transmission cycle. Adapted from White et. al.[11]

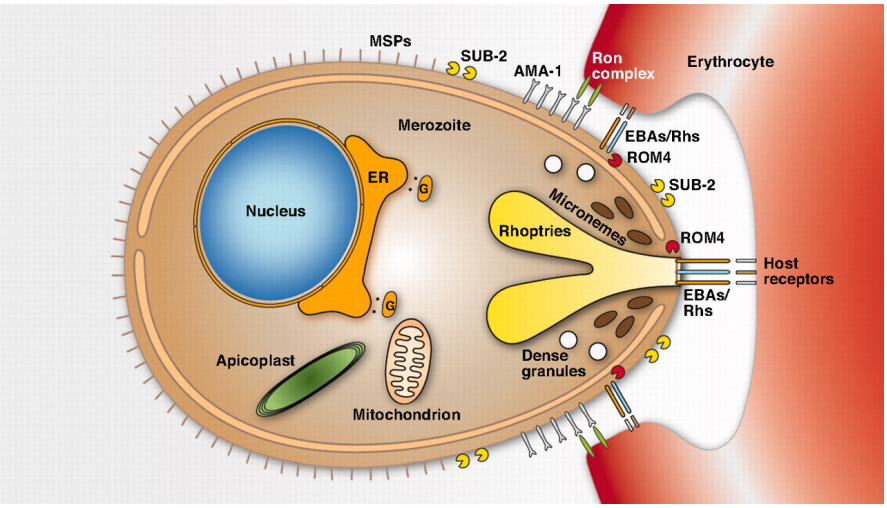

Figure 1.3: Schematic representation of *Plasmodium falciparum* merozoite invasion of an erythrocyte, highlighting key organelles (nucleus, apicoplast, mitochondrion, ER) and invasion machinery (micronemes, rhoptries, dense granules) as well as surface and secreted proteins (MSPs, AMA-1, EBAs/Rhs, RON complex, SUB-2, ROM4) that mediate host receptor engagement and erythrocyte entry.. Adapted from Kappe et. al.[53]

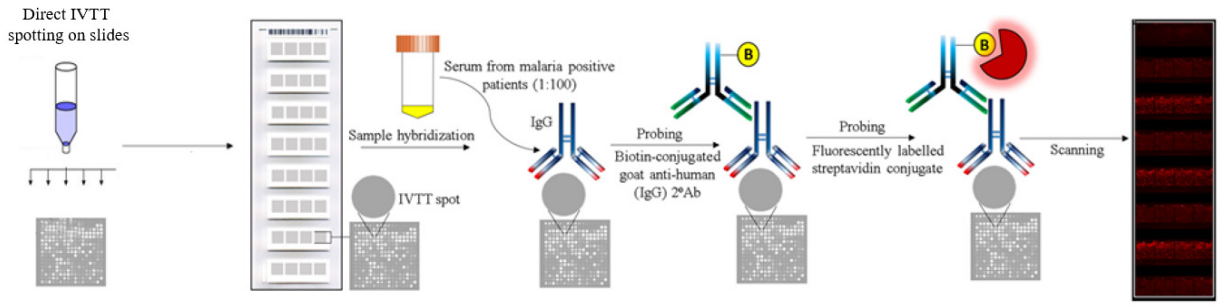

Figure 1.4: Schematic representation of traditional protein microarray experimentation and workflow. Antigens are expressed and directly spotted onto slides with no purification steps. A single slide contains thousands of antigen spots. Patient serums can then by hybridized on the slides and read out with fluorescently labeled secondary antibodies. Finally, slides are scanned to produce an image with varying fluorescent signal responses based on the antibody response of the patient. Adapted from Venkatesh et al. 2019.[54]

1.6. References

1. WHO. World Malaria Report 2023. Geneva: WHO; 2023. World malaria report 2023
2. World Health Organization. World Malaria Report 2024: Addressing Inequity in the Global Malaria Response. Geneva: WHO; 2024. World malaria report 2024
3. Lay, K. The Guardian. Malaria cases rise for fifth year as disasters and resistance hamper control efforts. Published Dec 11, 2024. Malaria cases rise for fifth year as disasters and resistance hamper control efforts | Global health | The Guardian
4. Centers for Disease Control and Prevention (CDC). Impact of Malaria. 2023. Malaria's Impact Worldwide | Malaria | CDC
5. McDonnell, MR., Beat Malaria (United Nations Foundation). World Malaria Report 2023: What you need to know. Published Dec 2023. World Malaria Report 2023: What You Need to Know – United to Beat Malaria
6. Samantharoy, S. Health Policy Watch. Global Malaria Progress Stalled With Nearly 600,000 Deaths in 2023. Dec 2023. Global Malaria Progress Stalled With Nearly 600,000 Deaths In 2023 - Health Policy Watch
7. Venkatesan, P. WHO world malaria report 2024. The Lancet Microbe, Volume 6, Issue 4, 101073. WHO world malaria report 2024 - The Lancet Microbe
8. Ehrlich, HY, Some, F, Bazie, T, Ebou, C, Dembele, E. Tracking antimalarial drug resistance using mosquito blood meals: a cross-sectional study. Lancet Microbe. 2023; Volume 4, Issue 6, e461 - e469. Tracking antimalarial drug resistance using mosquito blood meals: a cross-sectional study - The Lancet Microbe
9. MMV: Medicines for Malaria Venture. Lifecycle of the malaria parasite. 2025. Lifecycle of the malaria parasite | Medicines for Malaria Venture
10. Cowman AF, Healer J, Marapana D, Marsh K. Malaria: Biology and disease. *Cell*. 2016;167(3):610-24. doi:10.1016/j.cell.2016.07.055
11. White NJ, Pukrittayakamee S, Hien TT, Faiz MA, Mokuolu OA, Dondorp AM. Malaria. *Lancet*. 2014;383(9918):723-35. doi: 10.1016/S0140-6736(13)60024-0
12. Markus MB. Dormancy in *Plasmodium* species. Cell Press: *Trends in Parasitology*. 2012;28(2). https://doi.org/10.1016/j.pt.2011.10.005
13. Ashley EA, Pyae Phyo A, Woodrow CJ. Malaria. *Lancet*. 2018;391(10130):1608-21. doi:10.1016/S0140-6736(18)30324-6
14. Frischknecht F, Matuschewski K. Plasmodium Sporozoite Biology. Cold Spring Harb Perspect Med. 2017;7(5):a025478. Published 2017 May 1. doi:10.1101/cshperspect.a025478
15. Sinden RE. The cell biology of malaria infection of mosquito: Advances and opportunities. *Cell Microbiol*. 2015;17(4):451-66. https://doi.org/10.1111/cmi.12413
16. Duffy PE, Patrick Gorres J. Malaria vaccines since 2000: progress, priorities, products. *NPJ Vaccines*. 2020;5(1):48. Published 2020 Jun 9. doi:10.1038/s41541-020-0196-3
17. Dondorp AM, Fairhurst RM, Slutsker L, Macarthur JR, Breman JG, Guerin PJ, et al. The threat of artemisinin-resistant malaria. *N Engl J Med*. 2011;365(12):1073-5. 10.1056/NEJMp1108322
18. Dondorp AM, Fanello CI, Hendriksen IC, Gomes E, Seni A, Chhaganlal KD, et al. Artesunate versus quinine in the treatment of severe falciparum malaria in African children (AQUAMAT): An open-label, randomised trial. *Lancet*. 2010;376(9753):1647-57. 10.1016/S0140-6736(10)61924-1
19. Baird JK. 8-Aminoquinoline therapy for latent malaria. *Clin Microbiol Rev*. 2019;32(4):e00011-19. doi:10.1128/CMR.00011-19

20. WHO. Policy brief for the implementation of intermittent preventive treatment of malaria in pregnancy using sulfadoxine-pyrimethamine (IPTp-SP). Geneva: WHO; 2022.
21. Ranson H, Lissenden N. Insecticide resistance in African *Anopheles* mosquitoes: A worsening situation that needs urgent action to maintain malaria control. *Trends Parasitol*. 2016;32(3):187-96. doi:10.1016/j.pt.2015.11.010
22. RTS,S Clinical Trials Partnership. Efficacy and safety of RTS,S/AS01 malaria vaccine with or without a booster dose in infants and children in Africa: Final results of a phase 3, individually randomised, controlled trial. *Lancet*. 2015;386(9988):31-45. doi:10.1016/S0140-6736(15)60721-8
23. Datoo MS, Natama HM, Somé A, Bellamy D, Traoré O, Rouamba T, et al. Efficacy of a low-dose candidate malaria vaccine, R21/Matrix-M, with seasonal administration to children in Burkina Faso: A randomised controlled trial. *Lancet*. 2021;397(10287):1809-18. doi:10.1016/S0140-6736(21)00943-0
24. Uwimana A, Legrand E, Stokes BH, Ndikumana J-LM, Warsame M, Umulisa N, et al. Emergence and clonal expansion of in vitro artemisinin-resistant *Plasmodium falciparum* kelch13 R561H mutant parasites in Rwanda. *Nat Med*. 2020;26(10):1602-8. doi:10.1038/s41591-020-1005-2
25. Hemingway J, Ranson H, Magill A, Kolaczinski J, Fornadel C, Gimnig J, et al. Averting a malaria disaster: Will insecticide resistance derail malaria control? *Lancet*. 2016;387(10029):1785-8. doi:10.1016/S0140-6736(15)00417-1
26. Scherf A, Lopez-Rubio JJ, Riviere L. Antigenic variation in Plasmodium falciparum. *Annu Rev Microbiol*. 2008;62:445-470. doi:10.1146/annurev.micro.61.080706.093134
27. Smith JD, Rowe JA, Higgins MK, Lavstsen T. Malaria's deadly grip: cytoadhesion of *Plasmodium falciparum*-infected erythrocytes. Cell Microbiol. 2013;15(12):1976-83.
28. Doolan DL, Dobano C, Baird JK. Acquired immunity to malaria. Clin Microbiol Rev. 2009;22(1):13-36.
29. Gardner MJ, Hall N, Fung E, White O, Berriman M, Hyman RW, et al. Genome sequence of the human malaria parasite *Plasmodium falciparum*. Nature. 2002;419(6906):498-511.
30. Doolan DL, Mu Y, Unal B, Sundaresh S, Hirst S, Valdez C, et al. Profiling humoral immune responses to *Plasmodium falciparum* infection with protein microarrays. Proteomics. 2008;8(22):4680-94. Doi: 10.1002/pmic.200800194
31. Crompton PD, Kayala MA, Traore B, Kayentao K, Ongoiba A, Weiss GE, et al. A prospective analysis of the Ab response to *Plasmodium falciparum* before and after a malaria season by protein microarray. Proc Natl Acad Sci USA. 2010;107(15):6958-63. https://doi.org/10.1073/pnas.1001323107
32. Cham GK, Turner L, Kurtis JD, Mutabingwa TK, Fried M, Jensen AT, et al. Hierarchical, domain-specific acquisition of antibodies to *Plasmodium falciparum* erythrocyte membrane protein 1 in Tanzanian children. Infect Immun. 2010;78(11):4653-9.
33. Ondigo BN, Park GS, Gose SO, Ho BM, Ochola LA, Ayodo G, et al. Standardization and validation of a cytometric bead assay to assess antibodies to multiple *Plasmodium falciparum* antigens. Malar J. 2012;11:427. https://doi.org/10.1186/1475-2875-11-427
34. Momoh EO, Ghag SK, White J, Mudeppa DG, Rathod PK. Multiplex Assays for Analysis of Antibody Responses to South Asian *Plasmodium falciparum* and *Plasmodium vivax* Malaria Infections. Vaccines (Basel). 2023;12(1):1. doi:10.3390/vaccines12010001
35. Chung AW, Alter G. Systems serology: profiling vaccine induced humoral immunity against HIV. Trends Immunol. 2017;38(12):1029-44.

36. Rappuoli R, Bottomley MJ, D'Oro U, Finco O, De Gregorio E. Reverse vaccinology 2.0: Human immunology instructs vaccine antigen design. J.E.M. 2016;213(4):469-81. 10.1084/jem.20151960
37. Campo JJ, Dobano C, Sacarlal J, Guinovart C, Mayor A, Angov E, et al. Immune responses elicited by the RTS,S/AS01E malaria vaccine in African infants and children: assessment with immunopeptidomics. Vaccine. 2015;33(45):6089-98.
38. Ahsan H. Monoplex and multiplex immunoassays: approval, advancements, and alternatives. *Comp Clin Path*. 2022;31(2):333-345. doi:10.1007/s00580-021-03302-4
39. Fischinger S, Fallon JK, Michell AR, et al. A high-throughput, bead-based, antigen-specific assay to assess the ability of antibodies to induce complement activation. *J Immunol Methods*. 2019;473:112630. doi:10.1016/j.jim.2019.07.002
40. Jones L, Brown K. Technological advances enabling multiplexed microsphere assays. *Cytometry A*. 1999;38(2):78-85.
41. Luminex Corporation. xMAP® technology overview. Austin, TX: Luminex; 2001.
42. Doe RP, Zhang Y, Li H. Analysis of bead-based immunoassays using flow cytometry. *Cytometry B Clin Cytom*. 2005;68(1):1-9.
43. Cox C. Bead-Based Multiplex Immunoassays: Procedures, Tips, and Tricks. *Methods Mol Biol*. 2021;2261:263-276. doi:10.1007/978-1-0716-1186-9_16
44. Graham H, Chandler DJ, Dunbar SA. The genesis and evolution of bead-based multiplexing. *Methods*. 2019;158:2-11. doi:10.1016/j.ymeth.2019.01.007
45. Kamya MR, Arinaitwe E, Wanzira H. Comparative evaluation of ELISA and multiplex bead-based assays for malaria antigens. *Am J Trop Med Hyg*. 2007;77(3):428-35.
46. Dent AE, Patel P, Ndebele M. Geographic variation in malaria antigen immunogenicity assessed by multiplexing. *PLoS One*. 2015;10(7):e0132307.
47. Luminex Corporation. xMAP® Cookbook: Bead coupling protocols. Austin, TX: Luminex; 2010.
48. Mudeppa DG, Rathod PK.2013. Expression of Functional *Plasmodium falciparum* Enzymes Using a Wheat Germ Cell-Free System. Eukaryot Cell12: doi: 10.1128/EC.00222-13
49. Wilson R, Patel V, Thompson A. Affinity-based bead capture for high-throughput multiplexing. *J Immunol Methods*. 2014;409:62-70.
50. Smith J, Lee R. Optimizing small affinity tags in multiplex immunoassays. *Protein Expr Purif*. 2016;118:45-53.
51. Doolan DL, Crompton PD. High-throughput systems-level approaches for malaria antigen prioritization. *Trends Parasitol*. 2015;31(5):246-54.
52. Weiss, DJ, Dzianach, PA, Saddler, A, Lubinda, J, Browne, A. et al. Mapping the global prevalence, incidence, and mortality of *Plasmodium falciparum* and *Plasmodium vivax* malaria, 2000-22: a spatial and temporal modelling study. The Lancet, Volume 405, Issue 10483, 979 - 990
53. Kappe SH, Vaughan AM, Boddey JA, Cowman AF. That was then but this is now: malaria research in the time of an eradication agenda. Science. 2010;328(5980):862-866. doi:10.1126/science.1184785
54. Venkatesh, A., Jain, A., Davies, H., Periera, L., Maki, J. N., Gomes, E. et al. (2019) Hospital-derived antibody profiles of malaria patients in Southwest India Malar J 18, 138 10.1186/s12936-019-2771-5

Chapter 2 | Multiplex Assays for Antibody Responses to Malaria.

Reproduced in part from Momoh, E.O., Ghag, S.K.*, White, J., Mudeppa, D.G., Rathod, P.K. "Multiplex Assays for Analysis of Antibody Responses to South Asian Plasmodium falciparum and Plasmodium vivax Malaria Infections". Vaccines* ***2024****, 12, 1.*

**Equal contribution*

E.O.M. and S.K.G. investigated, curated data, and contributed to writing the manuscript. D.G.M. and P.K.R. developed methodologies, curated and visualized data, wrote and edited the manuscript. J.W. contributed to enrolling malaria patient samples into the MESA ICEMR program, assisted in investigating parasite growth inhibition studies and in writing the manuscript.

Abstract

Malaria remains a major global health challenge, causing approximately 0.5 million yearly deaths. To understand naturally acquired immunity in adult human populations in malaria-prevalent regions, improved serological tools are needed, particularly where multiple malaria parasite species co-exist. Slide-based and bead-based multiplex approaches have helped characterize antibodies in malaria patients from endemic regions, but these require pure, well-defined antigens. To efficiently bypass antigen purification steps, codon-optimized malaria antigen genes designed with N-terminal FLAG-tag and C-terminal Ctag sequences were expressed in a wheat germ cell-free system and directly adsorbed onto functionalized BioPlex beads. In this pilot study, 15 *P. falciparum* antigens, 8 *P. vivax* antigens, and negative control (GFP) were adsorbed individually on functionalized bead types through their Ctag. To validate the multiplexing powers of this platform, 10 *P. falciparum*-infected patient sera from a US NIH MESA-ICEMR study site in Goa, India, were tested against all 23 parasite antigens. Serial dilution of sera revealed variations in potency and breadth of patient antibodies to various parasite antigens. Individual patients revealed informative variations in immunity to *P. falciparum* versus *P. vivax*. This multiplex approach to malaria serology can answer key questions on varying immunity to different human malaria parasite species and different parasite antigens. This approach can be scaled to track the dynamics of antibody production during one or more human parasite infections.

2.1. Introduction

Plasmodium falciparum (*Pf*) and *Plasmodium vivax* (*Pv*) are primary causative agents of human malaria. Together they are responsible for over 240 million malaria cases yearly, resulting in roughly 600,000 deaths.[1] Despite the deployment of efficacious antimalarials, insecticides, and bed nets, the decline in the worldwide parasite burden has stalled in recent years. [2,3] Repeated exposure to malaria parasites produces antibody responses to many antigens and confers naturally acquired immunity. [4-6] Understanding variations in serum antibody responses in malaria patients can offer insights into serological markers for submicroscopic infections, activated hypnozoites, and protective immunity. Multiplexed slide-based protein arrays offer an important approach for malaria parasite antigen prioritization. [6-12] A single glass-based array can report on differential antibody binding from patient sera to hundreds of parasite antigens in parallel.[8, 13, 14]

As part of a global collaboration through the US NIH International Centers of Excellence for Malaria Research (ICEMRs), malaria protein arrays have been used to study immunity against *P. falciparum* and *P. vivax.* [6, 11, 12, 14-21.] Traditionally, protein arrays have been fabricated using unpurified malaria antigens spotted directly onto glass slides. [10, 11] This is often in the absence of antigen validation for correct folding or purity. Thus, important disease biomarkers may be masked.[6, 10, 11, 16, 22-26] On the other hand, slide-based arrays can offer the capacity for versatile fabrication and customization for specialized applications.

More recent methods for dissecting broad immune responses include the multiplexing of antigens using the bead-based BioPlex array system.[27-29] Using spectrally unique beads carrying unique antigens, the platform is well-suited for interrogating many antigens simultaneously. [30] Previous bead-based methods have detected malaria patient antibody responses.[31-41.] However, in these earlier studies, malaria antigen panels had limited representation. In addition, standard antigen coupling to beads was preceded by laborious purification of individual antigens from translation lysates, which can limit the complexity of larger antigen panels.

There is a need for antigen arrays that include *Pf* and *Pv* polymorphic antigens, particularly from local infected communities. In the present study, a streamlined bead-based protein array platform is described for the dissection of naturally acquired immunity in malaria patients. Recombinant parasite antigens were selectively adsorbed from translated lysates onto beads modified with an affinity reagent. Such modified beads measured the antibody titers against 23 *Pf* and *Pv* antigens from 10 patient sera. Expansion of these methods will help dissect patient antibody profiles, identify multiple important malarial serological markers, and will help to improve our understanding of differential immunity in malaria patients.

2.2 Materials and Methods

2.2.1 Sample collection with ethics statement

Patient samples were collected as part of a US National Institutes of Health (NIH) sponsored Malaria Evolution in South Asia-International Center of Excellence for Malaria Research (MESA-ICEMR). Plasma samples were collected from symptomatic malaria-positive patients at Goa Medical College (Goa, India). Written informed consent was obtained from all volunteers. A detailed description of the study site, enrollment, and sample processing has been published elsewhere.[42] Naïve human sera from malaria-free individuals were used as negative controls or from individuals who were treated for malaria and who were symptom-free for at least three years while living in non-endemic regions.

2.2.2 Antigen constructs

Malaria antigen genes were designed to carry a 5' XhoI restriction site followed by a start codon (ATG) and a Flag-tag (DYKDDDDK) coding sequence. On the 3' of antigen, a Ctag (GAAEPEA) coding sequence and a stop codon (TGA) were followed by an EagI restriction site. Codons of the antigen constructs were optimized on the GeneArt server to express in a wheat-based protein expression system. Optimized genes were chemically synthesized (GeneArt, Thermo Fisher Scientific, Waltham, MA) and

subcloned into a cell-free vector as earlier described (Mudeppa et al.). Plasmids were purified using Qiagen kits (Qiagen, Germantown, MD), and the resulting DNA products were validated by Sanger sequencing.

2.2.3 In vitro transcription

In vitro transcription of malaria antigens was carried out as previously described.[43, 44] For small-scale batch-method protein expression, 50 µl reactions contained 4 µg of plasmid DNA, transcription buffer (80 mM HEPES-KOH pH 7.8, 16 mM magnesium acetate, two mM spermidine, 25 mM β-mercaptoethanol), ten units of ribonuclease inhibitor (Promega, Madison, WI), 50 units of SP6 RNA polymerase (New England Biolabs (NEB), Ipswich, MA), and three mM each of GTP, ATP, CTP, and UTP. The transcription mixture was incubated at 37°C for 4 hours, followed by purification using Microspin G25 columns (GE Healthcare, Chicago, IL). For scaled-up bilayer method-based translations, a 600 µL transcription mixture contained 45 µg of plasmid DNA, 1.5x transcription buffer, 100 units of ribonuclease inhibitor (Promega), 900 units of SP6 RNA polymerase (NEB), and 4.5 mM each of GTP, ATP, CTP, and UTP. The mixture was incubated at 37°C for 4 hours, followed by centrifugation at 25°C at 10,000 x g for 5 minutes. The mRNA in the supernatant was used for wheat germ cell-free translations.

2.2.4 Cell-free expression of malarial antigens

For the initial verification of expressions, a batch translation method was used for radiolabeling the antigens. The cell-free translation of purified mRNA was carried out using an in-house preparation of wheat germ lysate. (43). A 50 µL translation contained 10 µL mRNA, four units of wheat germ lysate, one µg creatine kinase, 40 units of ribonuclease inhibitor, and protein expression buffer (30 mM HEPES-KOH pH 7.8, 100 mM potassium acetate, 2.7 mM magnesium acetate, five mM DTT, 0.4 mM spermidine, 1.2 mM ATP, 0.25 mM GTP, 16 mM creatine phosphate, 0.3 mM concentration of 19 amino acids ((-)leucine), and 800 nCi 14C leucine (Moravek, Brea, CA)). Translation reactions were placed in a 26 °C incubator for 4 hours, followed by centrifugation at 10,000 x g at 4°C. Soluble fractions were

boiled with Laemmli Sample buffer with 2% β-mercaptoethanol (β-me) and resolved by sodium dodecyl sulfate-polyacrylamide gel electrophoresis (SDS-PAGE). The gels were dried in a gel dryer for two hours and then exposed to a phosphor imager screen (GE Healthcare). The screen was scanned on a GE Typhoon FLA 9000 Gel Imager to visualize the position of radiolabeled proteins. For scaled-up translations, 500 µl of mRNA was mixed with an equal volume of wheat germ extract (to give a final OD of 120 A260 units), 80 µg creatine kinase, 40 units of ribonuclease inhibitor (Promega), and 0.1% TritonX-100. To each well of a six-well flat bottom culture plate, 10 mL of protein expression buffer was added. 1 mL of the translation reaction mixture was injected into the bottom of each well, creating two separate layers. Plates were incubated at 26 °C for 20 hours.

2.2.5 Functionalization of Luminex beads with anti-Ctag antibodies

Carboxylated color-coded magnetic Luminex beads were further functionalized by covalent coupling of the anti-Ctag antibody by following the manufacturer's instructions. Briefly, in a typical coupling reaction, 1x106 beads (Luminex, Austin, TX) were vortexed and sonicated and then kept on the magnetic stand to pipette out the buffer solutions. The beads were resuspended in a 50 µl solution of 0.1 M MES pH 4.5 activation buffer containing 5.5mg per ml each of N-Hydroxysulfosuccinimide (sulfo-NHS, Thermo Fisher Scientific) and carbodiimide (EDC, Thermo Fisher Scientific). After 25 minutes of activation at room temperature in the dark, beads were washed on a magnetic stand twice with 0.1 M MES pH 5.0. Next, in a series of 100 µl reactions, one million activated beads were mixed with 0.1 M MES pH 5.0 buffer containing 0 to 75 µg per ml of biotinylated anti-Ctag antibody (ThermoFisher Scientific) and incubated in the dark at room temperature for two hours with end-to-end rotation. Anti-Ctag antibody functionalized beads (AFBs) were washed three times with storage buffer PBS-TBN (PBS, 0.1% BSA, 0.02% Tween20, 0.05% sodium azide) and stored in the same buffer at 4° C. The AFBs were counted using a hemocytometer. Covalent attachment of anti-Ctag antibody to beads was confirmed using streptavidin-conjugated R-phycoerythrin (SAPE, Thermo Fisher Scientific) on BioPlex 200 system (Luminex). In a 96-well plate, triplicates of 2000 counts of beads (from each concentration of AFBs per

well) were added. Unless mentioned, all binding assays in this report were carried in 100 µl of buffer solutions. The AFBs were separated from the storage buffer by placing the plate on a handheld magnetic washer (Luminex) for 90 seconds. Microspheres were washed once with assay buffer (0.1% BSA in PBS), followed by the addition of 100 µl of serially diluted SAPE. The plate was incubated in the dark at room temperature for 30 minutes with orbital shaking at 800 RPM. The unbound SAPE was washed from AFBs once with 100 µl assay buffer. The AFBs were resuspended in 100 µL assay buffer and read on a BioPlex 200.

2.2.6 Adsorption of Ctagged *Pf*MSP1-42 on functionalized beads from wheat germ translated lysates (WGL)

Optimization of malarial antigen adsorption to AFBs was carried out using *Pf*MSP1-translated lysates. The *Pf*MSP1 translated lysate from the bilayer reaction was centrifuged at 20,000 x g for 10 minutes at 4 °C followed by the collection of *Pf*MSP1 in supernatants of translated lysates for further studies. To a series of 15 ml tubes containing 1 million of each concentration of AFBs, 0 to 9 mg (0 to 5 ml of WGL) of supernatant of *Pf*MSP1 WGL were added, and the final volume was adjusted to 7.5 ml with binding buffer (20 mM Tris pH 7.5, 100 mM NaCl, 0.05% TritonX-100). The mixtures were incubated in the dark at room temperature with end-to-end rotation for two hours. The tubes were spun at 4000 x g for 5 min to remove unbound proteins. The beads were washed thrice with binding buffer, followed by transfer to 1.5 ml microcentrifuge tubes. The beads were washed again with storage buffer (Phosphate Buffered Saline pH 7.4, with 0.045% Tween, 0.1% BSA, and 0.05% Azide) on a magnetic stand. The antigen adsorbed AFBs were stored in storage buffer at four °C, and the AFBs count was determined using a hemocytometer.

2.2.7 Validation of adsorbed *Pf*MSP1 on antibody functionalized beads

Adsorbed *Pf*MSP1 on AFBs was validated in a multiplex assay using anti-flag antibodies on the BioPlex 200 system. In a 96-well plate, triplicates of 2000 counts of each set of *Pf*MSP1 adsorbed AFBs were

mixed with 100 ng per ml of anti-flag rabbit antibodies (Abcam, Waltham MA) in assay buffer in triplicates. The plate was incubated in the dark at room temperature for one hour with orbital shaking at 800 RPM, followed by three washes with assay buffer. AFBs were resuspended in 100 µL assay buffer containing 100 ng per ml of PE-conjugated goat F(ab')2 anti-rabbit antibodies (Thermo Fisher Scientific). The plate was incubated for 30 minutes with orbital shaking, followed by three five-minute washes with assay buffer, and fluorescence was quantified on the BioPlex 200 system as described earlier.

Large-scale adsorption of individually translated malarial antigens from WGL on separate bead sets was carried out in a 15 ml reaction volume. To overcome the variations in antigen expression levels in the wheat germ system and differential coating on beads, a saturating volume of optimized antigen-translated lysates was used for adsorption onto functionalized beads. Approximately one million AFBs were mixed with 10 ml of wheat germ lysate (WGL) and an additional five ml of binding buffer. Subsequently, the wheat germ-expressed proteins were subjected to three rounds of washing in a binding buffer. After the washing step, the malaria antigen-adsorbed beads were quantified using a hemocytometer and combined to achieve a consistent concentration of each adsorbed AFB per milliliter of storage buffer. AFBs were visualized using rabbit anti-flag and R phycoerythrin-conjugated goat anti-rabbit antibodies. To validate the pooled antigen-coated beads, an anti-flag rabbit antibody was used at one µg per ml, and binding was extended to four hours.

2.2.8 Patient antibody binding studies in multiplex assay

Patient sera were initially diluted 50-fold in assay buffer. These 50-fold diluted sera were subjected to 5 more dilutions, with 3-fold serial dilutions relative to the previous one. Each malaria antigen-adsorbed and a GFP-adsorbed bead set was dispensed to obtain 2000 beads per type per well. Beads were washed twice with assay buffer (PBS, 0.1% BSA). Each serially diluted serum (100µl) was added to three wells and incubated in the dark for an hour at room temperature. After washing off the unbound sera, 100 µl of goat anti-human IgG-PE (Millipore Sigma, Burlington, MA), at 6 µg/ml, was added to each well and incubated for 30 min as earlier. The microspheres were washed three times in assay buffer, resuspended in

100 µl of assay buffer, and read on the BioPlex 200 system. To calculate half maximal titers, saturating binding curves of patient antibodies to target antigens were generated on Prism 10 (GraphPad, San Diago, CA). By utilizing the equation for one site binding models (Y = Bmax*X/(Kd + X)), half-maximal binding values (Kd) were calculated. Reciprocals of these Kd values are called reciprocals of half-maximal titers (MT50)

2.3. Results

2.3.1 Antigen selection

Toward the identification of a set of malaria serological markers to define submicroscopic infections, activation of hypnozoites, and protective immunity for antibody binding studies in the Indian subcontinent, the following reports were considered. In a MESA-ICEMR initiated *P. falciparum* whole genome sequencing project, clinical isolates from Indian patients were genetically distinct compared to the isolates from the rest of the world. [45] Most of these Indian malaria parasite genomes displayed several polymorphisms in known drug targets, serological markers, and vaccine candidates. In this research, we investigated clinical isolates originating from Goa, India, to evaluate the influence of specific polymorphisms on patient antibody binding to a specific antigen. To accomplish this, we examined mutations present in the *Pf*MSP1 gene from nine clinical isolates sourced from Goa, leading to the construction of six distinct *Pf*MSP1 variants, each characterized by a unique set of mutations (Figure 1). Notably, all identified mutations from these clinical isolates were clustered within the amino acid region spanning from position 1533 to 1692, corresponding to the 42 kDa portion of the C-terminal segment of *Pf*MSP1 (Figure 1A). Furthermore, it is noteworthy that some variants were shared among multiple patients, while others were exclusive to individual patients (Figure 1B). In recent serological studies conducted in India (12, 16), top reactive *P. falciparum* and P. vivax serological markers, distinct from those observed in other regions of the world, were reported. To validate these identified markers, we selected five markers each from *P. falciparum* and P. vivax. In this study, we included a panel of 15 *P. falciparum* and 8 P. vivax antigens, and a negative control (GFP) (Table 1). Of the 15 *P. falciparum*

antigens, eight were derived from truncated constructs of *Pf*MSP1 and its variants, while five were based on the previously reported top reactive *P. falciparum* serological markers identified in India. *Pf*AMA1 and *Pf*Rh5 were selected based on a literature search for globally reported vaccine targets. Within the group of eight P. vivax antigens, two were truncated constructs of *Pv*MSP1s, five were sourced from the top reactive P. vivax markers identified in India, and one was derived from *Pv*AMA1.

2.3.2 Rapid generation of malaria antigen-coated BioPlex beads

To overcome the limitations of the purification of malaria antigens for serological studies, a method was designed for the selective adsorption of malaria antigens onto beads from translated lysates. A commercially available CaptureSelect™ biotinylated anti-Ctag conjugate (anti-Ctag ab), a Camelid single-domain 13 kDa antibody fragment (VHH) was utilized to achieve this possibility. Initially, its versatility was tested by purifying Ctagged *Pf*MSP1 and GFP on resin coupled with this single-domain antibody. After binding *Pf*MSP1 or GFP translated lysates onto the anti-Ctag ab column, a simple wash with buffer solutions and gentle elution with a competing peptide yielded more than 80% pure *Pf*MSP1 antigen (supplemental data; Figure S1B). Such efficient capture of the malaria antigens from wheat-translated lysates with minimum background, higher purification yields, and purity was difficult to obtain using conventional purification resins. The quality of the wheat germ-expressed Ctagged *Pf*MSP1 antigen was further verified by immunizing rabbits to generate antibodies. A rabbit-generated anti-*Pf*MSP1 antibody detected a single band of 190kDa protein from 3D7 *P. falciparum* lysates (supplemental data; Figure S1C), corresponding to the size of full-length *Pf*MSP1. The anti-*Pf*MSP1 rabbit antibody also displayed parasite growth inhibitory activity in cell cultures (supplemental data; Figure S1D). Next, a preliminary study assessed the ability of the anti-Ctag ab coupled to BioPlex beads in efficient adsorption of Ctagged malaria antigen (supplemental data; Figure S2). When a purified *Pf*MSP1 is attached to a bead either chemically (Figure S2A) or adsorbed on an anti-Ctag ab functionalized bead (Figure S2C), or *Pf*MSP1 adsorbed directly from the translated lysates to an anti-Ctag ab functionalized bead (Figure S2D), similar mean fluorescence (MFI) was observed on BioPlex 200. These results suggest the potential

ability of anti-Ctag ab functionalized BioPlex bead to efficiently adsorb Ctagged proteins from translated lysates with minimal interference from background proteins and chemicals. These results prompted us to maximize antigen adsorption and to expand the study of multiple malaria antigens from translated lysates.

A generalized scheme was designed for the wheat germ cell-free expression of malaria antigens and their selective adsorption on anti-Ctag antibody-coated beads. Select antigens were designed to have an N-terminal flag-tag and a C-terminal Ctag. This allowed us to conveniently track binding antigens to beads (Figure 2A). Carboxylated BioPlex beads were functionalized with various quantities of anti-Ctag antibodies using EDC-NHS chemistry. The chemically attached anti-Ctag antibody was quantified using streptavidin-conjugated R-phycoerythrin on the BioPlex200 system. A 50 µg of anti-Ctag ab at 0.5 mg/ml was sufficient for saturating the chemical attachment to one million beads (Figure 2B). Next, anti-Ctag functionalized beads were tested for their capacity to adsorb *Pf*MSP1 antigen. The *Pf*MSP1 adsorbed to anti-Ctag coated beads was monitored by anti-flag antibodies. Maximum adsorption of *Pf*MSP1 was achieved by adding nine mg equivalent of wheat germ lysate per one million anti-Ctag coated beads (Figure 2C).

2.3.3 Parallel Adsorption of malaria antigens on functionalized beads and validation

The quality of the 23 wheat-expressed antigens, along with a negative control, GFP, was ascertained through autoradiography (Figure 3A). All antigens derived from soluble fractions of translated lysates displayed singular bands with expected masses consistent with previously adapted codon optimization strategy for minimizing protein fragmentation.[45] Next, scaled-up cell-free expression of the 23 antigens was carried out individually in a six-well plate using a bilayer reaction method. Subsequently, antigens were directly pulled from the supernatant of translated lysates and adsorbed onto individual anti-Ctag coated beads sets. To mitigate potential disparities in antigen adsorption to beads stemming from variations in expression levels or accessibility to the Ctag moiety on antigens, a twofold excess of wheat germ lysate was used to saturate each bead set coated with anti-Ctag antibodies for two hours. The bead sets featuring adsorbed Ctagged antigens were consolidated, and their occupancy was tracked using anti-

flag antibodies (Figure 3B). An average mean fluorescence intensity (MFI) exceeding 5000, substantially surpassing the background noise level, was indicative of the maximal adsorption of each antigen to their respective beads.

2.3.4 Patient antibody levels to *P. falciparum* and P. vivax antigens

In preliminary serological investigations, it became evident that a single-point sera dilution did not consistently reveal the full spectrum of patient antibody reactivity to all antigens. Consequently, in this study, we employed a more comprehensive approach by utilizing seven-point serial diluted sera to unveil the extent of antibody reactivity in each patient sample against the complete array of antigens. In a multiplex assay, a panel of 23 antigens was systematically tested in triplicates, each time using sera samples at seven different dilutions from each patient. This approach was necessitated by the unique combination of affinities versus protein abundances inherent to each antigen-antibody interaction, which exhibited variability among patients. For instance, the IgG antibodies from patient 8 (P8) exhibited distinct serum dilution preferences for optimal binding to different antigens (Figure 4A). Notably, P8 IgG showed optimal binding to *P. falciparum* antigens 0620400 and 0422100 at dilutions of 0.74 and 2.2 µl/ml (corresponding to 1350 and 450-fold dilutions), respectively. Conversely, these same patient antibodies displayed optimal binding to *P. falciparum* antigens 0935600 and 1002100 at dilutions of 20 and 6.6 µl/ml (50 and 150-fold dilutions), respectively. Interestingly, at higher serum dilutions, some *P. falciparum* antigens (0935600 and 1002100) exhibited antibody levels near background, while lower serum dilutions inhibited the optimal binding of patient antibodies to other antigens (0620400 and 0930300 (19kDa)). Similarly, when serially diluted sera samples were examined against variants of *Pf*MSP1, distinct patient antibody binding preferences were uncovered (Figure 4B). The reciprocals of half-maximal titers (MT50) were calculated from non-linear binding curves of patient IgG to antigens. For instance, antibodies from P8 displayed a preference for the *Pf*MSP1-V1 variant, with an MT50 of 5 µl/ml, surpassing all other variants (MT50: 1.6 to 3.1 µl/ml) including the 3D7 construct (MT50: 2.56 µl/ml). Given that the V1 construct was isolated from P8, and harbored unique mutations compared to

other constructs (Fig 1B), it is plausible that the patient had been primed for the V1 sequences. This hypothesis gains further support from the observed minimal preference of P8 antibodies for constructs V4 and V6, which lacked overlapping V1 mutations. In contrast, such marked differences in MSP1 variant preference were not evident in patients P3 and P4. Patients enrolled in the MESA-ICEMR study (Supplemental Table 1) displayed MT50 values ranging from 0.01 to 10 µl/ml (corresponding to dilutions of 10 to 10,000) for all antigen constructs (Fig 4C). Notably, younger patients P1 (aged 15) and P2 (aged 17) exhibited either minimal or zero levels of antibodies, limited to India-specific markers (0422100, 01315400, and 0620400), while showing no reactivity towards *Pf*MSP1, *Pf*Rh5, or *Pf*AMA1. Among the remaining *P. falciparum*-infected samples (aged 20 and above), only five patients exhibited IgG binding to common *P. falciparum* antigens such as *Pf*MSP1 (0930300) and *Pf*Rh5(0424100). However, IgG from these patients did bind to at least one of the five tested Indian markers. Remarkably, patients originating from Orissa (OR) exhibited IgG reactivity to six (P3) and seven (P8) of the nine tested *P. falciparum* antigens. Similarly, a patient (P4) originating from West Bengal (WB) displayed IgG reactivity to four of the nine tested antigens. Despite all ten tested patient samples being confirmed for *P. falciparum* infections through microscopy, rapid diagnostic tests (RDT), and polymerase chain reaction (PCR) (Supplemental Table 1), six patients demonstrated IgG reactivity to P. vivax India-specific markers, indicating prior exposure to P. vivax.

2.4 Discussion

Malaria parasites utilize a complex combination of ligands to invade human red blood cells, eliciting a diverse array of antibody responses targeting both surface antigens and intracellular proteins. The identification of serological markers capable of delineating submicroscopic infections, the activation of hypnozoites, and the characterization of protective immunity is pivotal for the achievement of malaria elimination. Collaborative efforts have been directed toward identifying dominant serological markers for both *Plasmodium falciparum* and *Plasmodium vivax* in malaria transmission regions. However, these efforts have predominantly focused on areas outside the Indian subcontinent. Contrastingly, early

serological investigations conducted in India have unveiled a distinct set of highly seroreactive P. vivax antigens [12, 16]. Furthermore, the implications of antigenic polymorphisms in evading the host immune response remain to be understood.

In this study, we present a simple yet versatile bead-based antigen assay capable of quantifying antibody levels against malaria antigens in regions endemic to both *Pf* and *Pv*, such as India. Our approach combines the sensitivity and specificity inherent to bead-based technology with the robustness of a wheat cell-free antigen expression system. Additionally, we present a novel protocol for functionalizing beads to adsorb antigens from translated lysates. This multiplex approach affords the flexibility to tailor serological markers to the specific requirements of local transmission settings. Importantly, the antigen-adsorbed beads exhibit exceptional stability, with no observable antigen exchange between beads over a 90-day storage period at 4°C, a crucial feature for the storage and shipment of pooled beads. The absence of the antigen purification step enhances the method's scalability, enabling the concurrent analysis of hundreds of antigens.

By employing serially diluted sera instead of the conventional single-point dilution serological tests, we uncovered the absolute levels of patient IgG antibodies directed against all studied antigens. For instance, *Pf*MSP10 (0620400) exhibited the highest antibody levels (MT50: 10 µl/ml) in P8, while the lowest levels (MT50: < 0.02 µl/ml) were observed in P4. Similarly, *Pf*MSP1 (0930300) displayed a 2- to 10-fold variation in binding to patient antibodies compared to its variants. Notably, six out of the ten *P. falciparum*-infected samples exhibited low antibody titers against P. vivax antigens, especially those corresponding to India-dominant markers, indicating prior exposure to P. vivax.

In summary, the presented multiplexed serological method holds the potential to uncover the true level of antibody responses against numerous antigens from different human malaria parasites. Generated Serological data combined with clinical information from patients promises to be instrumental in the identification of serological markers capable of detecting submicroscopic infections and defining the parameters of protective immunity against malaria.

Chapter 2 Figures and Tables

	Sl. No.	Antigen ID	Common name	ORF fragment, (AAs)	MW, (kDa)
P. falciparum antigens	1	-	Green fluorescent protein (GFP)	1-238 (238)	26.9
	2	PF3D7_0930300	Merozoite surface protein1 (MSP1-19)	1612-1720(108)	12.1
	3	PF3D7_0930300	Merozoite surface protein1 (MSP1-42)	1361-1720 (360)	41.5
	4	PF3D7_0930300	MSP1-42 V1	1361-1720 (360)	41.4
	5	PF3D7_0930300	MSP1-42 V2	1361-1720 (360)	41.6
	6	PF3D7_0930300	MSP1-42 V3	1361-1720 (360)	41.4
	7	PF3D7_0930300	MSP1-42 V4	1361-1720 (360)	41.4
	8	PF3D7_0930300	MSP1-42 V5	1361-1720 (360)	41.4
	9	PF3D7_0930300	MSP1-42 V6	1361-1720 (360)	41.3
	10	PF3D7_1133400	Apical membrane antigen 1 (AMA1)	22-544 (523)	60.5
	11	PF3D7_0424100	Reticulocyte binding protein homologue 5	1-526 (526)	63.0
South Asia *P. falciparum* top reactive serological markers [12]	12	PF3D7_0422100	Transmembrane emp24 domain-containing protein	1-385 (385)	45.0
	13	PF3D7_1002100	EMP1-trafficking protein	1-631 (631)	69.7
	14	PF3D7_0315400	Conserved protein, unknown function	1-256 (256)	30.5
	15	PF3D7_0620400	Merozoite surface protein10	1-525 (525)	61.2
	16	PF3D7_0935600	Gametocytogenesis-implicated protein	1-512(512)	58.2
P. vivax antigens	17	PVX_099980	MSP1-19	1,622–1,729 (108)	11.8
	18	PVX_099980	MSP1-42	1325-1729 (428)	42.0
	19	PVX_092275	Apical membrane antigen 1 (AMA1)	43-487 (444)	50.1
South Asia *P. vivax* top reactive serological markers [12]	20	PVX_081830	Exported protein, unknown function	1-494 (496)	56.7
	21	PVX_116780	Protein transport protein SFT2, putative	1-268 (269)	29.0
	22	PVX_083560	Exported protein, unknown function	1-310 (311)	34.0
	23	PVX_121930	Exported protein, unknown function	1-289 (290)	32.4
	24	PVX_118705	Hypothetical protein, conserved	1-438 (439)	50.7

Table 2.1: Description of selected malarial antigens.

C

Variant	Patient Isolate	Amino acid positions												
		1533	1558	1559	1598	1599	1601	1602	1604	1620	1667	1676	1677	1692
3D7	---	D	P	Y	I	E	K	F	D	E	T	S	R	L
V1	P7 / P8	D	P	Y	**L**	**D**	**N**	**L**	**G**	**Q**	**K**	**N**	**G**	L
V2	P9 / P5 / P1 / P3	D	**H**	**N**	I	E	K	F	D	**Q**	**K**	**N**	**G**	**F**
V3	P9 / P5 / P1 / P3	D	**H**	**D**	I	E	K	F	D	**Q**	**K**	**N**	**G**	**F**
V4	P4	**N**	**T**	**N**	I	E	K	F	D	E	T	S	R	L
V5	P7	N	**H**	**N**	I	E	K	F	D	**Q**	**K**	**N**	**G**	L
V6	P2	**N**	**H**	**N**	I	E	K	F	D	E	T	S	R	L

Figure 2.1. *Pf*MSP1-42 (*PF*3D7_0930300) polymorphisms in Goan clinical isolates. (A) Schematic representation of full-length *Pf*MSP1 and (B) its C-terminal portion (*Pf* MSP1-42). The numbers on the schematics indicate the amino acid positions. The black bars on *Pf*MSP1-42 indicate the position of mutations. (C) Amino acid changes in 3D7 *Pf*MSP1-42 variants by position. The highlighted amino acids differ from the 3D7 sequences.

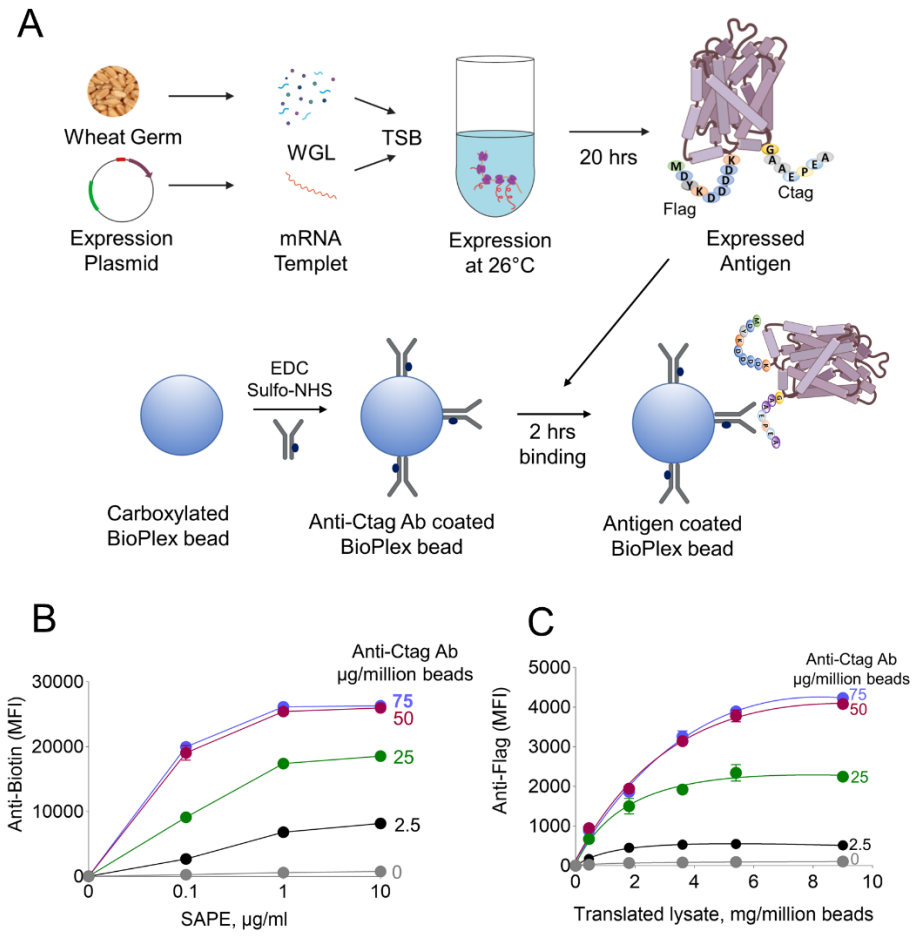

Figure 2.2. Overview of a methodology for a rapid generation of antigen-coated beads. (A) Illustration depicting the process of malaria antigen expression in wheat germ cell-free expression system and the selective adsorption onto functionalized beads. (B) Saturation curves showing the mean fluorescence intensities (MFI) of biotinylated anti-Ctag antibody chemically attached to BioPlex beads employing streptavidin-phycoerythrin antibody conjugate (SAPE) for detection and quantification. (C) Titration for optimal adsorption of a *Pf*MSP1 (*PF*3D7_0930300) onto functionalized BioPlex beads utilizing anti-Flag antibodies.

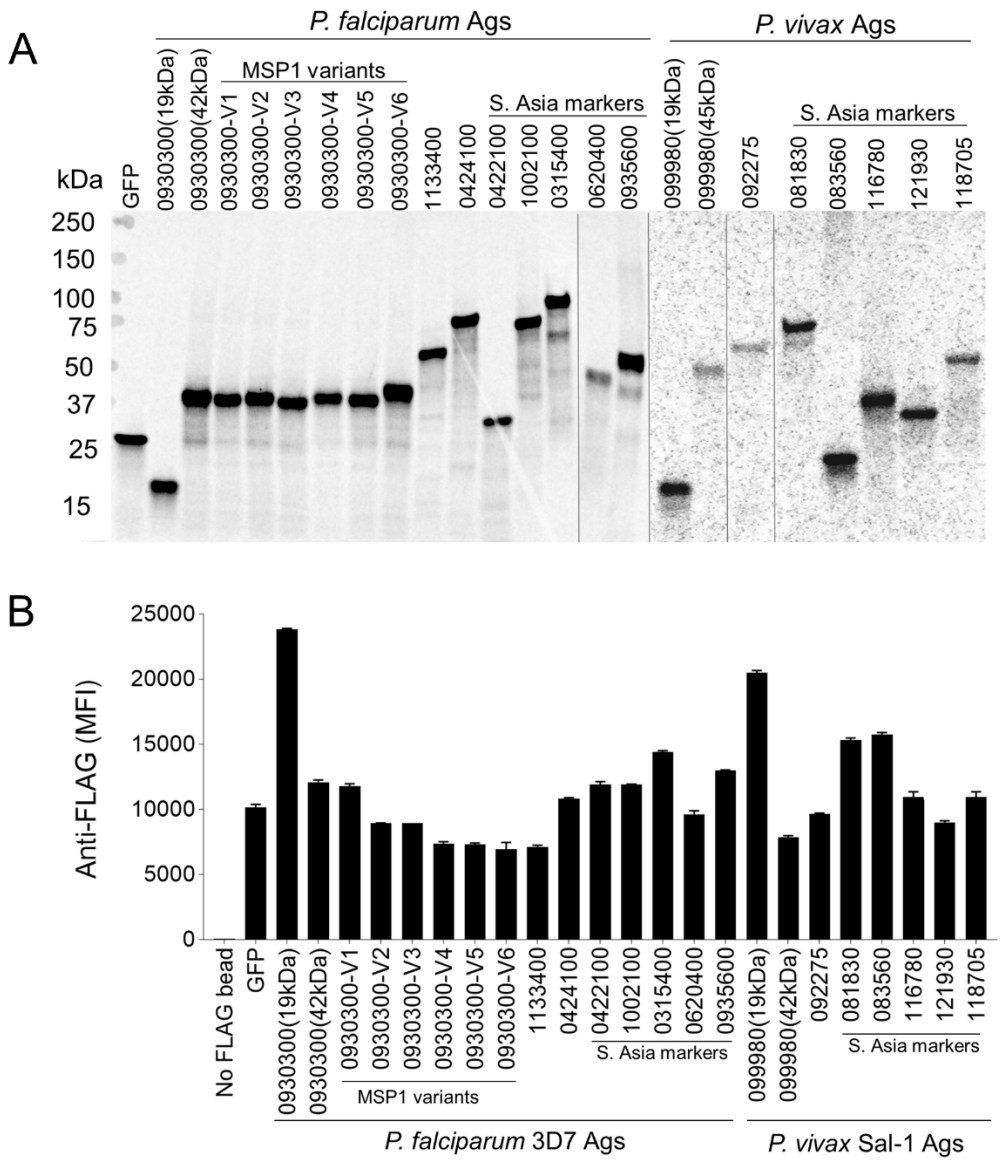

Figure 2.3. Validation of malaria antigen expression and adsorption onto functionalized beads. (A) An autoradiogram verifies the quality of malaria antigens expressed in the wheat cell-free system. (B) Confirmation of malaria antigen adsorption onto beads using anti-flag antibodies.

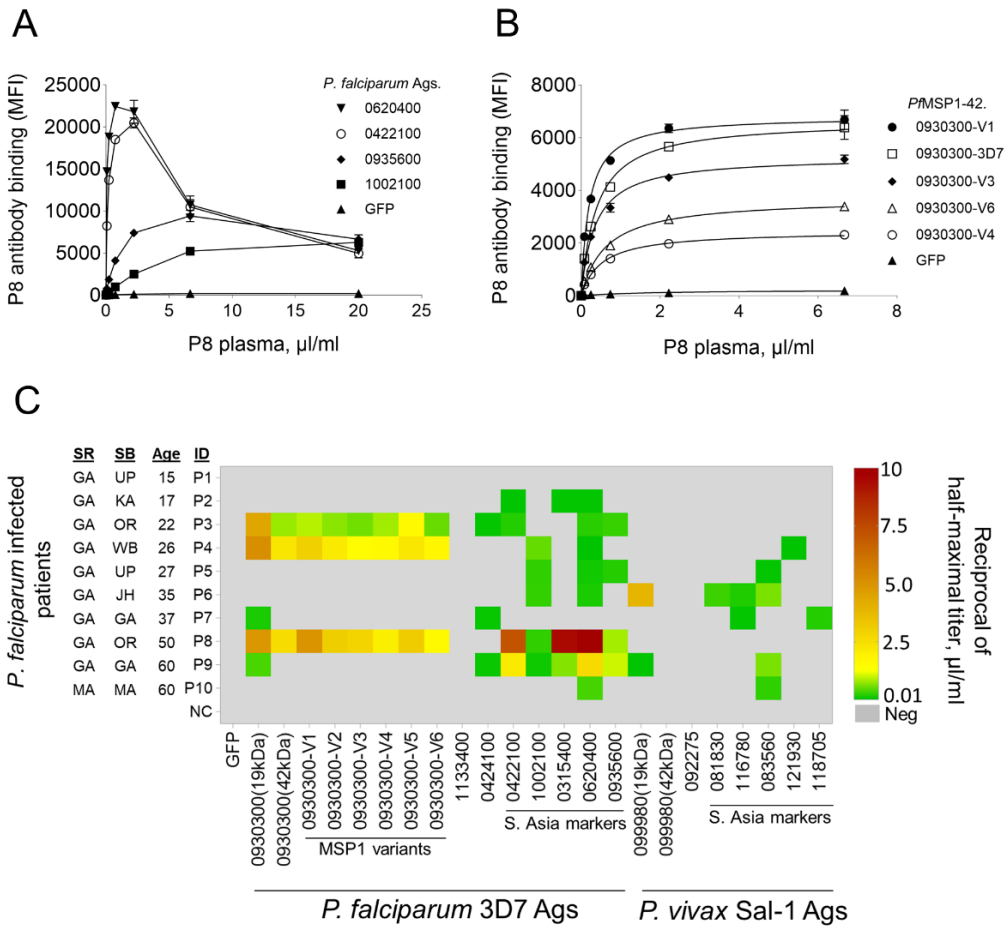

Figure 2.4. The magnitude of patient IgG responses to malaria antigens. (A) Assessment of IgG antibody levels against *P. falciparum* and P. vivax antigens by testing serially diluted patient serum. (B) Representative binding curves generated for the calculation of reciprocals of Half-Maximal titers. (C) Seroreactivity profiles for *P. falciparum* and P. vivax antigens. Patient samples are organized in ascending order of age, with migration status determined by their State of Birth (SB) and State of Residence (SR). GA-Goa; UP-Utter Pradesh; KA-Karnataka; OR-Orissa; WB-West Bengal; JH- Jharkhand; MA-Maharashtra.

2.5 Supplemental Methods and Data:

2.5.1 Degree of anti-c-tag antibody coating onto beads

CaptureSelect anti c-tag antibodies purchased from Thermofisher scientific are conjugated with biotin. To test the degree of coating, activated beads were modified with various concentrations of anti c-tag antibody to determine the optimal antibody concentration needed to coat 200,000 beads for maximum signal. The biotinylated anti-c-tag antibodies coated on the beads were detected using streptavidin-phycoerythrin conjugate (SAPE). The mean fluorescence intensity (MFI) curves of bead sets modified with various concentrations of anti c-tag antibody are shown in S1. Using bead sets modified with no anti c-tag antibody, MFI signals remain at background levels. As bead-coated antibody concentration increases, there is an observed signal increase. Our preliminary results determined the optimal anti c-tag antibody concentration to be 20 μg/200k beads. Increased concentrations gave similar or reduced signals suggesting beads saturation. To verify saturation, we generated a standard curve (figure S2a) to calculate the degree of anti c-tag coating using spectrophotometry to measure biotinylation on the coated bead sets. The fluorescence of the biotinylated anti c-tag was measured prior to coupling which was used to generate the standard curve. We also measured the fluorescence post-coupling to determine how much antibody was bound to the beads. Finally, we generated a saturation curve for the degree of coating (figure S3). From our data, we confirm that the beads are fully coated at a concentration of 20mg/200k beads, increasing the anti c-tag concentration saturates the bead surface hampering the binding efficiency.

2.5.2 Capturing of MSP1 antigens onto beads and multiplex analysis:

Preliminary attempts to determine the optimal concentration of WGL required for bead saturation were conducted. Here, we quantify the binding of various concentrations of anti-c-tag coated beads to the dual-tagged MSP1 antigen affinity captured directly from the WGL. Figure 3 shows the MFI curves of bead sets modified with various anti-c-tag antibody concentrations. Using uncoated bead sets, MSP1 MFI signals remain at background levels at all tested protein concentrations. As anti-c-tag antibody concentration increases there is an observed increase in MSP1 signals. At high concentrations of anti-c-

tag antibody (20-80 μg), there was no significant increase in signal as MSP1 concentration increased. Also, the graph approaches saturation as the concentration of WGL increases from 600-1000 μL. This antigen-antibody binding interaction shows a clear correlation between the concentration of anti-c-tag antibodies and antigen capture from the wheat germ lysate. Future optimization experiments include incubation time tests and coated beads stability assay. Traditional coupling methods require a protein purification step must before capture. Due to the difficulty in purifying malaria surface proteins, the Rathod lab recently developed a method to override the protein purification process by direct capturing c-tagged antigens from the wheat germ lysate using antibody-coated beads. Multiple papers have shown that c-tagged antigens could be isolated in high purity using capture columns coated with camelid antibodies that recognize the c-tag. Here, we utilize the antibody-capturing ability on the multiplexing bead surfaces. This allows for a single step of protein capture from lysates, onto the modified beads. After this capture step, antigens bound to the modified beads can bind to anti-flag antibodies forming a bead-antigen-antibody complex that can be analyzed for multiplex binding studies (figure S4).

2.5.3 Stability and drift of adsorbed antigens on Anti-Ctag functionalized beads (AFBs):

A stability assay was conducted to assess the longevity of antigens adsorbed onto the anti-Ctag conjugated beads and the chance of drifting the antigens between beads. In these studies, all 25 sets of AFBs adsorbed with no flag tag antigen (negative control), GFP (positive control), and our proteins of interest were mixed and multiplexed against anti-flag antibodies (Figure S5). The observed fluorescence was recorded as day 1 MFIs. Mixed beads were stored in the dark at 4°C for 6 months. The multiplexing experiment was repeated on day 180 to record any change in MFI.

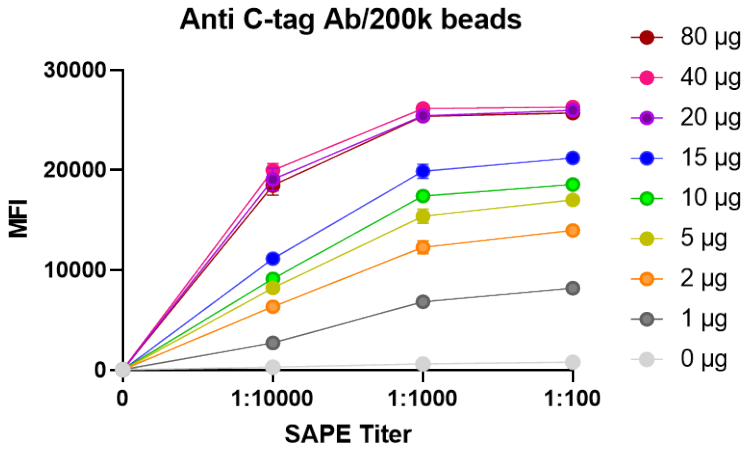

Figure S1: Streptavidin-Phycoerythrin (SAPE) titration of anti-c-tag antibody coated on 200,000 beads. Different bead regions were coated with various antibody concentrations ranging from 0 µg to 80 µg. Maximum signal detected at 20 µg/200k beads.

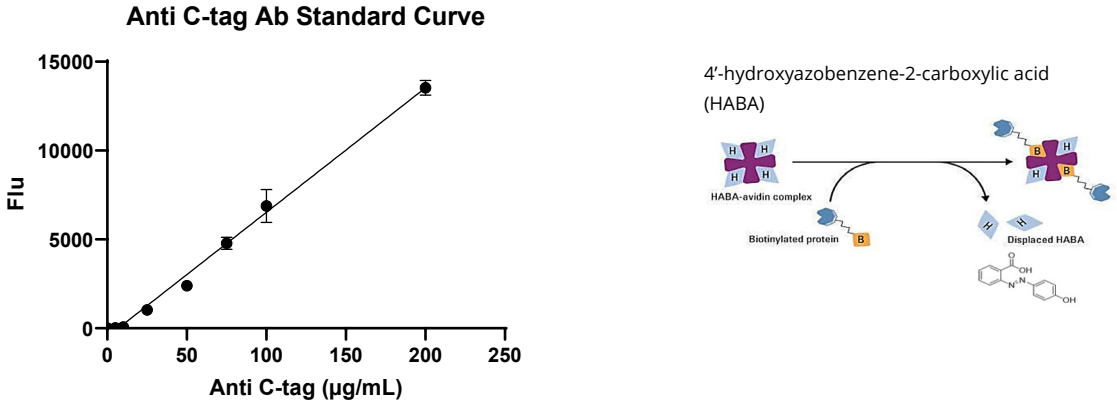

Figure S2a: Anti C-tag standard curve. A reporter agent containing fluorescent avidin and 4'-hydroxyazobenzene-2-carboxylic acid (HABA) was used for quantification. Avidin fluoresces at 520 nm when the weakly interacting HABA is displaced by biotin, measured by a plate reader.

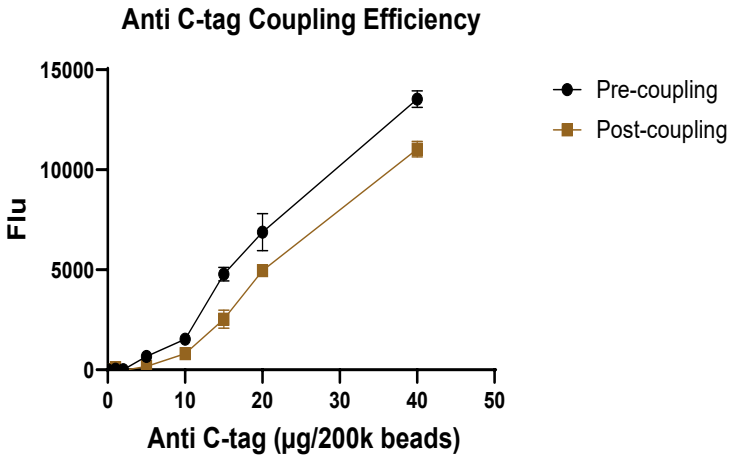

Figure S2b: Anti c-tag coupling efficiency. The Fluorescence of biotinylated anti c-tag was measured before and after coupling.

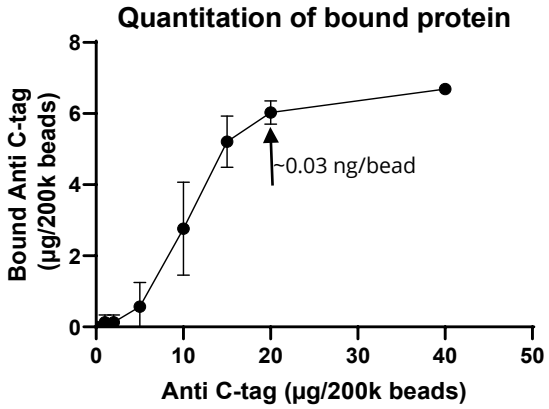

Figure S3: Degree of coating. Using the equation derived from the standard curve, the concentration of bound protein was calculated in nanograms. Based on the data, 20 µg is considered the optimal coating concentration per 200k beads.

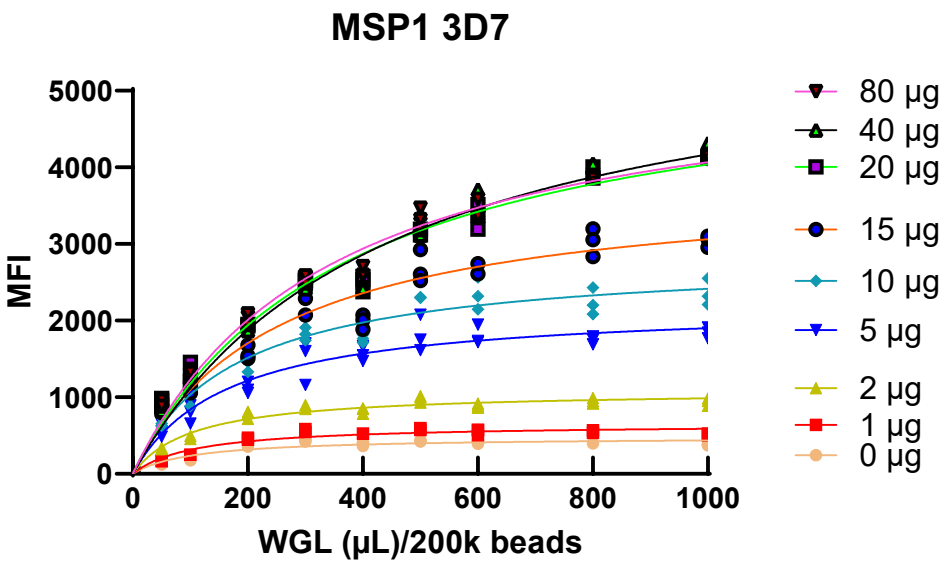

Figure S4: 0-80 µg of anti-c-tag antibody bound to MSP1 in WGL. 200,000 beads were coated with anti-c-tag antibodies at varying concentrations and pooled into a single tube. 10 concentrations of WGL MSP1 antigens were incubated with bead mix and pipetted into wells of a 96-well plate in triplicates. Each bead region was analyzed by the BioPlex instrument and mean fluorescence intensities (MFI) were plotted against WGL concentrations.

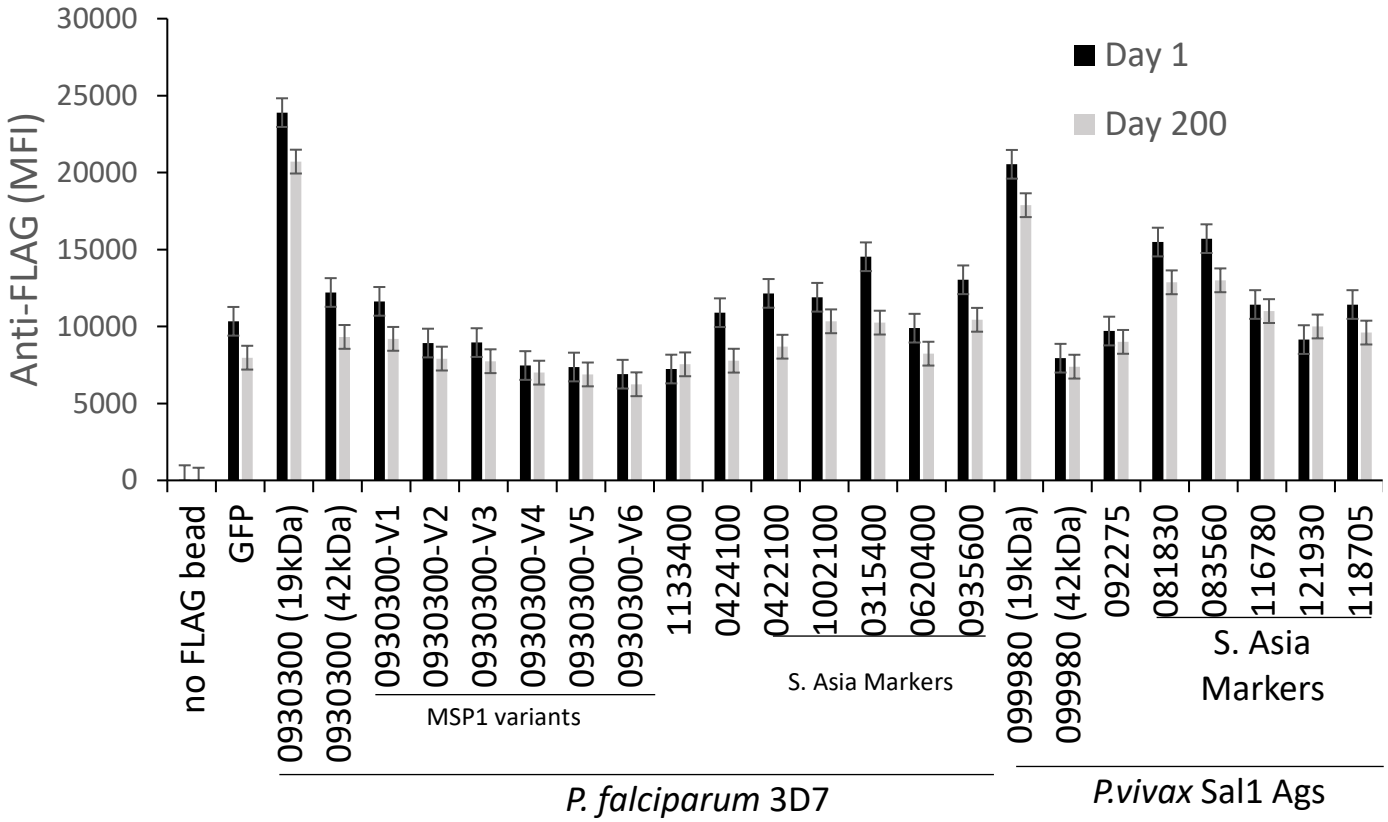

Figure S5: Stability and drift of antigens-adsorbed beads. No significant change in MFI over 6 months when probed with anti-FLAG antibodies indicates that the antigens are intact and stable on the beads. Similarly, no significant decrease in fluorescence over 6 months suggest that there is no exchange of adsorbed antigens between the beads sets.

2.6 References

1. Organization, W. H. 2018 World Malaria Report,
2. Hemingway, J., Shretta, R., Wells, T. N., Bell, D., Djimde, A. A., Achee, N., andQi, G. (2016) Tools and Strategies for Malaria Control and Elimination: What Do We Need to Achieve a Grand Convergence in Malaria? PLoS Biol **14**, e1002380 10.1371/journal.pbio.1002380
3. Tse, E. G., Korsik, M., andTodd, M. H. (2019) The past, present and future of anti-malarial medicines Malar J **18**, 93 10.1186/s12936-019-2724-z
4. Doolan, D. L., Dobano, C., andBaird, J. K. (2009) Acquired immunity to malaria Clin Microbiol Rev **22**, 13-36, Table of Contents 10.1128/CMR.00025-08
5. Cohen, S., Mc, G. I., andCarrington, S. (1961) Gamma-globulin and acquired immunity to human malaria Nature **192**, 733-737 10.1038/192733a0
6. Crompton, P. D., Kayala, M. A., Traore, B., Kayentao, K., Ongoiba, A., Weiss, G. E. *et al.* (2010) A prospective analysis of the Ab response to *Plasmodium falciparum* before and after a malaria season by protein microarray Proc Natl Acad Sci U S A **107**, 6958-6963 10.1073/pnas.1001323107
7. Emili A. Q., C., G. (2000) Large-scale functional analysis using peptide or protein arrays Nat Biotechnol **18**, 393-397,
8. MacBeath, G., andSchreiber, S. L. (2000) Printing proteins as microarrays for high-throughput function determination Science **289**, 1760-1763 10.1126/science.289.5485.1760
9. Haab, B. B., Dunham, M. J., andBrown, P. O. (2001) Protein microarrays for highly parallel detection and quantitation of specific proteins and antibodies in complex solutions Genome Biol **2**, 10.1186/gb-2001-2-2-research0004
10. Davies, D. H., Wyatt, L. S., Newman, F. K., Earl, P. L., Chun, S., Hernandez, J. E. *et al.* (2008) Antibody profiling by proteome microarray reveals the immunogenicity of the attenuated smallpox vaccine modified vaccinia virus ankara is comparable to that of Dryvax J Virol **82**, 652-663 10.1128/JVI.01706-07
11. Doolan, D. L., Mu, Y., Unal, B., Sundaresh, S., Hirst, S., Valdez, C. *et al.* (2008) Profiling humoral immune responses to *P. falciparum* infection with protein microarrays Proteomics **8**, 4680-4694 10.1002/pmic.200800194
12. Venkatesh, A., Jain, A., Davies, H., Periera, L., Maki, J. N., Gomes, E. *et al.* (2019) Hospital-derived antibody profiles of malaria patients in Southwest India Malar J **18**, 138 10.1186/s12936-019-2771-5
13. Stillman, B. A., andTonkinson, J. L. (2000) FAST slides: a novel surface for microarrays Biotechniques **29**, 630-635 10.2144/00293*Pf*01
14. King, C. L., Davies, D. H., Felgner, P., Baum, E., Jain, A., Randall, A. *et al.* (2015) Biosignatures of Exposure/Transmission and Immunity Am J Trop Med Hyg **93**, 16-27 10.4269/ajtmh.15-0037
15. Arevalo-Herrera, M., Lopez-Perez, M., Dotsey, E., Jain, A., Rubiano, K., Felgner, P. L. *et al.* (2016) Antibody Profiling in Naive and Semi-immune Individuals Experimentally Challenged with *Plasmodium vivax* Sporozoites PLoS Negl Trop Dis **10**, e0004563 10.1371/journal.pntd.0004563
16. Uplekar, S., Rao, P. N., Ramanathapuram, L., Awasthi, V., Verma, K., Sutton, P. *et al.* (2017) Characterizing Antibody Responses to *Plasmodium vivax* and *Plasmodium falciparum* Antigens in India Using Genome-Scale Protein Microarrays PLoS Negl Trop Dis **11**, e0005323 10.1371/journal.pntd.0005323

17. Chen, J. H., Chen, S. B., Wang, Y., Ju, C., Zhang, T., Xu, B. *et al.* (2015) An immunomics approach for the analysis of natural antibody responses to *Plasmodium vivax* infection Mol Biosyst **11**, 2354-2363 10.1039/c5mb00330j
18. Felgner, P. L., Roestenberg, M., Liang, L., Hung, C., Jain, A., Pablo, J. *et al.* (2013) Pre-erythrocytic antibody profiles induced by controlled human malaria infections in healthy volunteers under chloroquine prophylaxis Sci Rep **3**, 3549 10.1038/srep03549
19. Baum, E., Sattabongkot, J., Sirichaisinthop, J., Kiattibutr, K., Davies, D. H., Jain, A. *et al.* (2015) Submicroscopic and asymptomatic *Plasmodium falciparum* and *Plasmodium vivax* infections are common in western Thailand - molecular and serological evidence Malar J **14**, 95 10.1186/s12936-015-0611-9
20. Stone, W. J. R., Campo, J. J., Ouedraogo, A. L., Meerstein-Kessel, L., Morlais, I., Da, D. *et al.* (2018) Unravelling the immune signature of *Plasmodium falciparum* transmission-reducing immunity Nat Commun **9**, 558 10.1038/s41467-017-02646-2
21. Liu, E. W., Skinner, J., Tran, T. M., Kumar, K., Narum, D. L., Jain, A. *et al.* (2018) Protein-Specific Features Associated with Variability in Human Antibody Responses to *Plasmodium falciparum* Malaria Antigens Am J Trop Med Hyg **98**, 57-66 10.4269/ajtmh.17-0437
22. Vigil, A., Davies, D. H., andFelgner, P. L. (2010) Defining the humoral immune response to infectious agents using high-density protein microarrays Future Microbiol **5**, 241-251 10.2217/fmb.09.127
23. Baum, E., Badu, K., Molina, D. M., Liang, X., Felgner, P. L., andYan, G. (2013) Protein microarray analysis of antibody responses to *Plasmodium falciparum* in western Kenyan highland sites with differing transmission levels PLoS One **8**, e82246 10.1371/journal.pone.0082246
24. Venkatesh, A., Jain, A., Davies, H., Periera, L., Maki, J. N., Gomes, E. *et al.* (2019) Hospital-derived antibody profiles of malaria patients in Southwest India Malar J **18**, 138 10.1186/s12936-019-2771-5
25. Kamuyu, G., Tuju, J., Kimathi, R., Mwai, K., Mburu, J., Kibinge, N. *et al.* (2018) KILchip v1.0: A Novel *Plasmodium falciparum* Merozoite Protein Microarray to Facilitate Malaria Vaccine Candidate Prioritization Front Immunol **9**, 2866 10.3389/fimmu.2018.02866
26. Oulton, T., Obiero, J., Rodriguez, I., Ssewanyana, I., Dabbs, R. A., Bachman, C. M. *et al.* (2022) *Plasmodium falciparum* serology: A comparison of two protein production methods for analysis of antibody responses by protein microarray PLoS One **17**, e0273106 10.1371/journal.pone.0273106
27. M.R. Wilson, J. S. W. (1988) A new microsphere immunofluorescence assay using flow cytometry J Immunol Methods **107**, 225-230,
28. T.M. McHugh, e. a. (1988) Simultaneous detection of antibodies to cytomegalvirus and herpes simplex virus using flow cytometry and a microsphere based fluorescence assay using flow cytometry J Clin Microbiol **26**, 1957-1961,
29. Fulwyler, M. J., andMcHugh, T. M. (1990) Flow microsphere immunoassay for the quantitative and simultaneous detection of multiple soluble analytes Methods Cell Biol **33**, 613-629, https://www.ncbi.nlm.nih.gov/pubmed/2084487
30. Graham, H., Chandler, D. J., andDunbar, S. A. (2019) The genesis and evolution of bead-based multiplexing Methods **158**, 2-11 10.1016/j.ymeth.2019.01.007

31. Fouda, G. G., Leke, R. F., Long, C., Druilhe, P., Zhou, A., Taylor, D. W., andJohnson, A. H. (2006) Multiplex assay for simultaneous measurement of antibodies to multiple *Plasmodium falciparum* antigens Clin Vaccine Immunol **13**, 1307-1313 10.1128/CVI.00183-06
32. Fernandez-Becerra, C., Sanz, S., Brucet, M., Stanisic, D. I., Alves, F. P., Camargo, E. P. *et al.* (2010) Naturally-acquired humoral immune responses against the N- and C-termini of the *Plasmodium vivax* MSP1 protein in endemic regions of Brazil and Papua New Guinea using a multiplex assay Malar J **9**, 29 10.1186/1475-2875-9-29
33. Dodoo, D., Atuguba, F., Bosomprah, S., Ansah, N. A., Ansah, P., Lamptey, H. *et al.* (2011) Antibody levels to multiple malaria vaccine candidate antigens in relation to clinical malaria episodes in children in the Kasena-Nankana district of Northern Ghana Malar J **10**, 108 10.1186/1475-2875-10-108
34. Fonseca, A. M., Quinto, L., Jimenez, A., Gonzalez, R., Bardaji, A., Maculuve, S. *et al.* (2017) Multiplexing detection of IgG against *Plasmodium falciparum* pregnancy-specific antigens PLoS One **12**, e0181150 10.1371/journal.pone.0181150
35. Priest, J. W., Plucinski, M. M., Huber, C. S., Rogier, E., Mao, B., Gregory, C. J. *et al.* (2018) Specificity of the IgG antibody response to *Plasmodium falciparum*, *Plasmodium vivax*, Plasmodium malariae, and Plasmodium ovale MSP119 subunit proteins in multiplexed serologic assays Malar J **17**, 417 10.1186/s12936-018-2566-0
36. Assefa, A., Ali Ahmed, A., Deressa, W., Sime, H., Mohammed, H., Kebede, A. *et al.* (2019) Multiplex serology demonstrate cumulative prevalence and spatial distribution of malaria in Ethiopia Malar J **18**, 246 10.1186/s12936-019-2874-z
37. Yman, V., White, M. T., Asghar, M., Sundling, C., Sonden, K., Draper, S. J. *et al.* (2019) Antibody responses to merozoite antigens after natural *Plasmodium falciparum* infection: kinetics and longevity in absence of re-exposure BMC Med **17**, 22 10.1186/s12916-019-1255-3
38. Ondigo, B. N., Park, G. S., Gose, S. O., Ho, B. M., Ochola, L. A., Ayodo, G. O. *et al.* (2012) Standardization and validation of a cytometric bead assay to assess antibodies to multiple *Plasmodium falciparum* recombinant antigens Malar J **11**, 427 10.1186/1475-2875-11-427
39. Priest, J. W., Plucinski, M. M., Huber, C. S., Rogier, E., Mao, B., Gregory, C. J. *et al.* (2018) Specificity of the IgG antibody response to *Plasmodium falciparum*, *Plasmodium vivax*, Plasmodium malariae, and Plasmodium ovale MSP119 subunit proteins in multiplexed serologic assays Malar J **17**, 417 10.1186/s12936-018-2566-0
40. Assefa, A., Ahmed, A. A., Deressa, W., Sime, H., Mohammed, H., Kebede, A. *et al.* (2019) Multiplex serology demonstrate cumulative prevalence and spatial distribution of malaria in Ethiopia Malar J **18**, ARTN 24610.1186/s12936-019-2874-z
41. Rogier, E., van den Hoogen, L., Herman, C., Gurrala, K., Joseph, V., Stresman, G. *et al.* (2019) High-throughput malaria serosurveillance using a one-step multiplex bead assay Malar J **18**, 402 10.1186/s12936-019-3027-0
42. Chery, L., Maki, J. N., Mascarenhas, A., Walke, J. T., Gawas, P., Almeida, A. *et al.* (2016) Demographic and clinical profiles of *Plasmodium falciparum* and *Plasmodium vivax* patients at a tertiary care centre in southwestern India Malar J **15**, 569 10.1186/s12936-016-1619-5
43. Mudeppa, D. G., Rathod, P. K. (2013) Expression of functional *Plasmodium falciparum* enzymes using a wheat germ cell-free system Eukaryot Cell **12**, 1653-1663 10.1128/EC.00222-13

44. Sawasaki, T., Morishita, R., Gouda, M. D., andEndo, Y. (2007) Methods for high-throughput materialization of genetic information based on wheat germ cell-free expression system Methods Mol Biol **375**, 95-106 10.1007/978-1-59745-388-2_5
45. Mudeppa, D. G., andRathod, P. K. (2013) Expression of functional *Plasmodium falciparum* enzymes using a wheat germ cell-free system Eukaryot Cell **12**, 1653-1663 10.1128/EC.00222-13

Chapter 3 | Uncovering the Protective Potential of Patient Sera

3.1 Introduction

Building on the promising findings from our pilot studies (Chapter 2), this chapter aims to explore the protective potential of infected patients' sera against malaria blood-stage parasites. While several human monoclonal antibodies have been extensively characterized and shown to effectively block parasite invasion and replication, relatively few studies have examined the functional protective capacity of antibodies present in patient sera. Understanding whether naturally acquired antibodies can mediate parasite inhibition is critical for both vaccine development and the identification of correlates of immunity.

Here, we designed a comparative growth and invasion inhibition assay framework incorporating three categories of interventions: (i) novel small-molecule inhibitor (Tartrolon E) and clinically validated drug compounds, including DSM265, and artemisinin; (ii) well-characterized monoclonal antibodies targeting erythrocytic-stage antigens such as MSP1, AMA1, and EBA175; and (iii) sera from malaria-exposed patients. This experimental approach enables a direct comparison of inhibition profiles, allowing us to assess whether patient sera exhibit protective capabilities comparable to or distinct from established small-molecule and monoclonal antibody interventions. Through this strategy, we seek to advance understanding of the mechanisms underlying immune-mediated control of malaria parasites and to inform future efforts in antigen prioritization and therapeutic development.

Growth and Invasion Inhibition Assays in Malaria Research

The erythrocytic stage of *Plasmodium falciparum* is central to malaria pathogenesis and disease manifestation, making it the primary target of most therapeutic and immunological interventions. During this stage, merozoites invade host erythrocytes, undergo asexual replication, and release daughter parasites that perpetuate infection.[1] Consequently, in vitro assays that quantify parasite growth and invasion have become indispensable for studying antimalarial drug efficacy, host-parasite interactions,

and immune responses. Two widely used assay platforms are growth inhibition assays (GIAs) and invasion inhibition assays (IIAs).[2]

Growth inhibition assays (GIAs): GIAs measure the ability of compounds, antibodies, or sera to suppress parasite replication over one or more erythrocytic cycles. The typical readouts include half-maximal inhibitory concentrations (IC_{50}), IC_{90} values, or percent inhibition relative to untreated controls.[1,2] These assays provide insights into drug potency, stage specificity, and resistance phenotypes. Traditional GIA methods rely on microscopy of Giemsa-stained blood smears or incorporation of [^{3}H]-hypoxanthine into parasite DNA. More recently, higher-throughput platforms employ parasite lactate dehydrogenase (pLDH) assays, DNA-binding dyes such as SYBR Green I coupled with flow cytometry or plate readers, and bioluminescence-based transgenic parasite lines.[3] The versatility of GIAs has enabled their use in evaluating a wide array of small-molecule inhibitors, monoclonal antibodies, and sera from malaria-exposed individuals.

Invasion inhibition assays (IIAs): While GIAs measure overall parasite growth and replication, IIAs specifically quantify the ability of interventions to block merozoite entry into erythrocytes. These assays are generally performed using synchronized parasite cultures enriched at the schizont stage, which release merozoites that attempt to invade fresh erythrocytes. Invasion-blocking activity is quantified by measuring the proportion of newly invaded ring-stage parasites in the presence of inhibitors, relative to untreated controls. IIAs provide mechanistic insights into receptor-ligand interactions, reveal stage-specific vulnerabilities, and are particularly suited to testing monoclonal antibodies targeting merozoite surface antigens such as MSP1, AMA1, and EBA175.[4,5] Fluorescent labeling of merozoites or erythrocytes, combined with flow cytometry, has significantly enhanced throughput and precision in these assays compared to earlier microscopy-based approaches.[6]

Together, GIAs and IIAs provide a comprehensive framework for assessing interventions targeting the erythrocytic stages. GIAs are optimal for evaluating compounds or sera with broad activity across multiple cycles, while IIAs are indispensable for dissecting specific invasion-blocking mechanisms.

Importantly, IIAs can complement GIAs in distinguishing whether reduced parasite replication results from impaired invasion, intraerythrocytic growth inhibition, or both. This distinction is particularly relevant for antibodies or sera, where inhibitory activity may be antigen- and stage-dependent.

Overall, both assay platforms have played pivotal roles in antimalarial drug development and vaccine evaluation. GIAs are used routinely in preclinical and clinical pipelines to benchmark the potency of small-molecule inhibitors such as novel natural products, and artemisinin derivatives. IIAs, in contrast, are widely applied to evaluate vaccine candidates and monoclonal antibodies, as invasion-blocking activity is strongly associated with functional protection in preclinical models. Patient sera from malaria-endemic regions can be tested in both assays to assess naturally acquired immunity (NAI) and to identify antigenic targets that correlate with protective responses. Taken together, GIAs and IIAs provide robust and complementary in vitro tools to interrogate malaria parasite biology, evaluate therapeutic and immunological interventions, and prioritize candidates for translational development. Their continued refinement, including integration with high-throughput readouts and standardized protocols, remains essential for advancing malaria control and eradication efforts.[7]

3D7 Growth-Inhibition Assays with Small Molecules (Tartrolon E, Artemisinin, DSM265)

Historically, small-molecule compounds have been in the forefront malaria prevention, control and treatment strategies. Here, we use growth inhibition assays (GIAs) as the standard in vitro approach for evaluating the efficacy of three highly potent compounds.

Tartrolon E (TrtE): Tartrolon E is a marine-derived polyketide first reported from symbiotic bacteria associated with marine bivalves and, more recently, characterized for antiplasmodial activity. Two independent reports (one from the Rathod Lab) demonstrate exceptionally high potency of TrtE against *Plasmodium falciparum* asexual and sexual stages in vitro: sub-nanomolar IC_{50} values (i.e., nanomolar to sub-nanomolar range) and rapid parasiticidal activity within hours of exposure have been reported, making TrtE among the most potent small molecules described against blood stages.[8,9]

In addition to growth inhibition, TrtE shows activity against early sexual stages, suggesting potential transmission-blocking properties. Preliminary data suggest it disrupts intracellular development and parasite egress, although its precise mechanism of action remains under investigation. Importantly, Tartrolon E maintains activity against ART-resistant parasites, highlighting its potential as a next-generation therapeutic.

Artemisinin (ART) and derivatives: Artemisinins are endoperoxide-containing natural products (and semi-synthetic derivatives) that produce a fast and steep parasite kill in vivo and in vitro.[10] Mechanistically, activation of the endoperoxide bridge is linked to parasite-derived heme (from hemoglobin digestion) and possibly other iron sources. Activated ART forms carbon- and oxygen-centered radicals that alkylate multiple parasite proteins and lipids, producing a promiscuous "multi-target" effect and rapid parasite clearance.[10,11] GIAs typically show very low IC_{50} values for ART and derivatives (example: DHA-dihydroartemisinin) and time-kill assays demonstrate substantial parasite reduction within a single intraerythrocytic cycle.

Clinical and laboratory emergence of ART resistance is phenotypically detected as elevated survival in ring-stage survival assays (RSAs) and as delayed parasite clearance. Mutations in the *kelch13* (K13) propeller domain are the principal molecular markers associated with artemisinin partial resistance; strains harboring K13 mutations can show markedly higher RSA survival rates (for example, early Cambodian isolates showed survival increases from < 2% to > 10-40% in some cases) and slower in vivo clearance times.[12-14] However, Artemisin combination therapies (ACTs) remain the most effective malaria therapy currently in the market.

DSM265 (DHODH inhibitor): DSM265 is a selective inhibitor of *Plasmodium* dihydroorotate dehydrogenase (DHODH), an essential enzyme in the de novo pyrimidine biosynthesis pathway. Preclinical GIAs and parasite enzyme assays revealed potent, parasite-selective inhibition with low-nanomolar IC_{50s} and good selectivity indices against human DHODH, supporting further development as a long-acting antimalarial candidate.[15] In clinical development, DSM265 demonstrated desirable

pharmacokinetics (long half-life) and antimalarial activity in first-in-human studies and controlled human malaria infection (CHMI) trials.[16] In a CHMI prophylaxis study, DSM265 provided protection when given as a single dose prior to sporozoite challenge, and early therapeutic/efficacy studies demonstrated parasite clearance consistent with pharmacodynamic expectations; however, monotherapy was not sufficient for curative treatment of higher-density infections and combination strategies were recommended.[17-19] DSM265 illustrates how GIA data (potency and stage activity) inform dosing strategies and combination partner selection for slow-acting, long-half-life chemotypes.

Comparative GIA observations of TrTE, ART, and DSM265: ART derivatives show rapid killing but short duration, TrtE shows rapid and ultra-potent activity in vitro against multiple stages (suggesting utility as both therapeutic and potential transmission blocker), and DSM265 exhibits slow-acting but long-lasting activity suitable for prophylaxis or partner drug roles. Importantly, the translation from in vitro GIA potency to clinical efficacy depends on pharmacokinetics/pharmacodynamics, stage specificity, and host factors. For example, DSM265's long exposure enabled prophylactic efficacy in CHMI despite slower kill kinetics; conversely, artemisinins' rapid kill makes them indispensable in combination regimens despite emerging ring-stage tolerance in some regions.[15-19] The discovery of potent new chemotypes such as TrtE underscores the continued value of GIAs for lead identification, while also highlighting the need for detailed resistance-evolution studies and mechanistic work before clinical translation.[8,9]

Invasion-Inhibition Assays with Erythrocytic-Stage Monoclonal Antibodies (AMA1, MSP1, EBA175)

Invasion-inhibition assays (IIAs) provide a robust platform for evaluating the functional efficacy of monoclonal antibodies (mAbs) targeting blood-stage malaria antigens. These assays quantitatively measure the capacity of antibodies to prevent merozoite invasion of erythrocytes, offering critical validation for therapeutic and vaccine development.[20,21]

AMA1-Specific Monoclonal Antibodies: Apical Membrane Antigen 1 (AMA1) is an essential micronemal protein that facilitates tight junction formation during merozoite invasion of erythrocytes.

AMA1-specific mAbs inhibit this process by blocking interactions with the parasite protein RON2. In vitro, anti-AMA1 mAbs typically show modest inhibitory activity, with inhibition levels rarely exceeding 40-50% and IC_{50} values in the mid-to-high µg/mL range. High sequence polymorphism across *P. falciparum* strains limits their breadth of activity, making AMA1 a less favorable stand-alone vaccine target.[22,23]

MSP1-42-Specific Monoclonal Antibodies: Merozoite Surface Protein 1 (MSP1) is abundantly expressed on the merozoite surface and undergoes proteolytic processing critical for successful invasion. Antibodies against the 42 kDa C-terminal fragment (MSP1-42) are among the most potent invasion-blocking antibodies, with inhibition levels often exceeding 70% in vitro and IC_{50} values within the low µg/mL range. Due to its high surface expression and functional indispensability, MSP1-42 remains a leading candidate for protective immunity, though polymorphism and epitope accessibility present ongoing challenges.[24]

EBA175-Specific Monoclonal Antibodies: Erythrocyte Binding Antigen 175 (EBA175) mediates sialic acid-dependent binding to glycophorin A on erythrocytes. Anti-EBA175 mAbs disrupt this receptor-ligand interaction, yielding intermediate inhibitory activity in GIAs, typically 50-70% inhibition with IC_{50} values in the low-to-mid µg/mL range. While these antibodies effectively block the sialic acid-dependent invasion pathway, the parasite's ability to switch to alternate invasion ligands reduces overall efficacy.[25]

Growth-Inhibition Assays with Patient Sera from Malaria-Endemic Regions.

Growth-inhibition assays using sera from malaria-exposed patients provide a complementary approach to evaluate naturally acquired immunity. While monoclonal antibodies allow precise mechanistic dissection of antigen-specific inhibition, patient sera reflect the polyclonal and functionally diverse antibody repertoire present in endemic populations.[26] Serum-mediated GIAs assess the capacity of naturally acquired antibodies (NAAb) to inhibit erythrocytic-stage parasite replication in vitro, offering functional insight beyond what is captured by simple binding assays. Multiple cohort studies have shown that higher

pre-season GIA titers correlate with reduced risk of clinical malaria, particularly in young children transitioning from naïve to partially immune status.[27,28] Importantly, this correlation is both antigen- and strain-dependent, highlighting the influence of exposure history and immune breadth on protective outcomes.

Antigen-specific blocking or competition assays with endemic sera have identified AMA1 as a frequent target of inhibitory antibodies, although responses are often allele-specific. In contrast, MSP1-directed NAAb tend to act additively or synergistically with vaccine-induced antibodies, offering broader coverage across parasite strains when incorporated into combination therapies or multivalent immunogens.[29,30] These findings suggest that functional antibodies in patient sera may recapitulate some of the protective mechanisms observed with monoclonal antibodies, while also revealing additional targets or synergistic effects unique to naturally acquired immunity.

Methodological analyses indicate that sera from endemic populations may contain non-GIA mechanisms such as complement activation or opsonic phagocytosis, that contribute to protection independently of direct growth inhibition.[31] Consequently, GIAs should be integrated into a broader systems serology framework that includes binding profiles, Fc receptor engagement, and additional functional assays to comprehensively evaluate protective mechanisms.

Table 1 shows comparative inhibition profiles for established interventions (small molecules, monoclonal antibodies), and patient sera in erythrocytic-stage assays. By incorporating patient sera into the comparative experimental framework alongside small-molecule inhibitors and well-characterized monoclonal antibodies, this study aims to directly assess whether naturally acquired antibodies can mediate parasite inhibition at levels comparable to established interventions. This approach enables a nuanced understanding of the protective potential of patient-derived antibodies and informs antigen prioritization and vaccine design strategies based on real-world immune responses.

Intervention Type	Specific Agent / Antibody / Sera	Mechanism of Action	Max Inhibition (%)	notes
Small molecule	Tartrolon E	Parasite replication inhibitor	98	Highly potent; rapid action
Small molecule	DSM265	Dihydroorotate dehydrogenase inhibitor	95	Active against multiple stages
Small molecule	Artemisinin	Free-radical-mediated parasite killing	99	Standard clinical reference
Monoclonal Ab	mAb-MSP1-1	Blocks merozoite attachment	65	Modest inhibition, proteolytic processing,
Monoclonal Ab	mAb-AMA1	Blocks tight junction formation	80	High inhibition, polymorphic
Monoclonal Ab	mAb-EBA175	Blocks sialic acid-dependent binding to glycophorin A	70	Modest inhibition, redundant, invasion-switch limited
Patient sera	Endemic cohort, pooled sera	Polyclonal inhibition, multiple antigens	40-85	Heterogeneous activity; includes non-GIA mechanisms

Table 3.1: Adapted from combined sources.[8,10,15,22,24,25,28]

3.2 Materials and Methods

3.2.1 *P. falciparum* Growth EC50 Determination: Small-molecule inhibition assay

Asynchronous cultures were propagated in RPMI media supplemented with human red blood cells to 0.5% hematocrit and 0.5% parasitemia. Drugs were prepared in DMSO as a 400× dilution series and diluted 1:50 into media to yield a final DMSO concentration of 0.2%. Parasites were propagated at 37 °C for 72 h and growth was assessed using the SYBR Green method with minor modifications. SYBR green fluorescence was measured (ex./em. 485/535 nm) and data analysis was performed using GraphPad Prism 7. Prior to determining EC50, parasites were propagated for three intraerythrocytic cycles in media lacking drug before plating. All data were collected in triplicate.

3.3.2 *P. falciparum* Invasion EC50 Determination: Monoclonal Antibodies Assays.

The *P. falciparum* 3D7 line was maintained in continuous culture using fresh erythrocytes at 0.5% haematocrit and synchronized by two incubations in 5% sorbitol three hours apart. Synchronized early/mid trophozoites were adjusted to 0.5% parasitemia and then incubated with various mAb concentrations in 96 well plate (obtained from BEI resources at 1mg/ml) tested in triplicate. Final parasitemia was determined by sybr green staining. Briefly, parasite cultures were incubated with 2X syber green stain (in PBS) for 20 minutes in the dark. After incubation total volume in wells is brought to 200uL. Samples were read by flow cytometry (Accuri BD C6).

3.3.3 *P. falciparum* Invasion EC50 Determination: Patient Sera GIA.

Non-dialyzed naïve and patient sera were heat inactivated at 56 degrees Celsius for 30 minutes, and incubated at 37 degrees for 30 minutes. Control and patient sera were initially diluted 50-fold in assay buffer. These 50-fold diluted sera were subjected to 2-fold serial dilutions per well.
3D7 ring-stage parasites were synchronized twice by sorbitol lysis (5% D-sorbitol) and allowed to mature to late trophozoite/schizont stages. Parasites were cultured at 2% hematocrit in RPMI-1640 supplemented

with 25 mg/mL HEPES, 2 mg/mL sodium bicarbonate, 0.5% Albumax II, 0.3 mM hypoxanthine, and 0.1 mg/ml gentamicin. Cultures were maintained at 37 degrees C in an atmosphere of 5% CO_2, 5% O_2 and 90% N_2. Parasites were adjusted to 0.5% infected red cells with a final 0.5% hematocrit, 1:10 plasma dilution, and 100 mL final volume in 96-well flat-bottom microtiter plates in triplicates. The cultures were incubated for 26 hours to allow for schizont rupture and merozoite invasion (monitored by microscopy to ensure full schizont rupture). Final parasitemia was determined by sybr green staining. Briefly, parasite cultures were incubated with 2X syber green stain (in PBS) for 20 minutes in the dark. After incubation total volume in wells is brought to 200uL. Samples were read by flow cytometry (Accuri BD C6).

3.3 Results

3.3.1 *P. falciparum* 3D7 Growth EC50 Determination: Small-molecule inhibition assay

In line with the defining characteristics of historically successful antimalarials; high potency, tolerability, and efficacy across multiple parasite life-cycle stages, our proliferation assays reveal a striking potency profile for Tartrolon E (TrtE). As shown in Figure 3.1, TrtE demonstrated sub-nanomolar activity ($EC_{50} \approx$ 200 pM) against the asexual blood stages of *P. falciparum* (3D7 strain).

When compared to benchmark compounds, TrtE's inhibition profile was both steeper and more potent. Artemisinin (ART), the current frontline therapy, exhibited its expected nanomolar-range activity with a typical sigmoidal dose-response curve. However, TrtE achieved complete inhibition at far lower concentrations, with near-total suppression of proliferation observed at ~1 nM. Similarly, DSM265, a dihydroorotate dehydrogenase (DHODH) inhibitor in advanced clinical testing, showed comparable inhibitory activity, with a right-shifted dose-response curve relative to both TrtE and ART.

The data also highlight key pharmacodynamic differences among the three compounds. TrtE's inhibition curve is characterized by a sharp drop in proliferation, reflecting potent, rapid-acting activity. ART and DSM 265 maintained activity in the low-nanomolar range but with less complete suppression relative to TrtE at equivalent concentrations, consistent with its short half-life and stage-specific action.

Together, these findings establish TrtE as a highly potent inhibitor of *P. falciparum* blood-stage proliferation, with efficacy that surpasses ART in vitro and significantly outperforms DSM265. The sub-nanomolar EC_{50} values position TrtE among the most potent experimental antimalarials reported to date. Given its broad inhibitory profile and activity against blood stages, TrtE represents a promising candidate for further evaluation in combination therapies or as a next-generation antimalarial lead.

The inclusion of these compounds in growth inhibition assays provides robust positive controls for assessing parasite replication and invasion. Their predictable inhibitory effects establish reliable reference points for assay performance, allowing direct comparisons with experimental test conditions. This is particularly important for evaluating the protective potential of monoclonal antibodies and patient sera,

where the degree of inhibition may be more variable. By anchoring results to well-defined drug responses, TrtE, ART, and DSM265 serve as critical standards to validate assay sensitivity, reproducibility, and interpretability.

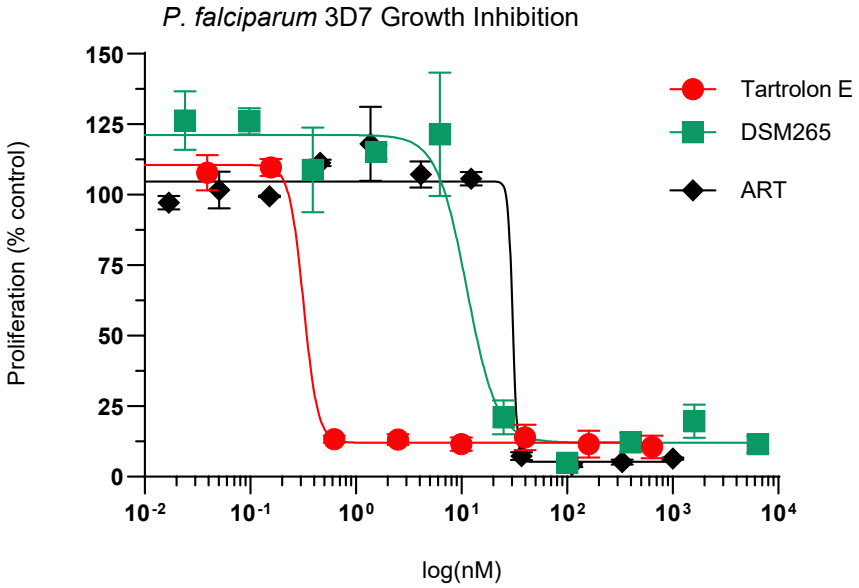

Figure 3.1: Dose-response profiles of Tartrolon E (TrtE, red circle), artemisinin (ART, black diamond), and DSM265 (green square) tested for their ability to inhibit *P. falciparum* (3D7) proliferation. EC50 determination are as follows: TrtE (0.28 nM), DSM 265 (19.8 nM), and ART (28 nM). Data represent mean ± SD from three independent experiments.

3.3.2 Inhibition Assays of *Plasmodium falciparum* 3D7 Using Erythrocytic Stage Monoclonal Antibodies

Monoclonal antibodies (mAbs) targeting blood-stage antigens of *Plasmodium falciparum* remain powerful tools for probing mechanisms of parasite invasion and growth inhibition. Among the most studied targets are merozoite surface protein 1 (MSP1), apical membrane antigen 1 (AMA1), and erythrocyte-binding antigen 175 (EBA175), each of which plays a distinct role in the invasion of erythrocytes. Growth inhibition assays (GIAs) using these antibodies allow for direct comparisons of their functional capacity to block parasite replication in vitro.

The results obtained for the *P. falciparum* 3D7 strain highlight a gradient of inhibitory potency across these antigens (Figure 3.2). Anti-AMA1 antibodies demonstrated the strongest inhibitory activity, maintaining over 80% inhibition across a broad concentration range and achieving half-maximal inhibition at approximately 0.4-0.5 mg/mL and nearly complete inhibition at sub-milligram concentrations with a steep dose-response profile. This finding aligns with the established role of AMA1 in forming the tight junction between merozoites and erythrocytes, a process critical for successful invasion, underscoring its potential as a protective antigen.

In contrast, antibodies targeting EBA175 exhibited intermediate potency, with a measurable but less pronounced inhibition of parasite proliferation (60-70%) compared to AMA1.This reflects the critical role of EBA175 in sialic acid-dependent binding to glycophorin A. However, the parasite's capacity to switch invasion pathways likely contributes to the incomplete inhibition observed. Although this pathway is important for erythrocyte entry, parasites can bypass it using alternative ligands, which likely explains the comparatively reduced inhibitory activity of EBA175-specific antibodies.

MSP1-specific antibodies displayed the weakest inhibitory activity, with incomplete suppression of parasite growth (40%) even at the highest concentrations tested. MSP1, while abundant on the merozoite surface and involved in erythrocyte invasion, undergoes extensive proteolytic processing, which may limit the accessibility of critical epitopes to antibody binding.

Together, these findings illustrate that not all erythrocytic antigens contribute equally to antibody-mediated inhibition of parasite growth. AMA1 emerges as the most effective target in this study, followed by EBA175, with MSP1 showing comparatively limited functional inhibition. These results provide a useful benchmark for comparing antibody-mediated inhibition to small-molecule compounds and patient sera responses. These results illustrate the differential inhibitory potential of monoclonal antibodies targeting distinct merozoite antigens. Importantly, they highlight how well-characterized mAbs provide strong positive controls in GIA studies, enabling direct comparisons to the functional activity of patient sera. By including monoclonal antibody benchmarks, it becomes possible to contextualize the protective capacity of naturally acquired antibodies and evaluate their contribution to blood-stage immunity.

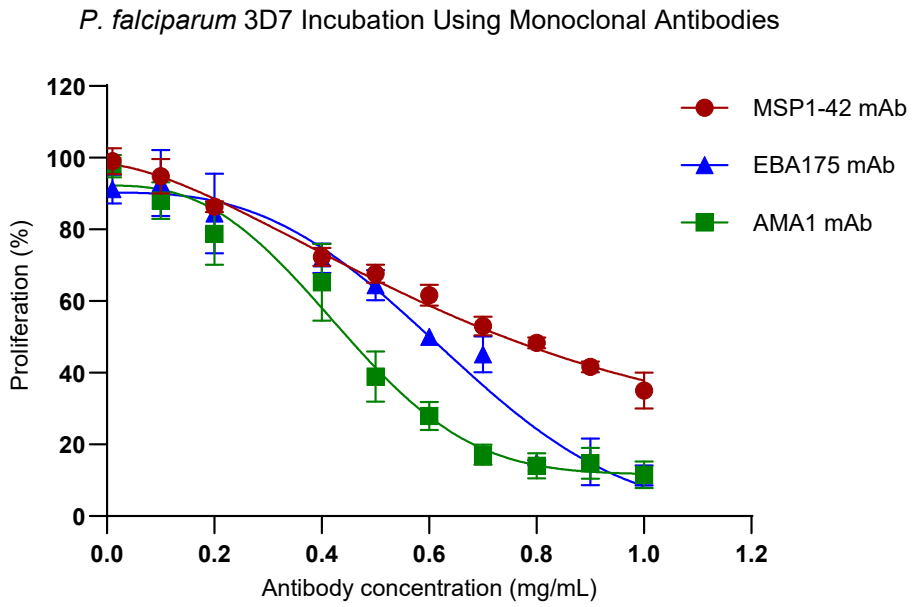

Figure 3.2: *P. falciparum* 3D7 strain comparative monoclonal antibodies growth inhibition assay. Red circle marker indicates MSP1Ab, blue triangle marker indicates EBA175 Ab, and green square marker indicates AMA1 Ab. Data represent mean ± SD from three independent experiments.

3.3.3 Growth Inhibition Assay of *Plasmodium falciparum* 3D7 Using Patient Sera

The growth inhibition assay (GIA) was performed to evaluate the inhibitory activity of patient-derived immune serum on the proliferation of *P. falciparum* 3D7 parasites. PBS and DMSO were included as positive and negative controls, respectively, while naive serum from a malaria-naive individual served as additional control. Parasite proliferation was measured across a range of serum dilutions, and percent proliferation relative to the PBS control was plotted (Figure 3.3).

PBS showed consistently high parasite proliferation across all dilutions, as expected, confirming that in the absence of inhibitory compounds or antibodies, the 3D7 strain maintains robust growth. Conversely, DMSO resulted in near-complete inhibition of parasite growth at high concentrations, demonstrating the assay's dynamic range and the capacity to detect inhibition. The immune serum exhibited nearly complete inhibition of parasite growth, particularly at lower dilutions (4 to 16-fold) similar to DMSO. At the lowest dilutions (4 - 64-fold), proliferation was markedly reduced compared with PBS, reflecting the presence of functional antibodies capable of interfering with parasite invasion or replication. As the serum was further diluted (256 -2048), the inhibition effect diminished, and proliferation approached that of PBS, suggesting a dose-dependent effect consistent with antibody-mediated activity. Interestingly however, the naive serum, obtained from an individual with no prior exposure to malaria, showed a proliferation curve nearly identical to immune serum, indicating a possibility of non-antimalaria specific inhibitory activity.

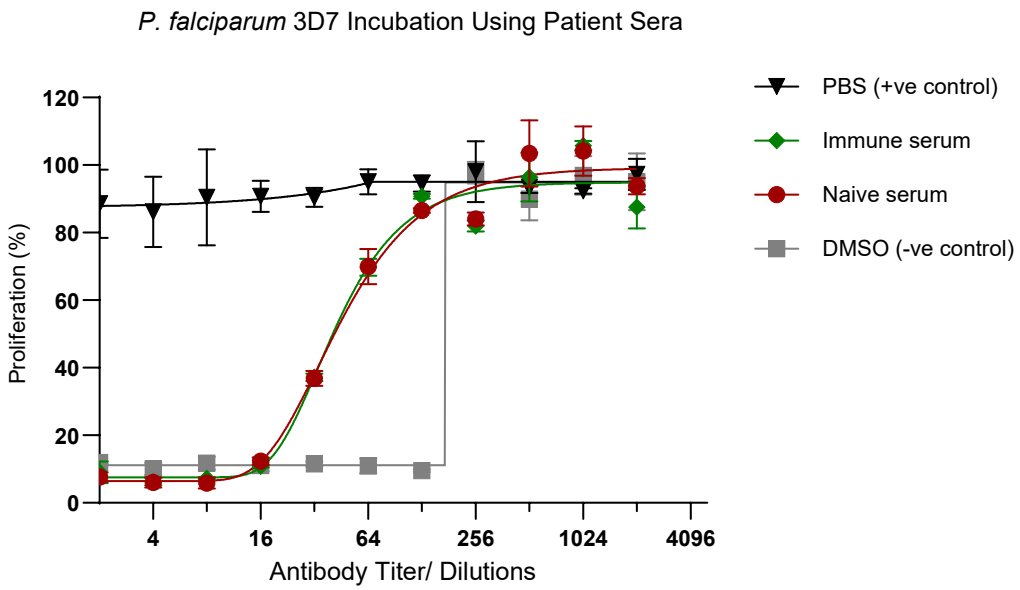

Figure 3.3. Growth-inhibition of *Plasmodium falciparum* 3D7 by patient sera.
Synchronized parasites were incubated with serial dilutions of immune serum (green markers) or naive serum (red markers). PBS served as the positive control for parasite proliferation (black triangles) and DMSO as a negative control (gray squares). Percent proliferation is expressed relative to PBS control. Immune sera produce dose-dependent inhibition; at dilutions ≥256 inhibition is reduced to ~20-25%. Data represent mean ± SD from three independent experiments.

3.4 Discussion

This chapter investigates the protective potential of small-molecule compounds, monoclonal antibodies, and patient sera against malaria blood-stage parasites. While several drug compounds and human monoclonal antibodies have been well-characterized and shown to inhibit parasite invasion and replication, relatively few studies have directly evaluated the capacity of naturally acquired antibodies in patient sera to confer protection. To address this, we employed growth/invasion inhibition assays as comparative tools, evaluating drug compounds, erythrocytic-stage monoclonal antibodies, and sera from individuals living in malaria-endemic regions. Together, these approaches provide a comprehensive framework to determine how different interventions impact parasite survival and inform strategies for antigen prioritization in vaccine development.[23,32]

In this study, three small-molecule compounds were evaluated: Tartrolon E, artemisinin (ART), and DSM265, a dihydroorotate dehydrogenase (DHODH) inhibitor. Proliferation assays revealed that Tartrolon E exhibits potent activity against the asexual blood stages of *P. falciparum* (3D7 strain), with sub-nanomolar inhibitory concentrations and near-complete growth inhibition at low doses. Artemisinin and DSM265 also demonstrated strong dose-dependent inhibition, consistent with their established activity against intraerythrocytic parasites. The consistency of these results with published data supports the robustness of the assay design and underscores the suitability of these small molecules as experimental controls. Importantly, their predictable and potent inhibitory effects provide a benchmark against which the protective capacity of monoclonal antibodies and patient sera can be compared.

Monoclonal antibodies (mAbs) targeting merozoite antigens offer precise tools to dissect antigen-specific immune responses. In GIAs/IIAs, they allow direct measurement of how targeting defined invasion ligands affects parasite survival. Three antibodies were tested: anti-MSP1, anti-AMA1, and anti-EBA175.

Anti-AMA1 antibodies showed the strongest inhibitory effect, maintaining >70% inhibition across a wide concentration range and reaching half-maximal inhibition at ~0.4-0.5 mg/mL. This reflects the essential role of AMA1 in merozoite invasion and its potential as a leading antigen for protective immunity. Anti-

EBA175 antibodies demonstrated intermediate inhibition, achieving ~60-70% inhibition at lower concentrations. Since EBA175 mediates sialic acid-dependent binding to glycophorin A, antibodies targeting this pathway effectively reduce invasion, though parasite plasticity in switching invasion mechanisms likely contributes to incomplete inhibition. Anti-MSP1 antibodies displayed the weakest inhibitory activity, with plateau at 40% inhibition at concentrations above 0.8 mg/mL. This reduced efficacy is consistent with MSP1's high polymorphism across parasite strains. Together, these results highlight the differential inhibitory potential of mAbs and emphasize their value as positive controls. Their inclusion provides a functional benchmark for interpreting the activity of patient sera, helping to contextualize naturally acquired immunity relative to well-characterized antigen-specific responses.

Patient sera from malaria-endemic regions provide a unique window into the complexity of naturally acquired immunity (NAI).[28] Unlike monoclonal antibodies, sera contain a diverse, polyclonal mixture of antibodies against multiple parasite antigens. GIAs using patient sera therefore capture the combined effect of naturally induced antibody responses, offering a more holistic assessment of functional immunity. Here, sera from exposed individuals were incubated with *P. falciparum* parasites, and their ability to inhibit invasion and replication within erythrocytes were quantified relative to control sera, PBS, and DMSO. Typically, stronger inhibitory activity is often observed in sera from highly exposed individuals, particularly adults who have acquired partial immunity, whereas sera from children or malaria-naïve donors typically show weaker effects.[27,31] The variability across samples reflects differences in exposure history, immune maturity, and parasite antigen diversity. In the patient sera assay covered in this chapter, immune sera showed typical inhibitory profiles, strong inhibitions at higher concentrations, and waning inhibitions as dilutions increased. We expected to see a contrasting difference between sera from an infected patient in malaria endemic region and sera from a naïve donor due to malaria specific antibodies present in the patient sample. Interestingly, control sera from a non-malaria-exposed donor showed a level of parasite growth inhibition comparable to that of sera from a malaria-exposed patient. This observation likely reflects the contribution of non-specific serum factors rather than malaria-specific immunity. Human serum contains innate inhibitory components, such as complement proteins, natural

antibodies, and other serum proteins, which can interfere with parasite growth in vitro. Additionally, assay conditions, including red blood cell donor variability, serum handling (dialysis, heat-inactivation), and parasite strain susceptibility may contribute to apparent inhibition in naïve sera. It is also possible that the patient sera contained low titers of functional malaria-specific antibodies, reducing the difference between naïve and immune serum. These results highlight that growth inhibition assays measure both specific and non-specific effects, and appropriate controls are essential to interpret malaria-specific antibody activity.

Also, partial inhibition observed even at high serum concentrations may be due to several factors;

- Redundant Invasion Pathways: *P. falciparum* can utilize multiple ligands to invade erythrocytes. Antibodies targeting a subset of these ligands may not fully block invasion, allowing residual growth.[33]
- Antibody Specificity and Affinity: Immune serum likely contains a heterogeneous mixture of antibodies, some of which may bind non-inhibitory epitopes or have lower affinity, limiting overall efficacy.[34]
- Functional Maturation of Antibodies: Not all antibodies generated in response to natural infection are equally inhibitory; some may require complement or other immune factors to exert full effect.[31,35]

Heterogeneity of responses underscores the complexity of protective immunity and the challenges in identifying a single antigen that can account for robust protection. By comparing patient sera results with those from small molecules and monoclonal antibodies, this study establishes a comprehensive framework for evaluating parasite inhibition. This comparative approach enables the assessment of naturally acquired antibodies against defined standards, helping to prioritize antigens for future vaccine development and improve our understanding of protective humoral immunity.

3.5 References

1. Desjardins RE, Canfield CJ, Haynes JD, Chulay JD. Quantitative assessment of antimalarial activity in vitro by a semiautomated microdilution technique. *Antimicrob Agents Chemother*. 1979;16(6):710-718. doi:10.1128/AAC.16.6.710
2. Noedl H, Wongsrichanalai C, Wernsdorfer WH. Malaria drug-sensitivity testing: new assays, new perspectives. *Trends Parasitol*. 2003;19(4):175-181. doi:10.1016/s1471-4922(03)00028-x
3. Smilkstein M, Sriwilaijaroen N, Kelly JX, Wilairat P, Riscoe M. Simple and inexpensive fluorescence-based technique for high-throughput antimalarial drug screening. *Antimicrob Agents Chemother*. 2004;48(5):1803-6. Doi: 10.1128/AAC.48.5.1803-1806.2004
4. Kennedy AT, Schmidt CQ, Thompson JK, Weiss GE, Cowman AF. Recruitment of Factor H as a Novel Complement Evasion Strategy for Blood-Stage *Plasmodium falciparum* Infection, *The Journal of Immunology*, Volume 196, Issue 3, February 2016, Pages 1239–124 10.4049/jimmunol.1501581
5. Sim BK, Narum DL, Chattopadhyay R, et al. Delineation of stage specific expression of Plasmodium falciparum EBA-175 by biologically functional region II monoclonal antibodies. *PLoS One*. 2011;6(4):e18393. Published 2011 Apr 14. doi:10.1371/journal.pone.0018393
6. Boyle MJ, Wilson DW, Richards JS, Riglar DT, Tetteh KK, Conway DJ, et al. Isolation of viable merozoites to define erythrocyte invasion events and advance vaccine and drug development. *Proc Natl Acad Sci USA*. 2010;107(32):14378-83. Doi: 10.1073/pnas.1009198107
7. Smilkstein M, Sriwilaijaroen N, Kelly JX, Wilairat P, Riscoe M. Simple and inexpensive fluorescence-based technique for high-throughput antimalarial drug screening. *Antimicrob Agents Chemother*. 2004;48(5):1803-9. 10.1128/AAC.48.5.1803-1806.2004
8. Chery-Karschney L, Patrapuvich R, Mudeppa DG, et al. Tartrolon E, a secondary metabolite of a marine symbiotic bacterium, is a potent inhibitor of asexual and sexual *Plasmodium falciparum*. *Antimicrob Agents Chemother*. 2024;68(2):e0068423. Doi: 10.1128/aac.00684-23
9. Cotto-Rosario A, Miller EYD, Fumuso FG, Clement JA, Todd MJ, O'Connor RM. The Marine Compound Tartrolon E Targets the Asexual and Early Sexual Stages of *Cryptosporidium parvum*. *Microorganisms*. 2022;10(11):2260. Published 2022 Nov 15. doi:10.3390/microorganisms10112260
10. Xie SC, Dogovski C, Hanssen E, et al. Haem-activated promiscuous targeting of artemisinin in *Plasmodium*. *Proc Natl Acad Sci U S A*. 2016;113(40):10950-5. PMID: 26694030. Doi:10.1038/ncomms10111
11. Mercer AE, Copple IM, Maggs JL, O'Neill PM, Park BK. The role of heme and the mitochondrion in the chemical and molecular mechanisms of mammalian cell death induced by the artemisinin antimalarials. *J Biol Chem*. 2011;286(2):987-96. PMID: 21059641.
12. Ariey F, Witkowski B, Amaratunga C, et al. A molecular marker of artemisinin-resistant *Plasmodium falciparum* malaria. *Nature*. 2014;505(7481):50-5. PMID: 24352249. Doi:10.1038/nature12876
13. Straimer J, Gnadig NF, Witkowski B, et al. K13-propeller mutations confer artemisinin resistance in *Plasmodium falciparum* clinical isolates. *Science*. 2015;347(6220):428-31. Doi:10.1126/science.1260867

14. Witkowski B, Duru V, Khim N, et al. A surrogate marker of artemisinin resistance-ring-stage survival assay. *Antimicrob Agents Chemother*. 2013;57(9):3560-6. PMID: 23784998.

15. Phillips MA, Lotharius, J, Marsh, K, White, J. et al., A long-duration dihydroorotate dehydrogenase inhibitor (DSM265) for prevention and treatment of malaria.Sci. Transl. Med.7,296ra111-296ra111(2015). DOI:10.1126/scitranslmed.aaa6645

16. Phillips MA, White KL, Kokkonda S, Deng X, White J, et al. A Triazolopyrimidine-Based Dihydroorotate Dehydrogenase Inhibitor with Improved Drug-like Properties for Treatment and Prevention of Malaria. *ACS Infectious Diseases* **2016**, *2* (12) , 945-957. https://doi.org/10.1021/acsinfecdis.6b00144

17. Sulyok M, Rueangweerayut R, Vanachayangkul P, et al. DSM265 for *Plasmodium falciparum* chemoprophylaxis: a randomised, double-blind, phase 1 trial with controlled human malaria infection. *Lancet Infect Dis*. 2017;17(6):636-44. PMID: 28363637. Doi:10.1016/S1473-3099(17)30139-1

18. McCarthy JS, Marquart L, Sekuloski S, et al. Safety, pharmacokinetics, and antimalarial activity of DSM265 in healthy volunteers: first-in-human single- and multiple-ascents. *Lancet Infect Dis*. 2017;17(6):645-53. PMID: 28363636.

19. Llanos-Cuentas A, et al. Antimalarial activity of single-dose DSM265 in patients with *P. falciparum* or *P. vivax* infection: proof-of-concept study. *Lancet Infect Dis*. 2018;18(8):874-83. PMID: 29909069.

20. Blackman MJ, Healer J. Apical membrane antigen 1 and its role in the invasion of erythrocytes by *Plasmodium falciparum*. Parasitology Today. 1998;14(11):448-53.

21. Healer J, et al. Neutralising antibodies block the function of RH5/Ripr/CyRPA complex during invasion of *Plasmodium falciparum* into human erythrocytes. Cell Microbiol. 2019;21(3):e13030.

22. Angage, D., Chmielewski, J., Maddumage, J.C. et al. A broadly cross-reactive i-body to AMA1 potently inhibits blood and liver stages of Plasmodium parasites. Nat Commun 15, 7206 (2024). https://doi.org/10.1038/s41467-024-50770-7

23. Healer J, et al. Mode of action of invasion-inhibitory antibodies directed against *Plasmodium falciparum* apical membrane antigen 1. Infect Immun. 2004;72(4):2129-38.

24. Harris SI, et al. Antibodies against Merozoite Surface Protein (MSP)1-19 are a major component of the immune response to malaria. J Exp Med. 2005;193(12):1403-12.

25. Paing MM, Salinas ND, Adams Y, et al. Shed EBA-175 mediates red blood cell clustering that enhances malaria parasite growth and enables immune evasion. Elife. 2018;7:e43224. 2018 Dec 17. doi:10.7554/eLife.43224

26. Kothari M, Wanjari A, Acharya S, et al. A Comprehensive Review of Monoclonal Antibodies in Modern Medicine: Tracing the Evolution of a Revolutionary Therapeutic Approach. Cureus. 2024;16(6):e61983. Published 2024 Jun 9. doi:10.7759/cureus.61983

27. Dent AE, Bergmann-Leitner ES, Wilson DW, et al. Antibody-mediated growth inhibition of *Plasmodium falciparum*: relationship to age and protection from parasitemia in Kenyan children and adults. *PLoS One*. 2008;3(10):e3557. doi:10.1371/journal.pone.0003557

28. Crompton PD, Miura K, Traore B, et al. In vitro growth-inhibitory activity and malaria risk in a cohort study in mali. *Infect Immun*. 2010;78(2):737-745. doi:10.1128/IAI.00960-0

29. Knudsen AS, Björnsson KH, Bassi MR, et al. Strain-Dependent Inhibition of Erythrocyte Invasion by Monoclonal Antibodies Against *Plasmodium falciparum* CyRPA. *Front Immunol*.

30. Miura K, Diouf A, Fay MP, et al. Assessment of precision in growth inhibition assay (GIA) using human anti-*Pf*RH5 antibodies. *Malar J*. 2023;22(1):159. Published 2023 May 19. doi:10.1186/s12936-023-04591-6 2021;12:716305. Published 2021 Aug 10. doi:10.3389/fimmu.2021.716305

31. Wanjala CNL, Bergmann-Leitner E, Akala HM, et al. The role of complement immune response on artemisinin-based combination therapy in a population from malaria endemic region of Western Kenya. *Malar J*. 2020;19(1):168. Published 2020 Apr 29. doi:10.1186/s12936-020-03242-4

32. Drew DR, Wilson DW, Elliott SR, et al. A novel approach to identifying patterns of human invasion-inhibitory antibodies guides the design of malaria vaccines incorporating polymorphic antigens. *BMC Med*. 2016;14(1):144. Published 2016 Sep 23. doi:10.1186/s12916-016-0691-6

33. Tijani MK, Lugaajju A, Persson KEM. Naturally Acquired Antibodies against *Plasmodium falciparum*: Friend or Foe?. *Pathogens*. 2021;10(7):832. Published 2021 Jul 2. doi:10.3390/pathogens10070832

34. Duncan CJ, Hill AV, Ellis RD. Can growth inhibition assays (GIA) predict blood-stage malaria vaccine efficacy?. *Hum Vaccin Immunother*. 2012;8(6):706-714. doi:10.4161/hv.19712

35. Rono J, Färnert A, Olsson D, Osier F, Rooth I, Persson KE. *Plasmodium falciparum* line-dependent association of in vitro growth-inhibitory activity and risk of malaria. *Infect Immun*. 2012;80(5):1900-1908. doi:10.1128/IAI.06190-11

Chapter 4 | Cross Resistance Studies of *PfDd2* Mutant Lines Against Novel DHODH Inhibitors

4.1 Introduction

Historically, the development and deployment of potent small-molecule antimalarials such as chloroquine, sulfadoxine-pyrimethamine, and artemisinin derivatives revolutionized malaria treatment. However, each of these drug classes has eventually been compromised by parasite resistance. Artemisinin-based combination therapies (ACTs), currently the global frontline treatment, are now facing resistance in Southeast Asia and parts of Africa, underscoring the urgent need for new therapeutic strategies.[1] In the past decade, high-throughput screening (HTS) against either intraerythrocytic parasites or *P. falciparum* enzymes have led to the identification of several novel chemical entities that reached clinical development. HTS also contributed to the validation of new parasite targets by providing different mechanisms of action from previously used antimalarials. One such candidate to reach Phase II clinical development include the pyrimidine bio synthetic enzyme dihydroorotate dehydrogenase (DHODH) inhibitor DSM265.[2] Through our work in collaboration with external partners, DHODH emerged as a strong target for malaria prophylaxis.[3]

PfDHODH: Structural Basis for Selective Inhibition

Plasmodium parasites rely exclusively on the de novo pyrimidine biosynthesis pathway for DNA and RNA precursors, making this pathway essential for survival in both blood and liver stages.[4-7] Dihydroorotate dehydrogenase (DHODH), a class II membrane-associated enzyme, catalyzes the fourth step by oxidizing dihydroorotate to orotate via flavin mononucleotide (FMN) and coenzyme Q (CoQ) (Figure 4.1).[8]

The *Plasmodium* enzyme forms a conserved α/β-barrel structure with an additional hydrophobic N-terminal extension that generates a tunnel-like pocket near the barrel top.[9,10] The active site, located within the barrel, binds FMN, while inhibitors can block activity either by occupying the barrel or by

binding within the tunnel. The tunnel site, due to its sequence variability and conformational flexibility, offers a route to selective inhibition.[10-12]

This tunnel binding pocket consists of three regions:[10,13]

1. **Hydrophilic pocket** - containing conserved residues His185 and Arg265.
2. **Hydrophobic pocket** - shaped by Phe188 and Phe227, which help position inhibitors.
3. **Hydrophobic channel** - leading toward FMN, lined by Val532, Ile272, and Ile263.

Unlike human host cells, which can salvage pyrimidines from their environment, *P. falciparum* parasites are entirely dependent on de novo pyrimidine biosynthesis for nucleotide production, making *Pf*DHODH indispensable for parasite survival. This dependency creates a therapeutic window that can be exploited by highly selective inhibitors that block parasite but not human DHODH activity.[14]

Development of *Plasmodium*-specific DHODH Inhibitors

Progress in developing selective inhibitors was limited until the *Pf*DHODH crystal structure was resolved. The first structure bound to a human DHODH inhibitor (A77-1726) revealed why the compound, though potent against HsDHODH, showed only weak activity against *Pf*DHODH.[15,16] Species-specific differences, particularly residues Met536, Phe174, Phe188, and Ile substitutions, create a smaller tunnel in *Pf*DHODH, altering inhibitor orientation and reducing hydrogen-bonding capacity.[17,18] Consequently, inhibitor binding in *Pf*DHODH is guided primarily by hydrophobic interactions, especially stacking with Phe188 and Phe227, while conserved residues His185 and Arg265 provide essential hydrogen bonds.[18,19]

Early efforts to modify A77-1726 yielded only moderate potency. Target-based high-throughput screening (HTS) then identified a thiophene-carboxamide scaffold, leading to Genz-667348.[20,21] This compound displayed selective nanomolar activity, with its benzimidazole moiety engaging the hydrophobic pocket

and its amide group hydrogen-bonding to His185 and Arg265.[22,23] However, despite promising in vitro and pharmacokinetic profiles, these inhibitors did not progress beyond late lead development.[22]

A second HTS campaign by our collaborators (UT Southwestern and MMV) produced DSM1, a triazolopyrimidine inhibitor that established the chemical foundation for current *Pf*DHODH inhibitors.[24-27] Structural studies showed its hydrophilic head group formed critical hydrogen bonds with His185 and Arg265, while the naphthyl tail occupied the hydrophobic pocket, inducing favorable stacking with Phe188.[26] Electron delocalization via the triazolopyrimidine N−1 was essential for potency, as replacement abolished activity. Further optimization revealed that bulky para-substituted phenyl groups, such as 4-SF5-Ph, provided the best balance of potency, stability, and exposure (as seen in DSM265).[27] Exploiting the C-5 position of DSM1 allowed extension into the narrow hydrophobic tunnel, producing DSM265 with superior drug-like properties.[13,28] Overall, these studies not only validated *Pf*DHODH as a clinically relevant target but also generated potent clinical candidates, with DSM265 representing the most advanced inhibitor to date.[29]

Triazolopyrimidine DSM265

DSM265 is a triazolopyrimidine-based compound with excellent potency against blood-stage parasites and long half-life properties compatible with single-dose therapy. DSM265 combines strong *Pf*DHODH inhibition with oral bioavailability and efficacy in vivo.[30] It engages the hydrophilic pocket through the triazolopyrimidine core, the hydrophobic channel via a CF2CH3 group, and the hydrophobic pocket with its 4-SF5-Ph substituent.[25-27] DSM265, developed by MMV and Takeda, has advanced through Phase IIa clinical trials, showing potential both as a single-dose cure and as weekly chemoprophylaxis.

Preclinical studies demonstrated its ability to cure *P. falciparum* infections in murine models, and early-phase human trials confirmed safety, tolerability, and efficacy in controlled human malaria infection studies.[30,31] DSM265 was thus considered one of the most promising non-artemisinin candidates in recent decades. In human Phase IIa clinical studies, DSM265, which has a long human half-life, was able to provide single dose cures of *P. falciparum* malaria in patients in Peru.[32] However, it showed lower efficacy against *P. vivax*, and resistant parasites that mapped to mutations in DHODH were identified in two relapsing *P. falciparum* patients. Importantly, DSM265 has both potent blood and liver-stage antischizontal activity, which supports the use of DHODH inhibitors for prophylaxis and provides superiority over compounds with only blood-stage activity for this indication.[33] Human sporozoite challenge studies showed that DSM265 prevented the emergence of *P. falciparum* infection if dosed a day prior to infection, providing a clinical proof of concept supporting the DHODH target for this indication.[31,34] Despite its good efficacy, DSM265 was shown to be both teratogenic and to result in testicular toxicity in certain preclinical species and thus was unable to meet the safety bar required for continued clinical development, particularly for use as a prophylactic over months during the transmission season in Africa, or in pregnant women (results unpublished).[35] While clinical development of DSM265 has been terminated, the clinical data obtained has validated DHODH as a strong target for malaria prophylaxis. As the current clinical malaria portfolio now lacks a DHODH inhibitor, there is strong justification to identify new DHODH inhibitors from a different chemical class that will combine the good efficacy of DSM265 with a safety profile that can support its development.[35, 36]

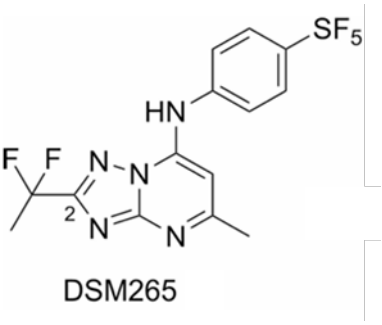

DSM265

<u>Emergence of Resistance to DHODH Inhibitor DSM 265</u>

Drug resistance remains a looming threat for any antimalarial introduced at scale. In-vitro studies have shown that continuous exposure of *P. falciparum* parasites to DSM265 results in the rapid emergence of resistant lines.[37] The sequencing of these resistant lines pioneered by the Rathod Lab has identified point

mutations clustered around the ubiquinone-binding pocket of *Pf*DHODH (figure 4.2). These mutations alter the interaction between DSM265 and its binding site, reducing inhibitor affinity without abolishing enzyme activity. For example, mutations such as Cys276Phe (C276F) and Gly181Ser (G181S) have been implicated in conferring substantial shifts in susceptibility.[30,37] The phenotypic consequences of these mutations can be quantified using in vitro growth inhibition assays (GIAs). Resistant parasite lines typically exhibit several-fold increases in the EC_{50} (half-maximal effective concentration) of DSM265 relative to wild-type strains, providing direct evidence of reduced drug sensitivity. For example, in selection assays, C276F and C276Y mutants show about an 18- to 32-fold increase in EC_{50}.[37] While DSM265 maintains potent activity against drug-naïve parasites, the selection of resistant lines demonstrates the evolutionary plasticity of *P. falciparum* and foreshadows the potential for resistance to emerge clinically if DSM265 or related inhibitors were deployed widely.

Cross-Resistance and the Need for New Target Profiling

Resistance mutations in *Pf*DHODH raise critical concerns not only about DSM265 itself but also about the broader drug discovery pipeline targeting this enzyme. Structurally distinct inhibitors may engage *Pf*DHODH in different ways, but those that share binding properties with DSM265 could be compromised by the same mutations.[38,39] This phenomenon, known as cross-resistance, can severely limit the clinical utility of a drug class. If resistant parasites selected under DSM265 pressure also show diminished susceptibility to novel *Pf*DHODH inhibitors, the therapeutic potential of the entire target class could be undermined.

The importance of cross-resistance surveillance has been highlighted in prior studies. Ross et al. (2018) systematically characterized DSM265-resistant *P. falciparum* Dd2 lines and demonstrated that several novel DHODH inhibitors exhibited reduced potency against these mutants.[38] At the same time, other inhibitors with distinct structural scaffolds retained activity, suggesting that rational design and scaffold diversity may overcome resistance.[39] These findings underscore the dual importance of understanding the molecular basis of resistance and evaluating the cross-resistance potential of next-generation candidates.[40]

Growth Inhibition Assays as a Tool for Studying Cross-Resistance

GIAs serve as a platform for quantifying drug susceptibility and resistance in *P. falciparum*. By exposing parasites to a range of inhibitor concentrations and measuring proliferation across the erythrocytic cycle, GIAs provide quantitative metrics such as IC_{50}/EC_{50} values, fold shifts in resistance, and stage-specific inhibition profiles. Methods including [^{3}H]-hypoxanthine incorporation, parasite lactate dehydrogenase (pLDH) activity, or SYBR Green I-based DNA quantification have all been widely used to generate robust dose-response curves.[41] These assays are indispensable for establishing the potency of new antimalarial compounds, confirming resistance phenotypes, and comparing the activity of drug candidates across wild-type and mutant parasite lines.

When applied to DSM265 and other *Pf*DHODH inhibitors, GIAs allow for direct head-to-head comparisons of drug susceptibility in resistant versus wild-type parasites. EC_{50} values shifted by several folds in resistant lines provide compelling evidence of altered target engagement, while preserved susceptibility to structurally distinct inhibitors highlights opportunities for drug design. Thus, GIAs not only serve as a functional readout of resistance but also guide the medicinal chemistry optimization process by identifying structural features that can evade resistance.

Objectives of the Current Study

Building on this background, the present work investigates cross-resistance of DSM265-resistant *P. falciparum* Dd2 lines against a panel of nine novel DHODH inhibitors. By expanding the resistance profiling beyond DSM265 itself, this study aims to identify compounds that retain potency against resistant parasites and thus represent viable scaffolds for future development. The key objectives are:

- To characterize DSM265-resistant *P. falciparum* Dd2 lines through growth inhibition assays and confirm shifts in EC_{50} relative to wild-type parasites.

- To evaluate cross-resistance profiles of resistant lines against nine chemically distinct DHODH inhibitors.

Through this work, we seek to expand the understanding of resistance liabilities in the *Pf*DHODH target class and to inform the development of durable, next-generation antimalarials.

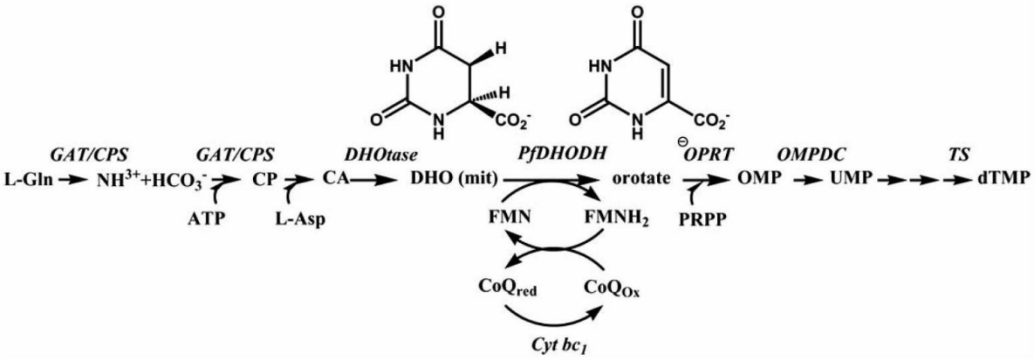

Figure 4:1: *PfDHODH* enzyme converts dihydroorotate (DHO) to orotate using ubiquinone; DSM265 competitively inhibits this reaction.[25]

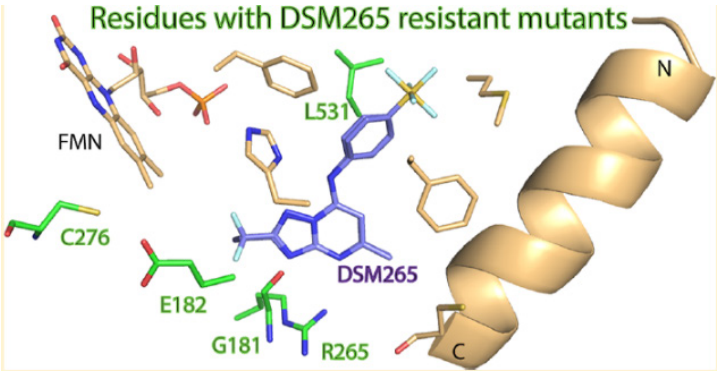

Figure 4.2: Resistance mutations (e.g., Cys276Phe, Gly181Ser) near the binding pocket reduce DSM265 efficacy, establishing the rationale for testing cross-resistance against diverse DHODH inhibitors.[37]

4.2 Materials and Methods

4.2.1 DSM265-Resistant *P. falciparum* Dd2 Clones Re-sequencing

For targeted *dhodh* sequencing, DNA was extracted from saponin-lysed parasites using the DNA extraction kit (Qiagen) and manufacturer's protocol. Briefly, frozen infected red blood cell (RBC) pellet was thawed at room temperature, during which most RBCs lysed. To initiate selective lysis, 1/20th volume of 3% saponin was added, and the suspension was incubated for 5 minutes at room temperature. Following incubation, 2 volumes of PBS were added, and the mixture was centrifuged at 4000 × g for 5 minutes. The pellet was washed twice more with the same volume of PBS, then transferred to a 1.5 ml microcentrifuge tube and centrifuged again at 4000 × g for 5 minutes, after which the supernatant was discarded. The resulting parasite pellet was resuspended in 200 µl PBS, followed by the addition of 20 µl proteinase K (supplied with the kit) and 4 µl RNase (100 mg/ml). Next, 200 µl buffer AL was added, and the sample was pulse-vortexed for 15 seconds, then incubated at 56 °C for 90 minutes with vortexing every 10 minutes. After a brief centrifugation to collect drops, 200 µl 100% ethanol was added, mixed by pulse vortexing, and spun briefly. The solution was carefully transferred into a mini spin column and centrifuged at 6000 × g for 1 minute. The column was placed into a clean tube while the collection tube was discarded. Washes were performed sequentially with buffer AW1 (6000 × g, 1 min) and buffer AW2 (20,000 × g, 3 min). To minimize buffer carryover, an additional centrifugation at 20,000 × g for 1 minute was performed. The column was transferred into a clean 1.5 ml tube, and DNA was eluted by adding 50 µl buffer AE, incubating for 1-2 minutes, and centrifuging at 6000 × g for 1 minute. The elution step was repeated using the initial eluate to maximize yield. After, the *P. falciparum dhodh* gene was PCR amplified using forward primer (CATTTAAGCCCCAAAACATTTTTAC) and reverse primer (GTGATAGATAGCTCCAGTCGATTTC) and submitted for sequencing to confirm point mutations.

4.2.2 *P. falciparum* Growth EC50 Determination

Asynchronous cultures were propagated in RPMI media supplemented with human red blood (O+) cells to 0.5% hematocrit and 0.5% parasitemia. Drugs were prepared in DMSO as a 400× dilution series (typically a 2- or 3-fold dilution series was used, yielding a final concentration in media ranging from 0.001−30 μM depending on the cell line) and were then diluted 1:40 into media to yield a final DMSO concentration of 0.2%. Parasites were propagated at 37 °C for 72 h and growth was assessed using the SYBR Green method with minor modifications. SYBR green fluorescence was measured (ex./em. 485/535 nm) and data analysis was performed using GraphPad Prism 10. Prior to determining EC50, parasites were propagated for three intraerythrocytic cycles in media lacking drug before plating. All data were collected in triplicate.

4.3 Results

4.3.1 DSM265-Resistant *P. falciparum* Dd2 Clones Re-sequencing

DSM265-resistant *P. falciparum* Dd2 parasites were previously generated through in vitro selection under continuous drug pressure at varying DSM265 concentrations. Whole-gene resequencing of the *Pfdhodh* locus was performed to confirm the presence of resistance-associated mutations. Four distinct amino acid substitutions were identified in the resistant lines: G181C, R265S, C276F, and L531F. Notably, the C276F mutation has also been observed in clinical isolates, underscoring its translational significance.

In this study, resequencing the parental Dd2 line and five DSM265-resistant clones confirmed the presence of these known *Pfdhodh* point mutations without evidence of additional novel mutations (Table 4.1). The resistant clones carried single mutations corresponding to specific nucleotide substitutions → amino acid changes: R10C1B (G541T → G181C), R2B B2D11 (A795T → R265S), R1BC1A and R1BC1B (G1593T → L531F), and R1AC1B (G827T → C276F). The parental Dd2 strain remained wild-type at these loci.

These results validate the stability of resistance-conferring mutations in DSM265-selected lines and confirm the absence of secondary mutations in *Pfdhodh* that might complicate the interpretation of cross-resistance studies.

Table 4.1:

Cell Line	Selection [265]	Pfdhodh nucleotide change	PfDHODH amino acid change
Dd2	na	na	na
R10C1B	22.8 nM	G541T (TGT)	G181C
R2B B2D11	36 nM	A795T (AGT)	R265S
R1BC1A	36 nM	G1593T (TTT)	L531F
R1BC1B	36 nM	G1593T (TTT)	L531F
R1AC1B	60 nM	G827T (TTT)	C276F

Confirmation of *Pf*DHODH amino acid substitutions in DSM265-resistant *P. falciparum* clonal lines. Sequences were analyzed using Geneious Prime software.

4.3.2 Verification of DSM265 resistant parasites EC_{50}

The effective concentration leading to 50% reduction in cell proliferation (EC_{50}) values of DSM265 were determined for the parental *P. falciparum* Dd2 wild-type (WT) strain and five DSM265-resistant clonal lines, with artemisinin (ART) included as a control compound. The DSM265 senstitive WT Dd2 parasites showed an EC_{50} of 5.18 ± 1.30 nM for DSM265, consistent with previous reports of sub- to low-nanomolar potency against DHODH in drug-sensitive parasites. In contrast, the resistant lines exhibited a substantial shift in DSM265 susceptibility, with EC_{50} values ranging from ~85 nM to 140 nM, representing an approximate 20- to 30-fold reduction in potency relative to WT parasites (Table 4.2). The Dd2 R10C1B line demonstrated the highest level of resistance, with a DSM265 EC_{50} of 140.2 ± 40.50 nM, while R2B and R1BC1B showed intermediate resistance (85.50 ± 15.30 nM and 110 ± 35.52 nM, respectively). The Dd2 R1AC1B line also displayed a similar resistance phenotype with an EC_{50} of 118.41 ± 37.29 nM. These findings indicate that different clonal selections confer varying degrees of cross-resistance, but all resistant lines show consistent loss of sensitivity compared with Dd2 WT.
In contrast, artemisinin maintained low-nanomolar EC_{50} values across all lines (1.10 ± 0.10 to 3.20 ± 0.10 nM). The absence of a significant shift in ART sensitivity across resistant clones confirms that resistance was specific to DSM265 and not due to global alterations in drug susceptibility. These results confirm that resistance phenotypes observed are directly attributable to mutations in the DHODH target pathway.

Table 4.2: Half-maximal inhibitory concentrations (EC_{50}) of DSM265 and artemisinin (ART) against *Plasmodium falciparum* Dd2 wild-type (WT) and DSM265-resistant clonal lines. Data sets were collected in triplicate for each concentration in the dose-response curve, and data were fitted in GraphPad Prism to determine the EC_{50} using the logI versus response equation. Reported values are presented as mean ± standard deviation with 95% confidence intervals (CI).

Clonal line	ART EC_{50} (nM) 95% CI	DSM 265 EC_{50} 95% CI (nM)
Dd2 WT	1.10 ± 0.10	5.18 ± 1.30
R10C1B	1.74 ± 0.11	140.2 ± 40.50
R2B	2.91 ± 0.28	85.50 ± 15.30
R1BC1A	1.80 ± 0.12	124.0 ± 20.58
R1BC1B	3.20 ± 0.10	110 ± 35.52
R1AC1B	1.81 ± 0.20	118.41 ± 37.29

4.3.3 Activity of Novel DHODH Inhibitors Against DSM265-Resistant Parasite Lines

To evaluate cross-resistance patterns and the potency of next-generation DHODH inhibitors, we determined EC_{50} values for a panel of DSM265-resistant *P. falciparum* Dd2 clones (R10C1B, R2B, R1BC1B, R1BC1A, and R1AC1B) and compared them to wild-type Dd2 parasites. Assays included artemisinin (ART) as a reference control, DSM265 as the parental DHODH inhibitor, and nine structurally distinct DSM compounds (DSM1465, DSM1463, DSM1469, DSM1389, DSM1200, DSM1398, DSM1342, DSM1459, DSM1510). All tested analogs retained nanomolar potency against DSM265-resistant clones, with EC_{50} values closely matching those observed for wild-type parasites. (Table 4.3, Figure 4.3)

DSM1465 demonstrated consistent sub-nanomolar potency across all lines. WT parasites were highly sensitive (0.23 ± 0.10 nM), and resistant clones showed EC_{50} values between 0.15 ± 0.04 nM (R2B) and 0.65 ± 0.01 nM (R1AC1B). Importantly, no significant right-shift was observed relative to WT, highlighting DSM1465 as a lead candidate with full retention of activity despite DSM265 resistance.

DSM1463 potency was similarly preserved. WT EC_{50} was 0.80 ± 0.15 nM, with resistant lines showing values from 0.40 ± 0.02 nM (R1BC1B) to 3.37 ± 0.19 nM (R1AC1B). While most resistant clones showed comparable or even slightly enhanced sensitivity, R1AC1B displayed a ~4-fold reduction in potency, suggesting allele-specific effects. Nonetheless, overall activity remained in the low-nanomolar range.

DSM1469 was the most potent compound tested, with EC_{50} values of 0.04 ± 0.02 nM (WT) and 0.040-0.27 nM across resistant clones. These data indicate complete preservation of inhibitory activity, irrespective of resistance mutations. The extremely low EC_{50} values highlight DSM1469 as an exceptionally promising scaffold with resilience to DSM265-associated resistance.

DSM1389 displayed low-nanomolar potency but showed clone-specific variation. WT parasites were inhibited at 1.20 ± 0.20 nM, while resistant clones ranged from 0.38 ± 0.07 nM (R1BC1B) to 5.15 ± 0.46

nM (R1AC1B). The elevated EC_{50} in R1AC1B suggests partial susceptibility to resistance mechanisms, although potency remained within a therapeutically favorable range.

DSM1200 potency was well preserved in resistant lines. The WT EC_{50} (0.26 ± 0.07 nM) compared closely with resistant values of 0.17-0.64 nM across clones. These results indicate minimal impact of DSM265 resistance mutations on DSM1200 activity.

DSM1398 remained effective while modest increases in EC_{50} were observed. WT parasites had an EC_{50} of 2.61 ± 0.72 nM, while resistant lines ranged from 0.42 ± 0.03 nM (R1BC1B) to 5.22 ± 0.23 nM (R1AC1B). The right-shift in R1AC1B (~2-fold higher than WT) points to allele-specific reductions in potency, though overall activity remains within a favorable nanomolar range.

DSM1342 showed excellent potency across all lines, with EC_{50} values of 0.39 ± 0.06 nM (WT) and 0.15-1.88 nM in resistant clones. No consistent pattern of resistance-linked loss of activity was observed, suggesting robustness to DSM265-associated mutations.

DSM1459 retained strong activity, with EC_{50} values of 0.23 ± 0.05 nM (WT) and 0.11-0.63 nM in resistant lines. Although resistant clones generally showed slightly higher EC_{50}s, the differences were <3-fold and biologically minor.

DSM1510 potency remained broadly intact, with WT parasites inhibited at 0.55 ± 0.15 nM and resistant clones showing 0.32-2.62 nM. R1AC1B demonstrated the largest increase (~5-fold vs WT), indicating partial susceptibility to DSM265 resistance mechanisms. Nonetheless, activity remained within a low-nanomolar range.

Overall, all novel DSM based DHODH inhibitors demonstrated particularly strong activity, with EC_{50} values ≤6 nM across all resistant clones, showing no cross-resistance relative to DSM265.

Interestingly, sensitivity patterns were not uniformly skewed toward resistance. Some novel DHODH inhibitors demonstrated greater potency in resistant lines compared to wild type, while others retained slightly stronger activity in WT parasites.

For example, DSM1465 displayed an EC_{50} of 0.23 ± 0.10 nM in WT but was even more potent against R2B (0.15 ± 0.04 nM) and R1BC1B (0.21 ± 0.02 nM). Similarly, DSM1459 showed enhanced inhibition in resistant clones such as R1BC1B (0.11 ± 0.02 nM) relative to WT (0.23 ± 0.05 nM). These findings suggest that some resistance-associated mutations may not reduce, and in certain cases may even improve, drug-target interactions for specific compounds.

By contrast, several compounds demonstrated slightly reduced potency in resistant lines relative to WT. DSM1398, for instance, showed an EC_{50} of 2.61 ± 0.72 nM in WT but shifted to 5.22 ± 0.23 nM in R1AC1B. Likewise, DSM1510 exhibited a WT EC_{50} of 0.55 ± 0.15 nM, increasing to 2.62 ± 0.12 nM in the same clone. These clone-specific shifts indicate that structural modifications in certain inhibitors may not fully circumvent resistance-conferring mutations.

Taken together, these observations emphasize the allele-specific effects of DHODH mutations. While some novel inhibitors, such as DSM1465 and DSM1459, appear to exploit compensatory changes in resistant parasites to maintain or even enhance potency, others such as DSM1398 and DSM1510 exhibit modest reductions in activity in select clones. This highlights the importance of evaluating new inhibitors across multiple resistant alleles to identify scaffolds with both potency and breadth of coverage.

DSM Inhibitors	Dd2 WT	R10C1B	R2B	R1BC1A	R1BC1B	R1AC1B
ART EC50 (nM) 95% CI	1.10 ± 0.10	1.74 ± 0.11	2.91 ± 0.28	1.80 ± 0.12	3.20 ± 0.10	1.81 ± 0.20
DSM 265 EC50 95% CI (nM)	5.18 ± 1.30	140.2 ± 40.50	85.50 ± 15.30	124.0 ± 20.58	110 ± 35.52	118.41 ± 37.29
DSM 1465 EC50 95% CI (nM)	0.23 ± 0.10	0.64 ± 0.05	0.15 ± 0.04	0.15 ± 0.05	0.21 ± 0.02	0.65 ± 0.01
DSM 1463 EC50 95% CI (nM)	0.80 ± 0.15	1.67 ± 0.07	0.45 ± 0.09	0.24 ± 0.02	0.40 ± 0.02	3.37 ± 0.19
DSM 1469 EC50 95% CI (nM)	0.04 ± 0.02	0.12 ± 0.01	0.043 ± 0.01	0.044 ±0.01	0.040 ± 0.01	0.27 ± 0.01
DSM 1389 EC50 (5% CI (nM)	1.20 ± 0.20	2.37 ± 0.14	0.53 ± 0.04	0.22 ± 0.02	0.38 ± 0.07	5.15 ± 0.46
DSM 1200 EC50 95% CI (nM)	0.26 ± 0.07	0.64 ± 0.03	0.40 ± 0.04	0.15 ±0.03	0.17 ± 0.02	0.48 ± 0.02
DSM 1398 EC50 95% CI (nM)	2.61 ± 0.72	3.70 ± 0.31	0.78 ± 0.04	0.40 ± 0.03	0.42 ± 0.03	5.22 ± 0.23
DSM 1342 EC50 95% CI (nM)	0.39 ± 0.06	0.78 ± 0.05	0.15 ± 0.06	0.30 ± 0.01	0.31 ± 0.03	1.88 ± 0.08
DSM 1459 EC50 95% CI (nM)	0.23 ± 0.05	0.50 ± 0.02	0.25± 0.04	0.13 ± 0.02	0.11 ± 0.02	0.63 ± 0.03
DSM 1510 EC50 95% CI (nM)	0.55 ± 0.15	1.00 ± 0.07	0.32 ± 0.05	0.32 ±0.01	0.47 ± 0.06	2.62 ± 0.12

Table 4.3: Half-maximal inhibitory concentrations (EC_{50}) of DSM265, artemisinin (ART), and nine novel DSM inhibitors against *Plasmodium falciparum* Dd2 wild-type (WT) and DSM265-resistant clones. EC_{50} values were determined from triplicate measurements at each drug concentration, and dose-response data were analyzed in GraphPad Prism using the log(inhibitor) versus response model. Results are reported as mean ± standard deviation with corresponding 95% confidence intervals (CI).

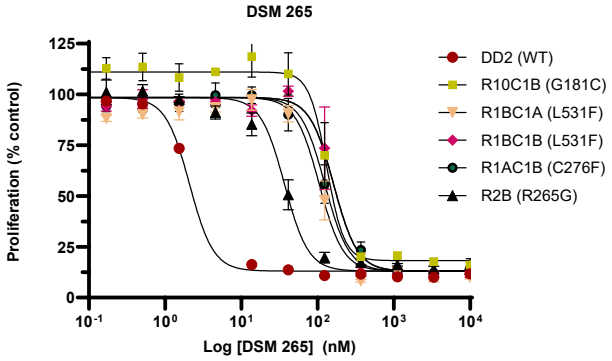
DSM 265
Proliferation (% control)
Log [DSM 265] (nM)
DD2 (WT)
R10C1B (G181C)
R1BC1A (L531F)
R1BC1B (L531F)
R1AC1B (C276F)
R2B (R265G)

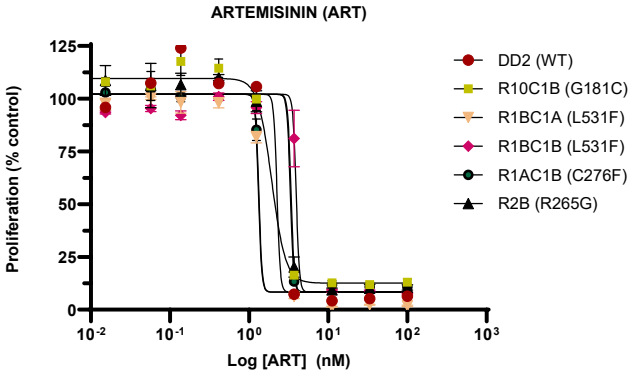
ARTEMISININ (ART)
Proliferation (% control)
Log [ART] (nM)
DD2 (WT)
R10C1B (G181C)
R1BC1A (L531F)
R1BC1B (L531F)
R1AC1B (C276F)
R2B (R265G)

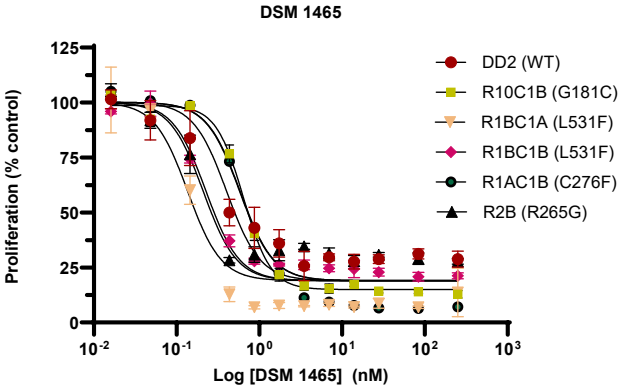
DSM 1465
Proliferation (% control)
Log [DSM 1465] (nM)
DD2 (WT)
R10C1B (G181C)
R1BC1A (L531F)
R1BC1B (L531F)
R1AC1B (C276F)
R2B (R265G)

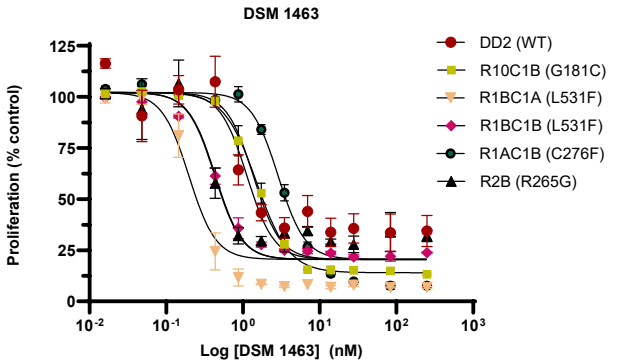
DSM 1463
Proliferation (% control)
Log [DSM 1463] (nM)
DD2 (WT)
R10C1B (G181C)
R1BC1A (L531F)
R1BC1B (L531F)
R1AC1B (C276F)
R2B (R265G)

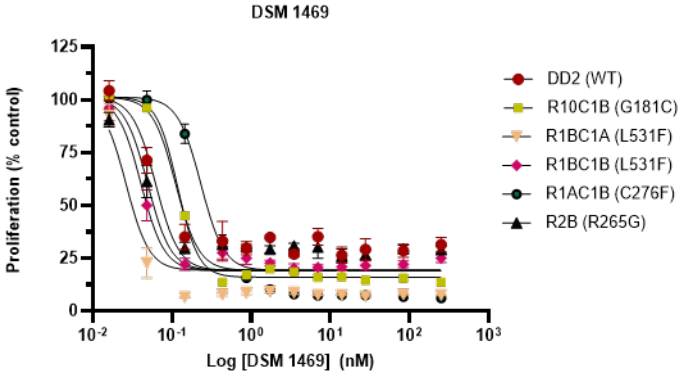
DSM 1469
Proliferation (% control)
Log [DSM 1469] (nM)
DD2 (WT)
R10C1B (G181C)
R1BC1A (L531F)
R1BC1B (L531F)
R1AC1B (C276F)
R2B (R265G)

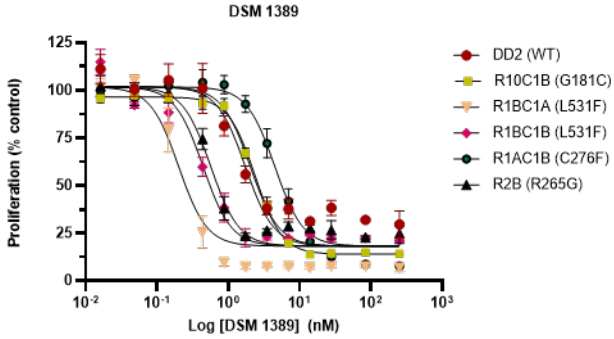
DSM 1389
Proliferation (% control)
Log [DSM 1389] (nM)
DD2 (WT)
R10C1B (G181C)
R1BC1A (L531F)
R1BC1B (L531F)
R1AC1B (C276F)
R2B (R265G)

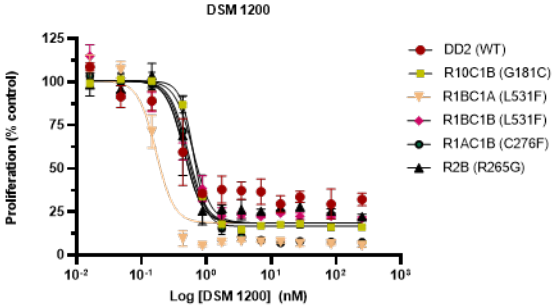
DSM 1200
Proliferation (% control)
Log [DSM 1200] (nM)
DD2 (WT)
R10C1B (G181C)
R1BC1A (L531F)
R1BC1B (L531F)
R1AC1B (C276F)
R2B (R265G)

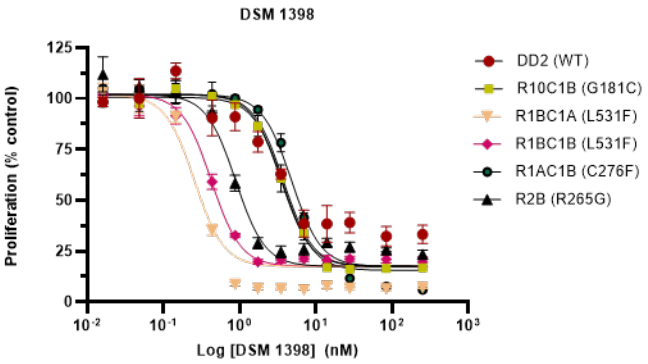
DSM 1398
Proliferation (% control)
Log [DSM 1398] (nM)
DD2 (WT)
R10C1B (G181C)
R1BC1A (L531F)
R1BC1B (L531F)
R1AC1B (C276F)
R2B (R265G)

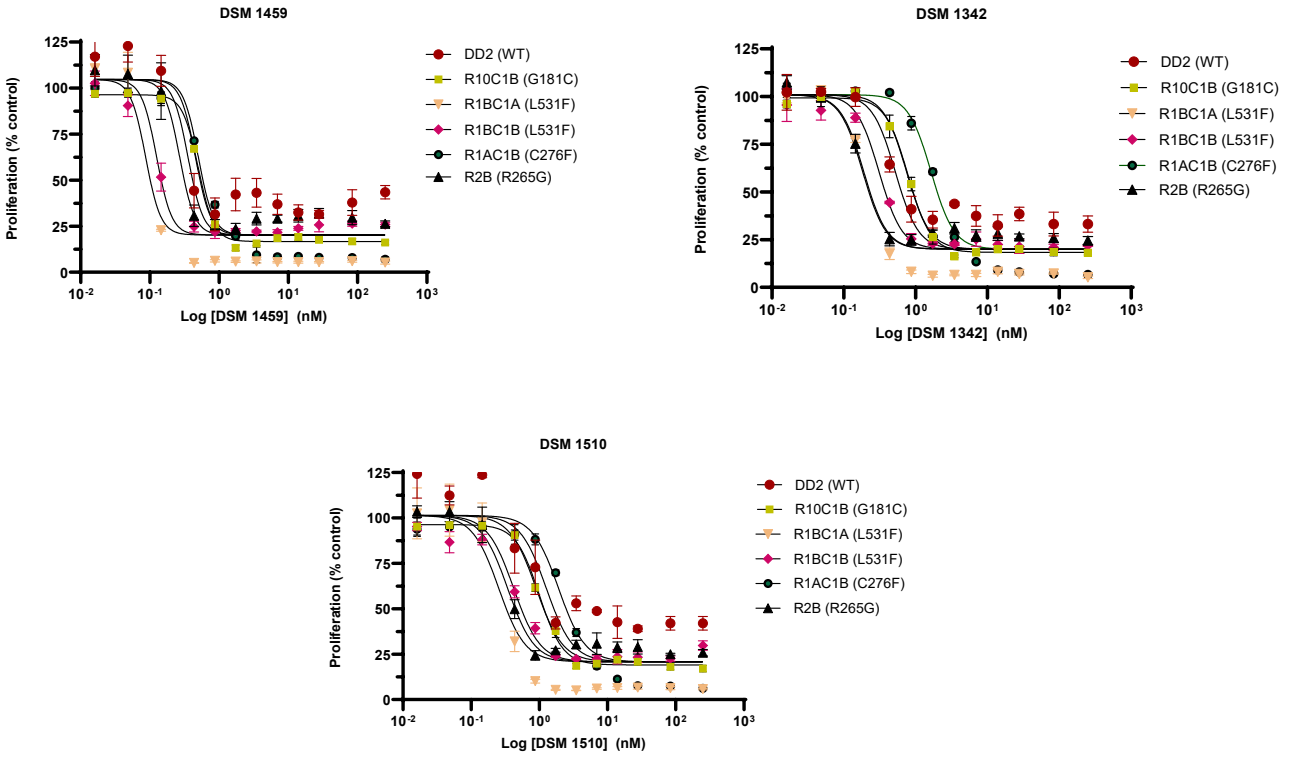

Figure 4.3: Half-maximal inhibitory concentrations (EC_{50}) of DSM265 and artemisinin (ART) and 9 DSM inhibitors against *Plasmodium falciparum* Dd2 wild-type (WT) and DSM265-resistant clonal lines. A- DSM265, B- ART, C- DSM165, D- DSM1463, E- DSM1469, F- DSM1389, G-DSM1200, H- DSM1398, I- DSM1432, J-DSM1459, K- DSM1210.

Data sets were collected in triplicate for each concentration in the dose-response curve, and data were fitted in GraphPad Prism to determine the EC_{50} using the logI versus response equation. Reported values are presented as mean ± standard deviation with 95% confidence intervals (CI).

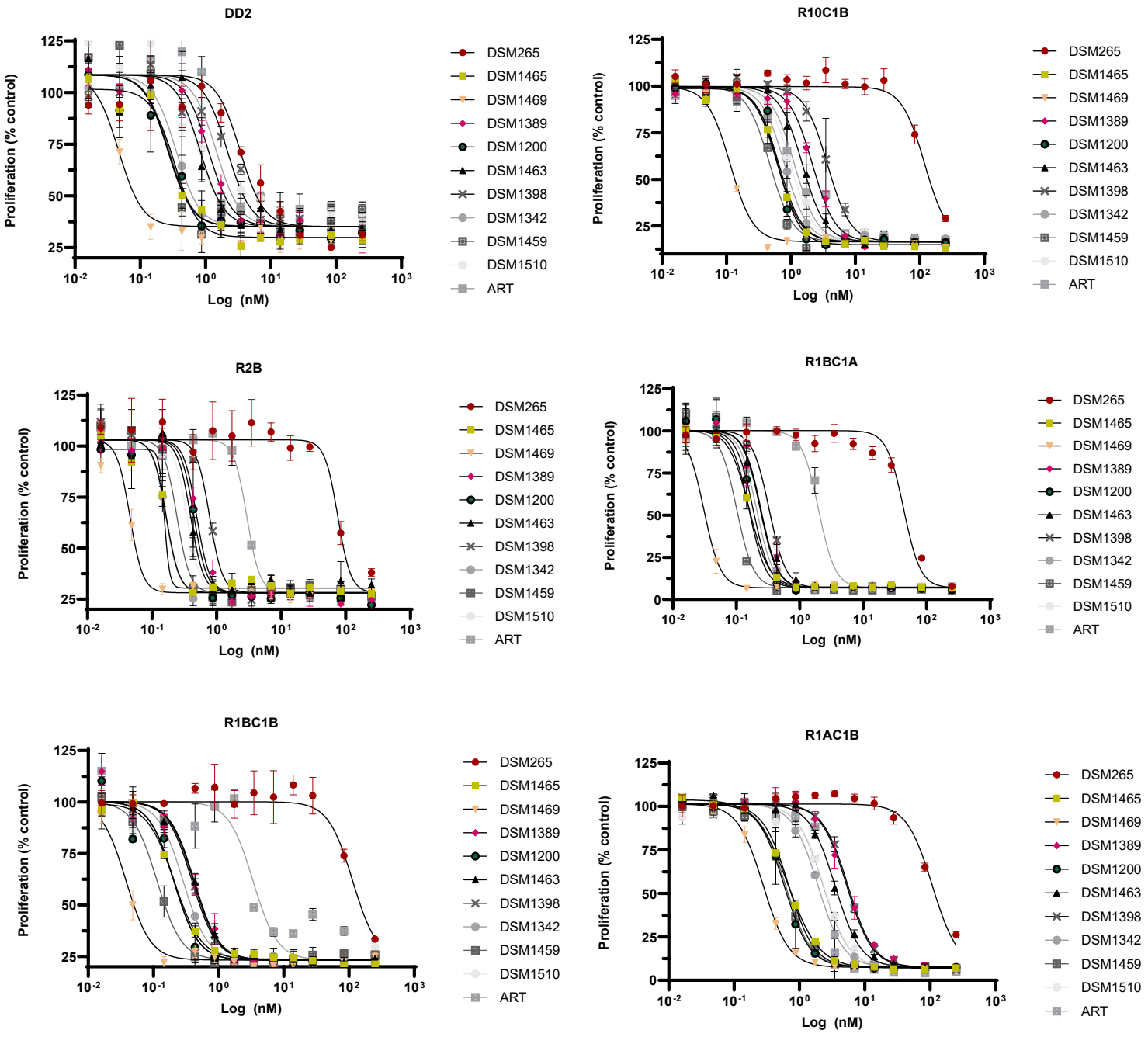

Figure 4: EC50 curves showing comparative parasite proliferation for DD2 and resistant lines (a- DD2, b- R10C1B, c- R2B, d- R1BCIA, e- R1BCIB, f- R1BC1B) against DSM 265, ART and all 9 novel DSM-based DHODH inhibitors. Data sets were collected in triplicate for each concentration in the dose-response curve, and data were fitted in GraphPad Prism to determine the EC_{50} using the logI versus response equation. Reported values are presented as mean ± standard deviation with 95% confidence intervals (CI).

4.4. Discussion

The emergence of resistance to antimalarial agents continues to pose a formidable challenge to global malaria control efforts, particularly for mechanistically novel compounds such as DHODH inhibitors. In this study, we evaluated the inhibitory profiles of a series of novel DHODH inhibitors against *P. falciparum* Dd2 clones carrying DSM265-resistance-associated mutations, with the aim of identifying compounds that maintain potency and broad coverage across resistant alleles. The data collectively underscore the critical importance of both structural optimization of DHODH inhibitors and detailed evaluation across multiple resistant backgrounds to anticipate and circumvent clinically relevant resistance.

Resequencing of the *Pf*dhodh locus in DSM265-selected clones confirmed the presence of four distinct amino acid substitutions (G181C, R265S, C276F, and L531F) previously reported to confer resistance.[37] The absence of additional novel mutations highlights the stability of these point mutations under continuous in-vitro selection, providing a defined framework to study cross-resistance. Importantly, one of these mutations, C276F, has been detected in clinical isolates, emphasizing the translational relevance of our findings. The differential distribution of these mutations across resistant clones allowed for an assessment of allele-specific effects on novel DHODH inhibitors.

Previous studies have indicated that mutations in the DHODH active site can impact inhibitor binding in a manner that is highly compound-specific.[30,37] Structural analyses have demonstrated that substitutions at residues such as C276 or L531 may alter the conformation of the inhibitor-binding pocket, potentially reducing binding affinity for some scaffolds while having minimal effect or even enhancing affinity for others.[37,38] The findings from the current study align with these observations: certain compounds retained full inhibitory potency across all resistant clones, whereas others exhibited modest shifts in EC_{50} values depending on the specific allele present.

Among the series evaluated, DSM1465 and DSM1469 emerged as standout candidates due to their remarkable retention of activity across resistant alleles. The lack of substantial right-shifts in EC_{50} values, even in clones carrying the C276F mutation (figure 4.4), suggests these compounds possess structural features that enable robust interactions with the altered DHODH active site. Such resilience is consistent with previous reports indicating that noncovalent interactions, including hydrogen bonding and hydrophobic contacts, can mitigate the impact of point mutations on inhibitor binding.[27,28,30,37] DSM1469, in particular, demonstrated sub-0.1 nM EC_{50} values across all lines, indicating near-maximal potency. The consistency of these results suggests that the compound may occupy multiple binding subsites within DHODH or engage in interactions outside the canonical active site, thereby reducing vulnerability to single-residue mutations.

DSM1463 and DSM1342 also displayed broadly preserved activity, although modest shifts were observed in specific clones. These patterns suggest that certain allelic variants can selectively influence inhibitor efficacy. The R1AC1B clone, carrying the C276F mutation, frequently exhibited reduced susceptibility to select compounds, emphasizing the importance of evaluating multiple resistance backgrounds when assessing novel inhibitors. Such observations are consistent with previous work on DSM265 cross-resistance, where differential binding effects were attributed to steric hindrance and altered hydrogen bonding at the mutation site.

The observation that some resistant clones demonstrated greater sensitivity than the wild-type parasite to certain inhibitors is particularly noteworthy. Compounds such as DSM1459 and DSM1465 exhibited enhanced potency against select resistant clones. This paradoxical increase in sensitivity may reflect conformational compensations in the DHODH enzyme that enhance inhibitor binding. Similar phenomena have been described in other systems, where resistance-conferring mutations inadvertently stabilize the enzyme in a conformation that favors binding of specific scaffolds.[42,43] These data highlight the potential for rationally designed inhibitors to exploit compensatory changes in mutant DHODH enzymes, offering a strategic avenue for the development of “resistance-proof” antimalarials.

Despite the overall retention of potency observed for most compounds, allele-specific differences were apparent. DSM1398 and DSM1510, for example, displayed modest right-shifts in EC_{50} against the R1AC1B clone. The selective reduction in potency suggests that subtle structural features of these inhibitors may be less compatible with the conformational changes induced by specific DHODH mutations. These findings underscore the mechanistic principle that even minor alterations within the active site can have compound-specific consequences for binding affinity. Structural studies of DHODH-inhibitor complexes have highlighted that residues such as C276 and L531 participate in both hydrophobic packing and hydrogen bonding networks critical for high-affinity binding.[37] Thus, substitutions at these positions are likely to selectively impact inhibitors with precise steric or electronic requirements.

The variability in sensitivity patterns also suggests that multi-clone screening is essential for accurate evaluation of cross-resistance potential. A compound that retains activity against one resistant allele may not necessarily retain it against others. This complexity highlights the need for comprehensive structure-activity relationship (SAR) studies in the context of resistance-associated mutations, to optimize both potency and breadth of coverage.

Therapeutic Implications

The preservation of low-nanomolar potency across most resistant clones has important implications for the development of next-generation DHODH inhibitors. DSM1465 and DSM1469, with their exceptional resilience to DSM265 resistance, represent promising lead candidates for clinical development. Their robust activity suggests that these compounds could maintain efficacy even in regions where DSM265 resistance has emerged, addressing a key limitation of current DHODH-targeted therapy. Furthermore, the observation that some inhibitors exhibit enhanced potency against resistant clones raises the possibility of designing compounds that selectively exploit resistance-associated conformational changes, potentially converting a liability into a therapeutic advantage.

From a translational perspective, these findings support that these novel DHODH inhibitors could serve as effective monotherapies or components of combination regimens. The retention of activity in multiple resistant backgrounds reduces the likelihood of cross-resistance and may prolong clinical utility. This aligns with prior observations that compounds designed to accommodate active site mutations can sustain potency in preclinical models.

The data also provide mechanistic insights into the molecular basis of DHODH inhibitor activity. The variable impact of resistance mutations across different scaffolds highlights the importance of the inhibitor's chemical structure, particularly its size, shape, and ability to form stabilizing interactions within the DHODH active site. This understanding could guide future medicinal chemistry efforts, particularly in the design of compounds with broad-spectrum activity against both wild-type and resistant *P. falciparum* isolates. Moreover, these findings underscore the importance of integrating resistance-informed design into early-stage drug discovery. By systematically evaluating compounds across diverse resistant alleles, researchers can identify scaffolds that combine both high potency and resilience to resistance, a strategy increasingly recognized as essential for sustainable antimalarial development.[40]

While the current study provides comprehensive in vitro evaluation of DHODH inhibitor potency against multiple DSM265-resistant clones, several limitations should be acknowledged. First, in vitro resistance profiles may not fully capture the complexity of clinical resistance, which can involve compensatory mechanisms outside the target enzyme, such as altered drug metabolism, efflux, or host-parasite interactions. Second, the study focused on single-point mutations, whereas clinical isolates may carry multiple co-occurring mutations or genetic backgrounds that influence susceptibility.[37] Nonetheless, the defined clonal lines used here provide a robust platform for mechanistic investigation of cross-resistance and rational inhibitor design.

In summary, the findings of this study highlight the promising potential of novel DHODH inhibitors to overcome DSM265-associated resistance. The compounds evaluated exhibited a spectrum of activity

patterns, with some retaining full potency across all resistant clones and others showing allele-specific shifts. Notably, several inhibitors demonstrated paradoxically enhanced activity against resistant lines, suggesting opportunities to exploit conformational changes induced by resistance mutations. These results underscore the importance of evaluating multiple resistant alleles during preclinical development and provide a framework for the rational design of DHODH inhibitors with both potency and breadth of coverage.

Collectively, these observations inform future drug development strategies aimed at sustaining the clinical utility of DHODH-targeted antimalarials. By prioritizing scaffolds that are resilient to resistance-conferring mutations and capable of maintaining nanomolar potency across diverse parasite backgrounds, researchers can develop next-generation therapies that address the growing threat of drug-resistant malaria.[44,45]

4.5. References

1. Hanboonkunupakarn B, Tarning J, Pukrittayakamee S, Chotivanich K. Artemisinin resistance and malaria elimination: Where are we now?. *Front Pharmacol*. 2022;13:876282. Published 2022 Sep 23. doi:10.3389/fphar.2022.876282
2. Palmer, M.,Deng, X., Watts, S., Krilov, G. et al. Potent Antimalarials with Development Potential Identified by Structure-Guided Computational Optimization of a Pyrrole-Based Dihydroorotate Dehydrogenase Inhibitor Series. J. Med. Chem. 2021, 64, 9, 6085-6136. https://doi.org/10.1021/acs.jmedchem.1c00173
3. White J, Dhingra SK, Deng X, et al. Identification and Mechanistic Understanding of Dihydroorotate Dehydrogenase Point Mutations in *Plasmodium falciparum* that Confer in Vitro Resistance to the Clinical Candidate DSM265. *ACS Infect Dis*. 2019;5(1):90-101. doi:10.1021/acsinfecdis.8b00211
4. Krungkrai J. Purification, characterization and localization of mitochondrial dihydroorotate dehydrogenase in *Plasmodium falciparum*, human malaria parasite. *Biochim Biophys Acta*. 1995;1243(3):351-360. doi:10.1016/0304-4165(94)00158-t
5. Hyde JE. Targeting purine and pyrimidine metabolism in human apicomplexan parasites. *Curr Drug Targets*. 2007;8(1):31-47. doi:10.2174/138945007779315524
6. Gardner MJ, Hall N, Fung E, et al. Genome sequence of the human malaria parasite *Plasmodium falciparum*. *Nature*. 2002;419(6906):498-511. doi:10.1038/nature01097
7. McRobert L, McConkey GA. RNA interference (RNAi) inhibits growth of *Plasmodium falciparum*. *Mol Biochem Parasitol*. 2002;119(2):273-278. doi:10.1016/s0166-6851(01)00429-7
8. Phillips MA, Lotharius J, Marsh K, et al. A long-duration dihydroorotate dehydrogenase inhibitor (DSM265) for prevention and treatment of malaria. *Sci Transl Med*. 2015;7(296):296ra111. doi:10.1126/scitranslmed.aaa6645
9. Hoelz L.V.B., Calil F.A., Nonato M.C., Pinheiro L.C.S. and Boechat N. (2018) *Plasmodium falciparum* dihydroorotate dehydrogenase: a drug target against malaria. Future Med. Chem. 10, 1853-1874 10.4155/fmc-2017-0250
10. Hurt D.E., Widom J. and Clardy J. (2006) Structure of *Plasmodium falciparum* dihydroorotate dehydrogenase with a bound inhibitor. Acta Crystallogr. D Biol. Crystallogr. 62, 312-323 10.1107/s0907444905042642
11. Walse B., Dufe V.T., Svensson B., Fritzson I., Dahlberg L., Khairoullina A. et al. (2008) The structures of human dihydroorotate dehydrogenase with and without inhibitor reveal conformational flexibility in the inhibitor and substrate binding sites. Biochemistry 47, 8929-8936 10.1021/bi8003318
12. Malmquist N.A., Gujjar R., Rathod P.K. and Phillips M.A. (2008) Analysis of flavin oxidation and electron-transfer inhibition in *Plasmodium falciparum* dihydroorotate dehydrogenase. Biochemistry 47, 2466-2475 10.1021/bi702218c
13. Deng X., Gujjar R., El Mazouni F., Kaminsky W., Malmquist N.A., Goldsmith E.J. et al. (2009) Structural plasticity of malaria dihydroorotate dehydrogenase allows selective binding of diverse chemical scaffolds. J. Biol. Chem. 284, 26999-27009 10.1074/jbc.m109.028589
14. Cassera MB, Zhang Y, Hazleton KZ, Schramm VL. Purine and pyrimidine pathways as targets in *Plasmodium falciparum*. *Curr Top Med Chem*. 2011;11(16):2103-2115. doi:10.2174/156802611796575948
15. Baldwin J., Farajallah A., Malmquist N., Rathod P. and Phillips M. (2002) Malarial dihydroorotate dehydrogenase: substrate and inhibitor specificity. J. Biol. Chem. 277, 41827-41834 10.1074/jbc.M206854200
16. Baldwin J., Michnoff C.H., Malmquist N.A., White J., Roth M.G., Rathod P.K. et al. (2005) High-throughput screening for potent and selective inhibitors of *Plasmodium falciparum* dihydroorotate dehydrogenase. J. Biol. Chem. 280, 21847-21853 10.1074/jbc.m501100200

17. Davies M., Heikkilä T., McConkey G.A., Fishwick C.W.G., Parsons M.R. and Johnson A.P. (2009) Structure-Based design, synthesis, and characterization of inhibitors of human and *Plasmodium falciparum* dihydroorotate dehydrogenases. J. Med. Chem. 52, 2683-2693 10.1021/jm800963t
18. Liu S., Neidhardt E.A., Grossman T.H., Ocain T. and Clardy J. (2000) Structures of human dihydroorotate dehydrogenase in complex with antiproliferative agents. Structure 8, 25-33 10.1016/S0969-2126(00)00077-0
19. Heikkilä T., Thirumalairajan S., Davies M., Parsons M.R., McConkey A.G., Fishwick C.W.G. et al. (2006) The first De novo designed inhibitors of *Plasmodium falciparum* dihydroorotate dehydrogenase. Bioorg. Med. Chem. Lett. 16, 88-92 10.1016/j.bmcl.2005.09.045
20. Heikkilä T., Ramsey C., Davies M., Galtier C., Stead A.M.W., Johnson A.P. et al. (2007) Design and synthesis of potent inhibitors of the malaria parasite dihydroorotate dehydrogenase. J. Med. Chem. 50, 186-191 10.1021/jm060687j
21. Patel V., Booker M., Kramer M., Ross L., Celatka C.A., Kennedy L.M. et al. (2008) Identification and characterization of small molecule inhibitors of *Plasmodium falciparum* dihydroorotate dehydrogenase. J. Biol. Chem. 283, 35078-35085 10.1074/jbc.M804990200
22. Booker M.L., Bastos C.M., Kramer M.L., Barker R.H. Jr, Skerlj R., Sidhu A.B. et al. (2010) Novel inhibitors of *Plasmodium falciparum* dihydroorotate dehydrogenase with anti-Malarial activity in the mouse model. J. Biol. Chem. 285, 33054-33064 10.1074/jbc.M110.162081
23. Lukens A.K., Ross L.S., Heidebrecht R., Javier Gamo F., Lafuente-Monasterio M.J., Booker M.L. et al. (2014) Harnessing evolutionary fitness in *Plasmodium falciparum* for drug discovery and suppressing resistance. Proc. Natl Acad. Sci. U.S.A. 111, 799-804 10.1073/pnas.1320886110
24. Gujjar R., Marwaha A., El Mazouni F., White J., White K.L., Creason S. et al. (2009) Identification of a metabolically stable triazolopyrimidine-based dihydroorotate dehydrogenase inhibitor with antimalarial activity in mice. J. Med. Chem. 52, 1864-1872 10.1021/jm801343r
25. Kokkonda S., Deng X., White K.L., El Mazouni F., White J., Shackleford D.M. et al. (2020) Lead optimization of a pyrrole-Based dihydroorotate dehydrogenase inhibitor series for the treatment of malaria. J. Med. Chem. 63, 4929-4956 10.1021/acs.jmedchem.0c00311
26. Gujjar R., El Mazouni F., White K.L., White J., Creason S., Shackleford D.M. et al. (2011) Lead optimization of aryl and aralkyl amine-Based triazolopyrimidine inhibitors of *Plasmodium falciparum* dihydroorotate dehydrogenase with antimalarial activity in mice. J. Med. Chem. 54, 3935-3949 10.1021/jm200265b
27. Phillips M.A., White K.L., Kokkonda S., Deng X., White J., El Mazouni F. et al. (2016) A triazolopyrimidine-based dihydroorotate dehydrogenase inhibitor with improved drug-Like properties for treatment and prevention of malaria. ACS Infect. Dis. 2, 945-957 10.1021/acsinfecdis.6b00144
28. Coteron J.M., Marco M., Esquivias J., Deng X., White K.L., White J. et al. (2011) Structure-Guided lead optimization of triazolopyrimidine-Ring substituents identifies potent *Plasmodium falciparum* dihydroorotate dehydrogenase inhibitors with clinical candidate potential. J. Med. Chem. 54, 5540-5561 10.1021/jm200592f
29. Calic PPS, Mansouri M, Scammells PJ, McGowan S. Driving antimalarial design through understanding of target mechanism. *Biochem Soc Trans*. 2020;48(5):2067-2078. doi:10.1042/BST20200224
30. Phillips M.A., Lotharius J., Marsh K., White J., Dayan A., White K.L. et al. (2015) A long-Duration dihydroorotate dehydrogenase inhibitor (Dsm265) for prevention and treatment of malaria. Sci. Transl. Med. 7, 296ra111 10.1126/scitranslmed.aaa6645
31. McCarthy JS, Lotharius J, Rückle T, et al. Safety, tolerability, pharmacokinetics, and activity of the novel long-acting antimalarial DSM265: a two-part first-in-human phase 1a/1b randomised study. *Lancet Infect Dis*. 2017;17(6):626-635. doi:10.1016/S1473-3099(17)30171-8
32. Llanos-Cuentas A., Casapia M., Chuquiyauri R., Hinojosa J.-C., Kerr N., Rosario M. et al. (2018) Antimalarial activity of single-dose Dsm265, a novel plasmodium dihydroorotate dehydrogenase

inhibitor, in patients with uncomplicated *Plasmodium falciparum* or *Plasmodium vivax* malaria infection: a proof-of-Concept, open-label, phase 2a study. Lancet Infect. Dis. 18, 874-883 10.1016/S1473-3099(18)30309-8
33. Belard, S, Ramharter, M. DSM265: a novel drug for single-dose cure of *Plasmodium falciparum* malaria.The Lancet Infectious Diseases, Volume 18, Issue 8, 819 - 820
34. Flannery EL; Foquet L; Chuenchob V; Fishbaugher M; Billman Z; Navarro MJ; Betz W; Olsen TM; Lee J; Camargo N; Nguyen T; Schafer C; Sack BK; Wilson EM; Saunders J; Bial J; Campo B; Charman SA; Murphy SC; Phillips MA; Kappe SH; Mikolajczak SA, Assessing drug efficacy against *Plasmodium falciparum* liver stages in vivo. JCI Insight 2018, 3, e92587
35. Palmer MJ, Deng X, Watts S, et al. Potent Antimalarials with Development Potential Identified by Structure-Guided Computational Optimization of a Pyrrole-Based Dihydroorotate Dehydrogenase Inhibitor Series. *J Med Chem*. 2021;64(9):6085-6136. doi:10.1021/acs.jmedchem.1c00173
36. Kokkonda S., El Mazouni F., White K.L., White J., Shackleford D.M., Lafuente-Monasterio M.J. et al. (2018) Isoxazolopyrimidine-based inhibitors of *Plasmodium falciparum* dihydroorotate dehydrogenase with antimalarial activity. ACS Omega 3, 9227-9240 10.1021/acsomega.8b01573
37. White J, Dhingra SK, Deng X, et al. Identification and Mechanistic Understanding of Dihydroorotate Dehydrogenase Point Mutations in *Plasmodium falciparum* that Confer in Vitro Resistance to the Clinical Candidate DSM265. *ACS Infect Dis*. 2019;5(1):90-101. doi:10.1021/acsinfecdis.8b00211
38. Ross LS, Lafuente-Monasterio MJ, Sakata-Kato T, et al. Identification of Collateral Sensitivity to Dihydroorotate Dehydrogenase Inhibitors in *Plasmodium falciparum*. *ACS Infect Dis*. 2018;4(4):508-515. doi:10.1021/acsinfecdis.7b00217
39. Ross LS, Gamo FJ, Lafuente-Monasterio MJ, et al. In vitro resistance selections for *Plasmodium falciparum* dihydroorotate dehydrogenase inhibitors give mutants with multiple point mutations in the drug-binding site and altered growth. *J Biol Chem*. 2014;289(26):17980-17995. doi:10.1074/jbc.M114.558353
40. Duffey,M., Blasco, B., Burrows,J.N., Wells,T., et al.Assessing risks of *Plasmodium falciparum* resistance to select next-generation antimalarials. Trends in Parasitology, 2021;37(8), Pages 709-721,https://doi.org/10.1016/j.pt.2021.04.006.
41. Barney R, Velasco M, Cooper CA, et al. Diagnostic Characteristics of Lactate Dehydrogenase on a Multiplex Assay for Malaria Detection Including the Zoonotic Parasite Plasmodium knowlesi. *Am J Trop Med Hyg*. 2021;106(1):275-282. Published 2021 Nov 15. doi:10.4269/ajtmh.21-0532
42. Freedy, A.M., Liau, B.B. Discovering new biology with drug-resistance alleles. *Nat Chem Biol* **17**, 1219-1229 (2021). https://doi.org/10.1038/s41589-021-00865-9
43. Hooper DC, Jacoby GA. Mechanisms of drug resistance: quinolone resistance. *Ann N Y Acad Sci*. 2015;1354(1):12-31. doi:10.1111/nyas.12830
44. Rottmann M, McNamara C, Yeung BK, et al. Spiroindolones, a potent compound class for the treatment of malaria. *Science*. 2010;329(5996):1175-1180. doi:10.1126/science.1193225
45. White NJ, Pukrittayakamee S, Hien TT, Faiz MA, Mokuolu OA, Dondorp AM. Malaria. *Lancet*. 2014;383(9918):723-735. doi:10.1016/S0140-6736(13)60024-0

Chapter 5 | Conclusion and Future Directions

5.1 Overview

This dissertation presented an integrated analysis of antimalarial immunity and resistance, emphasizing chemistry-driven tools to dissect antibody responses and small molecule activity against *Plasmodium falciparum*. The overall aim was to bridge antigen prioritization strategies with mechanistic assays that evaluate drug and antibody-mediated inhibition, thereby advancing the molecular understanding of malaria immunology and therapeutic resistance.

In Chapter 1, the background on malaria burden, immune evasion, and antigenic diversity underscored the central challenge: the parasite's ability to alter surface-expressed epitopes and employ redundant invasion pathways. This sets the stage for antigen prioritization and mechanistic assay development.

Chapter 2 described the optimization of bead-based multiplexing platforms to interrogate antibody responses against multiple malaria antigens simultaneously. By improving antigen immobilization chemistry, orientation, and detection sensitivity, these assays overcame limitations of earlier single-antigen ELISAs, allowing for a more comprehensive and physiologically relevant mapping of antibody repertoires.

In Chapter 3, growth and invasion inhibition assays were applied to evaluate the inhibitory effects of small molecules, monoclonal antibodies, and patient sera. Tartrolon E, DSM265, and artemisinin served as pharmacological benchmarks, demonstrating consistent inhibitory activity in erythrocytic stages. Monoclonal antibodies targeting MSP1, AMA1, and EBA175 exhibited differential inhibition, with AMA1-directed antibodies being the most potent, consistent with their direct role in merozoite invasion. Patient sera from malaria-endemic regions further highlighted the protective potential of naturally acquired immunity, reinforcing the relevance of multiplex assays for antigen prioritization.

Finally, Chapter 4 addressed the problem of drug resistance by characterizing cross-resistance of DSM265-selected mutant parasite lines against a panel of novel DHODH inhibitors. These studies revealed varying susceptibility patterns, highlighting both the vulnerability and adaptability of the *P. falciparum* DHODH enzyme. The results demonstrate that resistance mutations selected by one

compound can extend to structurally related inhibitors, providing mechanistic insights into resistance evolution and guiding rational design of next-generation antimalarials.

Collectively, the studies presented here demonstrate that combining chemical biology, immunological assays, and resistance profiling provides a multidimensional framework for dissecting host-parasite interactions and informing malaria control strategies.

5.2 Contributions to the Field

The major contributions of this dissertation can be summarized in three key areas:

5.2.1 Advancements in Antigen Prioritization Technologies

The bead-based multiplexing system described in Chapter 2 represents a significant methodological improvement over traditional ELISAs and protein microarrays. By addressing issues of antigen orientation and epitope masking through chemistry-based immobilization strategies, the developed assay provided a more physiologically relevant platform for assessing naturally acquired immune responses. This system enables parallel evaluation of >100 antigens using minimal patient sample volumes, which is particularly important in field studies where blood collection is limited. Such advances have direct implications for vaccine development by allowing for rapid, high-throughput antigen screening in diverse populations.[1-3]

5.2.2 Mechanistic Insights into Inhibition of Parasite Growth

Chapter 3 provided comparative analyses of three modalities of growth inhibition: small molecules, monoclonal antibodies, and patient sera. The use of pharmacological controls (Tartrolon E, DSM265, artemisinin) established reliable benchmarks for interpreting antibody- and sera-mediated inhibition. The identification of AMA1 as a highly potent antibody target supports continued exploration of AMA1-based vaccines or monoclonal therapies, while the relatively modest inhibition by MSP1 underscores the need for combination antigen approaches. Patient sera studies further validated that naturally acquired

immunity can confer growth inhibition, although with variable potency, pointing toward heterogeneity in immune responses across populations.[4,5]

5.2.3 Understanding and Anticipating Drug Resistance

Chapter 4 extended current knowledge on DHODH inhibitors by demonstrating cross-resistance among DSM265-selected mutant parasite lines. These findings reveal that while DSM265 resistance mutations compromise susceptibility to several related compounds, some novel inhibitors retain activity, suggesting opportunities for rational structure-activity optimization. This highlights the importance of resistance surveillance in drug development and demonstrates that mechanistic assays can help predict clinical resistance outcomes before large-scale deployment.[6-8]

5.3 Limitations of the Present Work

Despite the advances presented in this dissertation, several limitations warrant acknowledgment.

First, while bead-based multiplex assays allow for robust antigen screening, they remain limited by the availability and quality of recombinant antigen preparations. Many malaria antigens are large, conformationally complex, or membrane-bound, making expression and purification challenging. Improvements in expression systems could mitigate these limitations.[3]

Second, growth inhibition assays, although widely used, are limited in their ability to fully replicate in-vivo conditions. These assays do not account for the complexities of host immune networks, complement pathways, or tissue-specific sequestration that occur during malaria infection. As such, results should be interpreted as mechanistic proxies rather than absolute predictors of clinical efficacy.[9,10]

Third, the resistance studies in Chapter 4 were restricted to in vitro-selected mutant lines of *P. falciparum* Dd2 strain. While informative, these findings require validation in additional genetic backgrounds, particularly field isolates, to confirm their generalizability. Moreover, fitness costs associated with resistance mutations were not systematically addressed, an area that could significantly impact their epidemiological relevance.[11]

5.4 Future Directions

5.4.1 Expanding Antigen Discovery Platforms

Future work should focus on refining multiplex bead-based systems to include conformationally intact, post-translationally modified antigens. Integration with protein microarray and next-generation proteomic approaches could provide complementary insights. Coupling multiplex assays with systems serology, including Fc-effector function profiling, could enable a more holistic understanding of protective immunity. Machine learning approaches could also be applied to large-scale multiplex datasets to identify predictive immune signatures of protection.[12]

5.4.2 Combining Antibody and Drug-Based Strategies

Given the variable potency of monoclonal antibodies and patient sera, future studies could be done to investigate combination strategies that pair antibody-based interventions with small molecules (i.e. antibody-drug conjugates).[13] For instance, synergistic inhibition may be achieved by combining AMA1 antibodies with DHODH inhibitors or artemisinin derivatives. Such combination therapies could reduce the likelihood of resistance emergence and provide broader protection against diverse parasite strains.

5.4.3 Resistance Surveillance and Structural Optimization

The resistance profiling described in Chapter 4 should be expanded to include field-derived resistant isolates, longitudinal sampling from endemic regions, and structural biology approaches. Solving high-resolution structures of mutant DHODH enzymes bound to inhibitors could reveal mechanisms of resistance at the molecular level and guide medicinal chemistry optimization.[14] Furthermore, genome-editing technologies such as CRISPR-Cas9 can be leveraged to validate the fitness impact of resistance mutations and to model polygenic resistance phenotypes.[15]

5.4.4 Translational Applications and Clinical Relevance

The ultimate goal of this work is to advance translational malaria control strategies. Multiplex assays can be deployed in vaccine field trials to monitor antigen-specific antibody responses, while growth inhibition assays can serve as surrogate markers for vaccine efficacy. Resistance monitoring against DHODH inhibitors should be incorporated into clinical trial designs to anticipate resistance emergence before wide-scale use. Additionally, the framework established here could be adapted for other parasitic diseases where antigenic complexity and drug resistance remain barriers to control.

5.5 Concluding Remarks

Malaria continues to challenge global health due to the parasite's antigenic diversity, immune evasion strategies, and ability to develop drug resistance. This dissertation contributes to addressing these challenges by integrating chemistry-based immunoassays, mechanistic growth inhibition studies, and drug resistance profiling. The findings underscore the importance of multipronged strategies that combine antigen discovery, mechanistic dissection, and drug surveillance. Looking forward, advances in antigen engineering, structural biology, and integrative computational analysis hold promise for accelerating the development of effective vaccines and therapeutics. Ultimately, the tools and frameworks developed in this work provide a foundation for rational design of next-generation malaria interventions, with broader implications for combating other complex infectious diseases.

5.6 References

1. Crompton PD, Pierce SK, Miller LH. Advances and challenges in malaria vaccine development. *J Clin Invest*. 2010;120(12):4168-4178. doi:10.1172/JCI44423
2. Miura K, Orcutt AC, Muratova OV, Miller LH, Saul A, Long CA. Development and characterization of a standardized ELISA including a reference serum on each plate to detect antibodies induced by experimental malaria vaccines. *Vaccine*. 2008;26(2):193-200. doi:10.1016/j.vaccine.2007.10.064
3. Momoh, E.O., Ghag, S.K., White, J., Mudeppa, D.G., Rathod, P.K. "Multiplex Assays for Analysis of Antibody Responses to South Asian *Plasmodium falciparum* and *Plasmodium vivax* Malaria Infections". Vaccines 2024, 12, 1.
4. Cowman AF, Tonkin CJ, Tham WH, Duraisingh MT. The Molecular Basis of Erythrocyte Invasion by Malaria Parasites. *Cell Host Microbe*. 2017;22(2):232-245. doi:10.1016/j.chom.2017.07.003
5. Beeson JG, Drew DR, Boyle MJ, Feng G, Fowkes FJ, Richards JS. Merozoite surface proteins in red blood cell invasion, immunity and vaccines against malaria. *FEMS Microbiol Rev*. 2016;40(3):343-372. doi:10.1093/femsre/fuw001
6. Phillips M.A., Lotharius J., Marsh K., White J., Dayan A., White K.L. et al. (2015) A long-Duration dihydroorotate dehydrogenase inhibitor (Dsm265) for prevention and treatment of malaria. Sci. Transl. Med. 7, 296ra111 10.1126/scitranslmed.aaa6645
7. Ross LS, Gamo FJ, Lafuente-Monasterio MJ, et al. In vitro resistance selections for *Plasmodium falciparum* dihydroorotate dehydrogenase inhibitors give mutants with multiple point mutations in the drug-binding site and altered growth. *J Biol Chem*. 2014;289(26):17980-17995. doi:10.1074/jbc.M114.558353
8. Deng X., Gujjar R., El Mazouni F., Kaminsky W., Malmquist N.A., Goldsmith E.J. et al. (2009) Structural plasticity of malaria dihydroorotate dehydrogenase allows selective binding of diverse chemical scaffolds. J. Biol. Chem. 284, 26999-27009 10.1074/jbc.m109.028589
9. Duncan CJ, Hill AV, Ellis RD. Can growth inhibition assays (GIA) predict blood-stage malaria vaccine efficacy?. *Hum Vaccin Immunother*. 2012;8(6):706-714. doi:10.4161/hv.19712
10. Miura, K., Diouf, A., Fay, M.P. *et al.* Assessment of precision in growth inhibition assay (GIA) using human anti-*Pf*RH5 antibodies. *Malar J* **22**, 159 (2023). https://doi.org/10.1186/s12936-023-04591-6
11. French-Constant,R., Bass, C. Does resistance really carry a fitness cost? Current Opinion in Insect Science, 21, 2017, 39-46, https://doi.org/10.1016/j.cois.2017.04.011.
12. Curion, F., Theis, F.J. Machine learning integrative approaches to advance computational immunology. *Genome Med* **16**, 80 (2024). https://doi.org/10.1186/s13073-024-01350-3
13. Shastry, M., Gupta, A, Chandarlapaty, S, Young, M, et al. Rise of Antibody-Drug Conjugates: The Present and Future. *Am Soc Clin Oncol Educ Book* **43**, e390094(2023). DOI:10.1200/EDBK_390094
14. Hurt D.E., Widom J. and Clardy J. (2006) Structure of *Plasmodium falciparum* dihydroorotate dehydrogenase with a bound inhibitor. Acta Crystallogr. D Biol. Crystallogr. 62, 312-323 10.1107/s0907444905042642
15. Ansori AN, Antonius Y, Susilo RJ, et al. Application of CRISPR-Cas9 genome editing technology in various fields: A review. *Narra J*. 2023;3(2):e184. doi:10.52225/narra.v3i2.184